7-9-2015 12:00 AM

Hydrogen Exchange Mass Spectrometry for Studying Protein-Ligand Interactions

Modupeola A. Sowole
The University of Western Ontario

Supervisor
Lars Konermann
The University of Western Ontario

Graduate Program in Chemistry
A thesis submitted in partial fulfillment of the requirements for the degree in Doctor of Philosophy

Hydrogen Exchange Mass Spectrometry for Studying Protein-Ligand Interactions

(Thesis format: Integrated-article)

By

Modupeola A. Sowole

Graduate Program in Chemistry
A thesis submitted in partial fulfillment
of the requirements for the degree of
Doctor of Philosophy

The School of Graduate and Postdoctoral Studies
The University of Western Ontario
London, Ontario, Canada

Abstract

Hydrogen deuterium exchange (HDX) coupled with mass spectrometry is widely used for probing protein structure and dynamics. Protein-ligand interactions usually induce a reduction in the measured HDX rates an effect that may be ascribed to stabilization of the protein structure. This work aims to improve the general understanding of the changes in HDX patterns associated with ligand binding.

We initially applied HDX for studying differences between oxy-hemoglobin (Oxy-Hb) and aquomet-hemoglobin (Chapter 2). The results show that the α and β subunits respond differently to the oxy to aquomet transition with the heme binding pocket being destabilized in both cases. The results suggest that enhanced structural dynamics in the heme binding pocket may have adverse effects on heme-protein interactions.

Chapter 3 focuses on the different scenarios that can be encountered in an HDX experiment upon ligand binding. Myoglobin and hemoglobin were used as model systems, focusing on the oxy and deoxy states of both proteins. Our results demonstrate that ligand binding can be stabilizing or destabilizing, leading to decreased or increased HDX rates respectively.

In Chapters 4 HDX was used to probe the changes in structural dynamics of caseinolytic protease P (ClpP), an antibiotic drug target, after binding ADEP antibiotics. The mechanism of ADEP binding and the N-terminal structure of ClpP is not well understood with conflicting x-ray structures reported in literature. Our findings demonstrate that the N-terminus of ClpP remains quite unstructured after ADEP binding, while belt region undergoes tightening.

Pin 1, a peptidyl prolyl isomerase, binding to a cyclic peptide inhibitor was studied in Chapter 5. Characterization of Pin1-CRYPEVEIC interactions by other techniques has been difficult. This study demonstrates that binding of the inhibitor triggers an overall stabilization of Pin 1. We identify a loop that interacts with basic sites of the ligand and that becomes destabilized upon ligand binding. This destabilization is ascribed to steric clashes between the peptide inhibitor and the protein

Keywords: hydrogen-deuterium exchange, mass spectrometry, hemoglobin, myoglobin, ClpP, Pin1, ligand binding

Statement of Co-Authorship

The works in Chapters 2, 3, 4 and 5 were published in the following articles, respectively:

Modupeola A. Sowole and Lars Konermann (2013). Comparative Analysis of Oxy-Hemoglobin and Aquomet-Hemoglobin by Hydrogen/Deuterium Exchange Mass Spectrometry. *J. Am. Soc. Mass Spectrom. 24*, 997-1005. Reproduced with permission © 2013, Springer.

Modupeola A. Sowole and Lars Konermann (2014). Effects of Protein-Ligand Interactions on Hydrogen/Deuterium Exchange Kinetics: Canonical and Non-Canonical Scenarios. *Anal. Chem. 86,* 6715-6722. Reproduced with permission © 2014, American Chemical Society.

M. Sowole, J. Alexopoulos, Y.-Q. Cheng, J. Ortega, and L. Konermann (2013). Activation of ClpP Protease by ADEP Antibiotics: Insights from Hydrogen Exchange Mass Spectrometry. *J. Mol. Biol. 425* 4508-4519. Reproduced with permission © 2013, Elsevier.

Modupeola A. Sowole, B. T. Innes, M. Amunugama, D. W. Litchfield, C. J. Brandl, B. H. Shilton, and L. Konermann. (2015). Noncovalent Binding of a Cyclic Peptide Inhibitor to the Peptidyl-Prolyl Isomerase Pin1 Explored by Hydrogen Exchange Mass Spectrometry. *Can. J. Chem. 93,* 44-50 Reproduced with permission. © 2015, NRC Research Press.

The first draft of each of these articles was prepared by the author. Subsequent revisions were done by the author and Dr. Lars Konermann together. All experimental work was done by the author.

Dedication

This work is dedicated to God.

Acknowledgements

I am grateful to God Almighty for the successful completion of this degree program. Without life and good health, I could have done nothing.

I wish to acknowledge my supervisor Dr. Lars Konermann for his support, mentorship throughout the course of this journey. Working with you has been a great and wonderful experience. I cannot forget your words of advice to me when I first joined the lab "Always ask yourself before you leave the lab, have I done something towards an article today?"

A special thank you to members of my supervisory committee: Dr. Martin Stillman, Dr. Ken Yeung and Dr. Keith Griffith. I'll also like to say a big thank you to my examiners Dr. Norman Huner and Dr. Derek Wilson.

My experience in the Konermann laboratory would not have been so great without the wonderful people I call friends and colleagues. First I'll like to thank Dr. Yan (Lucy) Pan for showing me the ropes of HDX. She never got tired of my questions and was always available even during my practice times on the weekends. My sincere thanks to Dr. Bradley Stocks, for showing me that I can be an excellent repair woman with the right tools (the days of ice buckets). Many thanks to the current and former group members who have given their time in the form of educative discussions along the way like Siavash, Jenna, Yue, Edwardo, Antony, Ming, Sherry, Haidy, Robert, Courtney and Samuel. You have all touched my life in one way or the other.

A very special thanks to my husband, you have been a huge support through these past years. Your love and understanding is immensely appreciated. Thanks for all the nights you had to come stay with me while I work in the lab and your words of encouragement.

Finally, I would like to thank my family and good friends for all their support throughout the years. My gratitude is beyond words.

Table of Content

List of Figures

Chapter 1

Chapter 2

Chapter 5

List of Appendices

List of Symbols and Abbreviations

NMR	Nuclear Magnetic Resonance
UV-VIS	ultraviolet-visible
CD	circular dichroism
I_0	initial light intensity
I	transmitted intensity
A	absorbance
FRET	F□rster resonance energy transfer
R_o	F□rster radius
MS	Mass Spectrometry
MALDI	Matrix Assisted Laser Desorption/Ionization
ESI	Electrospray Ionization
LC	Liquid Chromatography
z_R	charge at Rayleigh limit
γ	surface tension
ε_o	vacuum permittivity
CRM	charge residue model
IEM	ion evaporation model
CEM	chain ejection model
m/z	mass to charge ratio
DC	Direct current
RF	radio frequency
Q-TOF	Quadrupole-Time of Flight
$^{\bullet}OH$	Hydroxyl radical
E_{pot}	potential energy
E_{kin}	kinetic energy
HDX	Hydrogen Deuterium Exchange
k_{op}	opening exchange rates

k_{cl}	closing exchange rates
k_{ex}	exchange rates
k_{ch}	chemical exchange rates
K_{op}	equilibrium constant
k_H	acid catalyzed exchange rates
k_{OH}	base catalyzed exchange rates
R	radius of the droplet
Hb	Hemoglobin
Mb	Myoglobin
K_d	dissociation constant
$\Delta_d G°$	dissociation free energies
$\Delta_{op} G°$	opening free energy
ITC	Isothermal titration calorimetry
Z	partition function
ClpP	Caseinolytic protease P
ADEP	Acyldepsipeptide
m/z	mass to charge ratio

Chapter 1. Introduction

1.1. Protein Structures

Proteins play important roles in virtually all biological processes. While performing their functions many proteins undergo conformational changes which are essential for enzyme catalysis, transport, or energy conversion.[1] Proteins adopt specific higher order structures via folding pathways that are still not fully understood.[2] Misfolding can lead to diseases such as Alzheimer's, Parkinson's and other disorders.[3] Even in the native state, proteins display considerable flexibility ranging from localized fluctuations to large conformational transitions. Ligand binding can trigger structural changes that lead to an increase or decrease in activity.[4-5] Ligands that cause such conformational switching include inhibitors, metal ions and hormones.[6] Deciphering protein conformational dynamics, folding pathways and ligand-induced structural changes remain a fundamental research goal.

1.2. Methods for Studying Protein Structure

Numerous methods are available for the study of protein structures. These techniques are useful for both biochemical and clinical applications. A brief discussion of the most common methods is given below.

1.3. "Traditional" Methods

1.3.1. X-ray crystallography

X-ray crystallography remains the gold standard for solving the 3D conformation proteins with atomic resolution. This method is amenable to the study of protein 3D structures because X-ray wavelengths are comparable to the ~1Å range typically encountered for chemical bonds. A basic X-ray diffractometer includes a radiation source, and a detector (Figure 1-1).

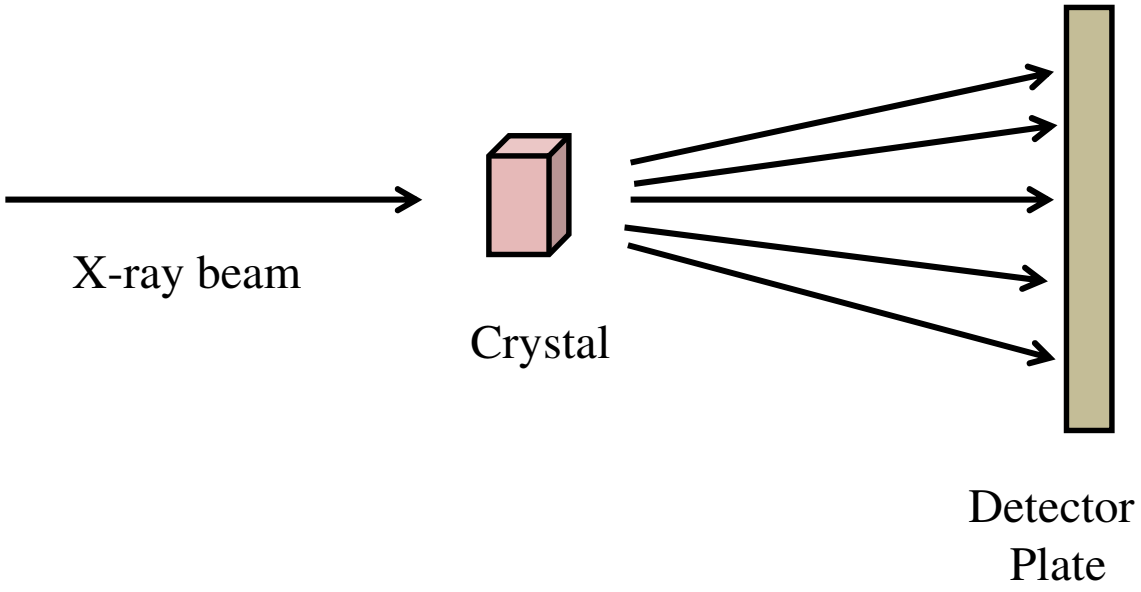

Figure 1-1: Schematic representation of an X-ray diffractometer

Protein X-ray crystallography was first implemented in the 1950s for solving the structure of hemoglobin and myoglobin.[7] The atomic coordinates derived from X-ray crystallography are usually accompanied by displacement parameters also known as B-factors. B-factor measures primarily the molecular disorder in the crystal and this is used as an indirect estimate of the dynamics of the protein. B-factor also measures other errors in addition to thermal motions in proteins crystal structures.[8] It is widely recognized that proteins are not static structures and they constantly sample different conformational states in solution.[9] The dynamic information on protein crystals are therefore limited because the proteins are modelled as single conformations.[10-11] Although X-ray crystallography is widely used, crystal growth remains a challenge as not all proteins are amenable to crystallization. Also, X-ray data provide static pictures, thereby glossing over the intrinsic dynamics of proteins.

1.3.2. Nuclear Magnetic Resonance (NMR) Spectroscopy

NMR spectroscopy represents another tool for studying proteins. NMR is a phenomenon during which nuclei absorb particular radio frequencies in a strong external magnetic field. Depending on the type of interaction with the electromagnetic radiation insight can be gleaned into the nuclear identity and environment. For a nucleus to be NMR-visible, it must have a non-zero spin. Examples include ^{1}H, ^{13}C, ^{15}N and ^{31}P. The incorporation of deuterium into the protein backbone eliminates some NMR proton signals because ^{2}H is not an NMR-active nucleus.[12-13] NMR spectroscopy is a powerful technique for probing the structure and dynamics of biopolymers at the atomic level. NMR relaxation

measurements of ^{13}C or ^{15}N nuclei allow the study of molecular motions on the picosecond to microsecond time scales. Heteronuclear NMR can also be used to determine protein structures in solution.[14] The technique, however, suffers size limitation problems.[15]

1.3.3. Optical Methods

Optical techniques are widely used for probing protein structural features. Examples include UV-Visible (UV-VIS) absorption spectroscopy, circular dichroism (CD) and fluorescence spectroscopy. These methods are quite popular because they are easy to use, sensitive, and proteins can be studied directly under physiological conditions with good sample recovery after analysis. They represent, however, low resolution tools.

CD spectroscopy is an absorption-based method that measures the difference of left and right circularly polarized light. A CD spectrum is observable for chiral molecules. This technique is often used to evaluate secondary structural elements in proteins. Different structures generate characteristic CD signals. For example, proteins with a high α-helical content will give CD spectra with a minimum at 222 nm. β-sheet structures have a minimum around 215 nm, while for random coil structures the minimum appears at ~202 nm.[16] Tertiary structure information can also be obtained when wavelengths between 250-350 nm are scanned.[17]

UV-Vis spectroscopy works well when the protein contains a chromophore such as a conjugated π system. It is most useful for measuring protein concentrations. Also, small changes protein structure can be reflected in alterations of the absorption maxima. A good example is the conversion of oxyhemoglobin to deoxyhemoglobin. The change in the ligation

state of the heme chromophore is reflected by a shift in the absorption maxima from 415 nm to 430 nm.[18] Absorbance (A) is defined as

$$A = \log \frac{Io}{I} \qquad (1.1)$$

where I_0 is the initial light intensity and I is the transmitted intensity.[19] The absorbance of a chromophore is related to its concentration according to Beer Lambert's law.

$$A = \varepsilon \, C \, d \qquad (1.2)$$

where d is the pathlength of the cuvette, C is concentration and ε is the molar absorption coefficient.

Fluorescence spectroscopy is another optical technique that is routinely used for protein structural analyses. An electronically excited chromophore can relax to the ground state via photon emission to generate fluorescence. Tryptophan is the most commonly used intrinsic fluorophore.[20] F□rster resonance energy transfer (FRET) is fluorescence technique that is particularly useful for probing molecular structure. In FRET, the energy transfer from an excited donor fluorophore to an acceptor depends on the distance between the two fluorophores. [21] FRET efficiency is defined as

$$E = \frac{R_O^6}{R_O^6 + R^6} \qquad (1.3)$$

Where R is the distance between donor and acceptor and R_o is the F□rster radius for E = 0.5.

The sensitivity of FRET to distance has made it useful for probing distances within 3-8 nm, for example in the context of protein folding.[22-23] FRET can also lead to fluorescence quenching, a phenomenon that has been applied to proteins containing heme, retinal or other non-fluorescent chromophores.[24-27]

1.4. Mass Spectrometry

Mass spectrometry (MS) has evolved as an indispensable tool in proteomics research. MS represents a weighing balance for ions in the gas phase. Two ionization techniques are used in proteomics research which allows the transfer of intact protein analytes into the gas phase under soft conditions. They are referred to as Matrix Assisted Laser Desorption/Ionization (MALDI-MS) and Electrospray Ionization (ESI).[28] These ionization techniques allow the investigation of compounds with sizes ranging from a few Daltons (Da) to mega Daltons (MDa).[29-30] MALDI was developed in 1985 by Karas and Hillenkamp.[31] For MALDI, the analytes are embedded in a solid matrix containing ultraviolet-absorbing molecules. With the help of a laser pulse, gaseous analyte ions are formed. [32-33] Because ESI

is exclusively used throughout this work, the ESI mechanism will be discussed in detail in the following section.

1.4.1. The ESI Source

ESI is a "soft" technique that is capable of transferring proteins and peptides from solution into the gas phase. ESI has several advantages over MALDI. ESI can be coupled to liquid chromatography (LC) which enables on-line separations. ESI generates multiply charged ions, as opposed to the singly charged ions produced by MALDI. This allows the detection of large analytes on mass spectrometers with limited m/z range.

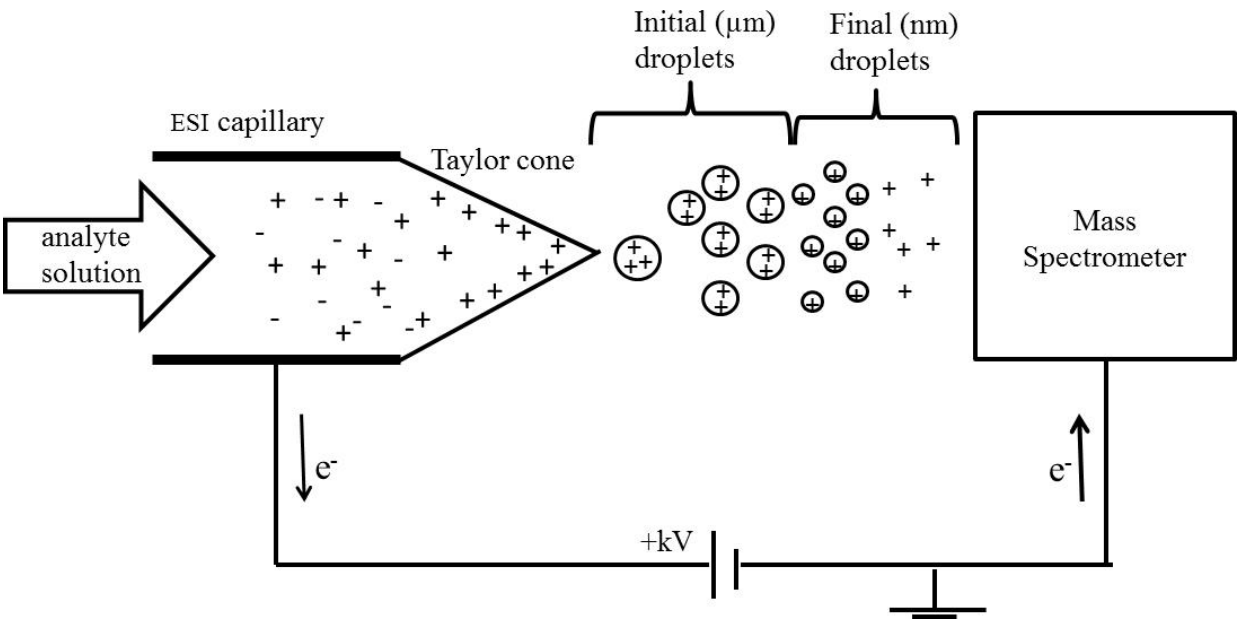

Figure 1-2: Schematic representation of an ESI source operated in positive mode

ESI occurs at atmospheric pressure. An analyte solution is infused into a metal capillary that is kept at a high voltage (~3kV in positive mode) relative to ground. This high voltage causes charge separation, where electrons are removed from solution (for example $2H_2O \rightarrow 4H^+ + 4e^- + O_2$). The solution at the tip of the capillary tip gets distorted into a Taylor cone which emits a mist of μm sized droplets (Figure 1-2).[34] The initial droplets undergo rapid solvent evaporation. The charge density on the shrinking droplets continues to increase until surface tension equals Coulombic repulsion, also known as the Rayleigh limit. At this point, the number z_R of elementary charges e is: [35]

$$z_R = \frac{8\pi}{e}\sqrt{\varepsilon_o \gamma R^3} \qquad (1.4)$$

where R is the droplet radius, ε_o is the vacuum permittivity, and γ is the surface tension.

Droplets close to z_R undergo jet fission. Several cycles of evaporation and jet fission ultimately produce gaseous analyte ions that can be detected by MS. [32-33, 36-37] To avoid the introduction of droplets and contaminants into the mass analyzer, a counter flow of gas is used for desolvation (usually N_2).[38] Nano-ESI is a variant of ESI that requires less sample volume than regular ESI. Nano-ESI droplets are believed to be at least 10 times smaller than those produced by regular ESI sources, leading to enhanced salt tolerance.[39] This makes nano-ESI ideal for the study of large protein complexes in electrolyte-containing solutions.

The ESI mechanism is widely debated, three scenarios have been put forward to explain how charged droplets form analytes ions. These are referred to as the charge residue model (CRM), ion evaporation model (IEM), and chain ejection model (CEM) (Figure 1-3).[37,40-41] The CEM and CRM apply to proteins. The CRM is thought to be operative for native (compact) proteins.[41] The droplet undergoes several evaporation/fission cycles until all the solvent is removed, leaving a dried out protein ion. Unfolded proteins likely follow the CEM where the polymer chain exits the droplet with concomitant exchange of mobile charge carriers (protons).[42]

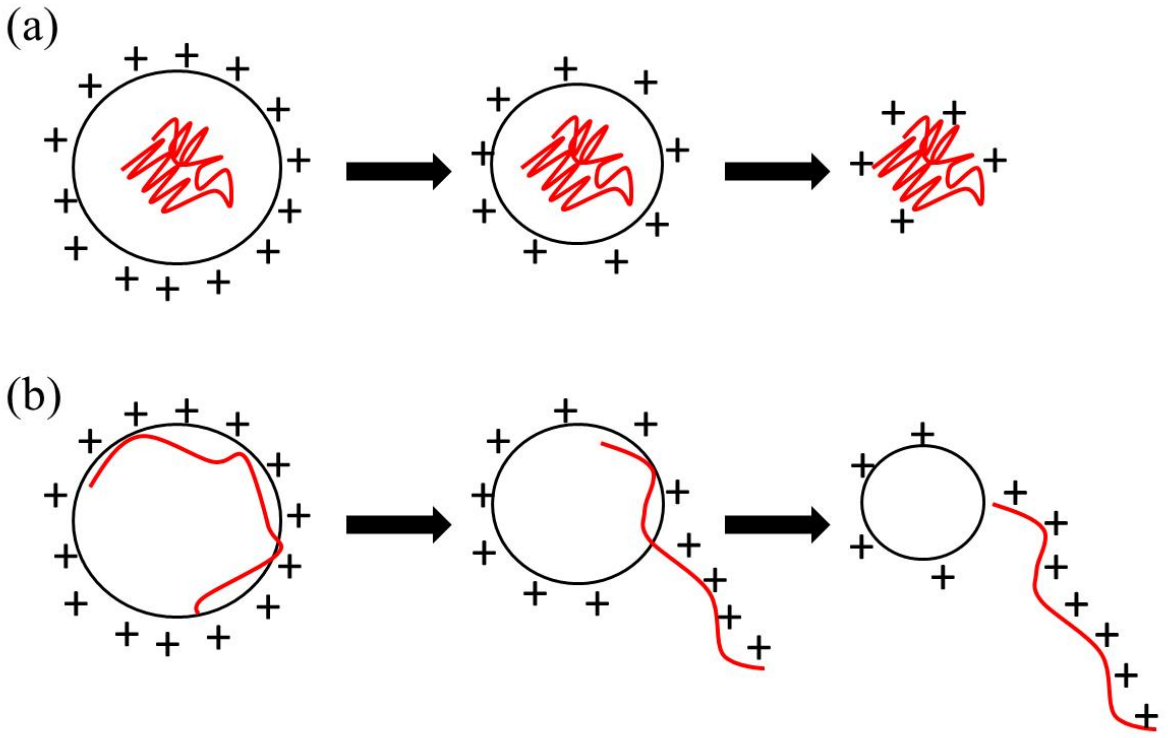

Figure 1-3: Summary of protein ESI mechanism for (a) CRM for the transfer of globular proteins into the gas phase, and (b) CEM used for unfolded proteins.

1.4.2. Mass Analyzers

The mass analyzer is used to separate charged analytes ions based on their m/z values. The charge state of a multiply protonated ion is given by

$$m/z = \frac{[M + zH]}{z} \qquad (1.5)$$

Ion separation can be achieved by using electric and/or magnetic fields.[43-44] Different mass analyzers, include quadrupoles, time of flight instruments, linear ion traps, [45] Orbitrap,[46-48] and Fourier transform ion cyclotron resonance devices.[49] Some of these mass analyzers can be coupled together for tandem MS applications. Only the quadrupole and the time of flight operation will be discussed in the next section, because they are directly relevant to the experiments of this work.

1.4.3. Quadrupole Mass Analyzer

The quadrupole is by far the most common mass analyzer. It consists of two pairs of cylindrical rods with opposite charges (Figure 1-4). With a radio frequency (RF) voltage applied to the quadrupole, all ions generated in the source can be transmitted to the detector. In this "RF-only" mode, the quadrupole acts as an ion guide (Figure 1-4b). The quadrupole can also be used as a mass filter when choosing a combination of direct current (DC) and RF

voltages. In this "mass-resolving" mode, only ions with a certain m/z value can pass through the quadrupole while all other ions collide with the rods because their trajectories are unstable (Figure 1-4c). Single quadrupoles have been used in early mass spectrometers. In modern instruments it is more common to use them in conjugation with other analyzers. In particular Q-TOF instruments use quadrupole for precursor selection in tandem MS.[50-54]

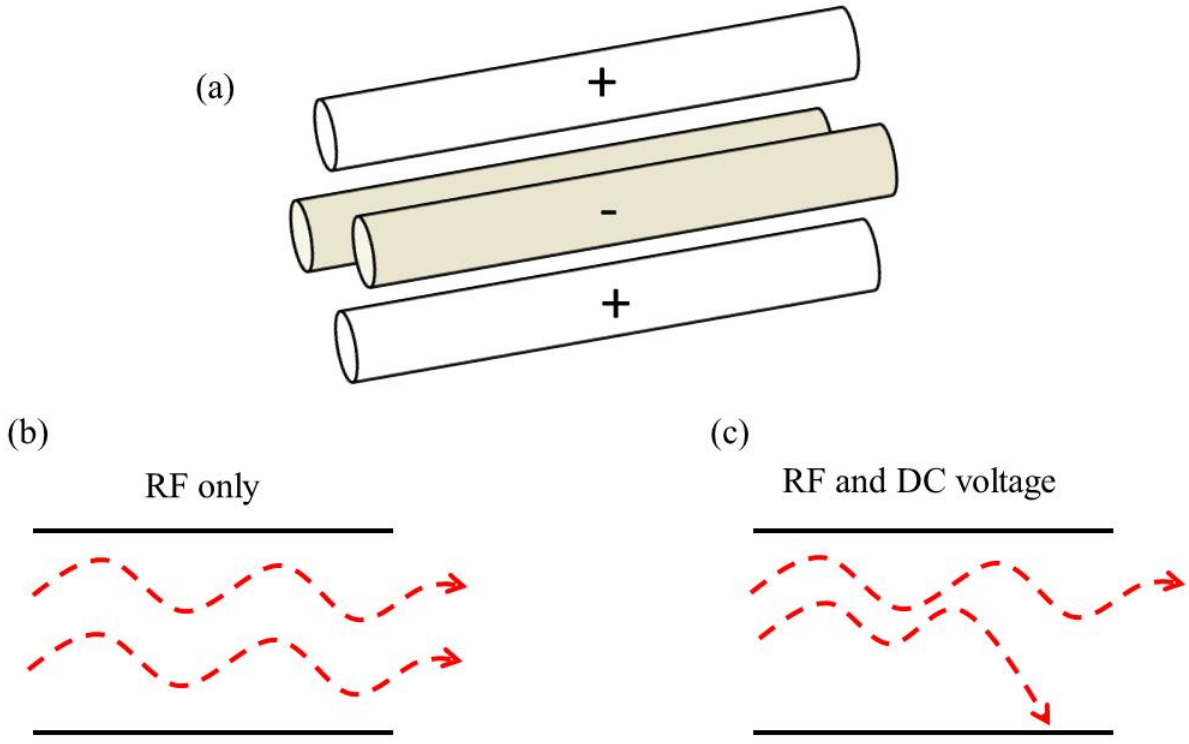

Figure 1-4: (a) Schematic representation of a quadrupole mass analyzer (b) RF only mode allows the passage of all analyte ions, and (c) quadrupole in mass filter mode

1.4.4. Time of Flight (TOF) Mass Analyzer

TOFs are able to separate ions of different m/z values without the need to scan across the mass range, a feature which is a huge advantage over quadrupole mass filters. In a TOF instrument, ions are accelerated into a flight tube by the application of a pusher pulse. Upon acceleration, the potential energy of the ion is converted into kinetic energy, and the time it takes for the ions to reach the detector can be calculated as follows

$$E_{pot} = E_{kin} \tag{1.6}$$

$$eUz = \frac{1}{2}mv^2 \tag{1.7}$$

From eq. 1.7, the time it takes to traverse the flight tube by an ion can be calculated as

$$t = d\sqrt{\frac{m}{e}\frac{1}{z2U}} \tag{1.8}$$

where *U*, *d, m, z* and □ represent the acceleration voltage, length of the flight tube, mass of the ion, charge state of the ion, and velocity of the ion, respectively. Equation 1.8 can be rewritten as:

$$t = k\sqrt{\frac{m}{z}} \tag{1.9}$$

Where $k = {}^{d}/_{\sqrt{2Ue}}$ is a parameter independent of the analyte

With conventional TOF instruments, slight deviations in the velocities of ions are not corrected for, two ions of the same m/z value with slightly different velocities will arrive at the detector at different times, leading to low mass resolution. The introduction of reflectron compensates for these velocity differences. Most modern instruments use an orthogonal acceleration geometry (oa-TOF) where the pusher pulse is applied in a perpendicular direction towards the incoming ion beam. (Figure 1-5).

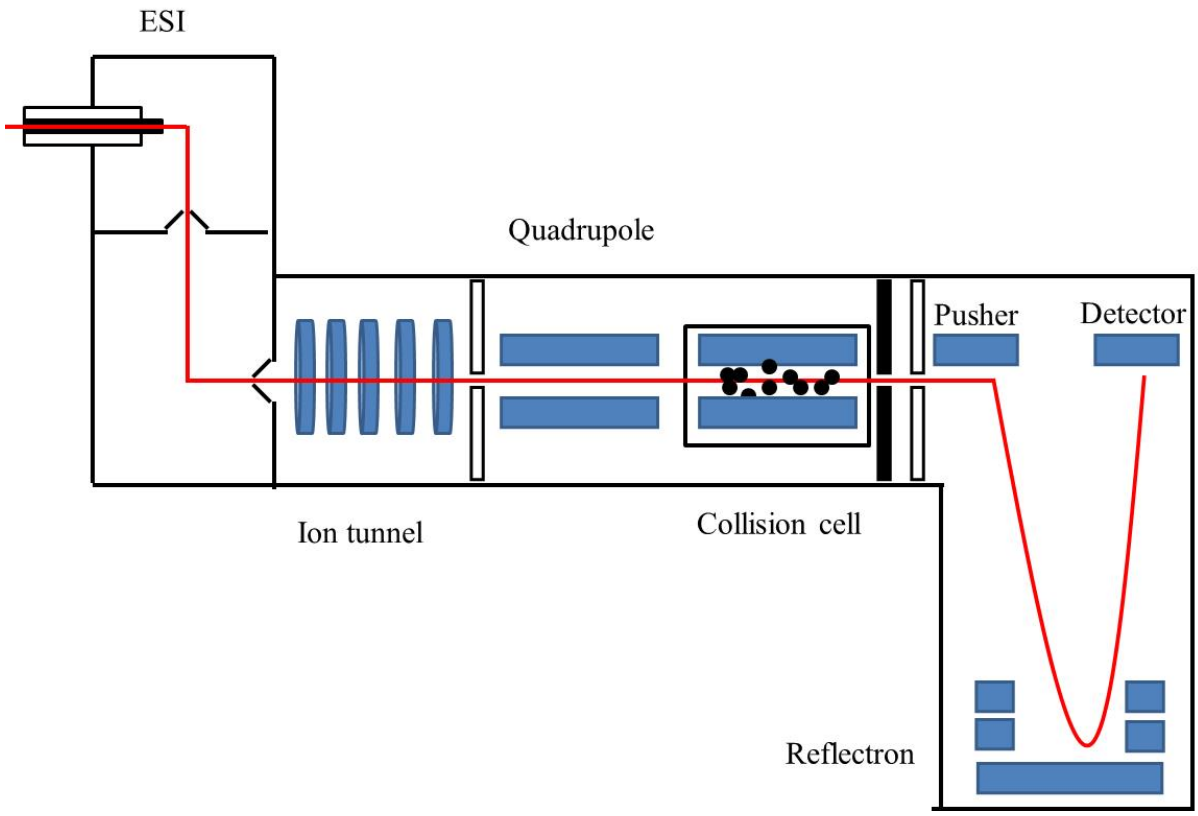

Figure 1-5: Schematic representation of an oaQ-TOF mass spectrometer equipped with a collision cell for collision-induced dissociation (CID). The red line indicates the ion trajectory.

The ion travelling with a higher velocity penetrates the reflectron further than one with a lower velocity. This ensures that the two ions arrive at the detector at the same time leading to sharper peaks and better resolution.[55]

1.5. Mass Spectrometry Based Methods for Characterizing Protein Structure and Dynamics.

1.5.1. Covalent Labeling

Covalent labeling is a common approach for examining protein conformations. This method can probe the solvent accessibility of side chains. Exposed sites react with the covalent probe very quickly, while buried regions are protected (Figure 1-6).[56]

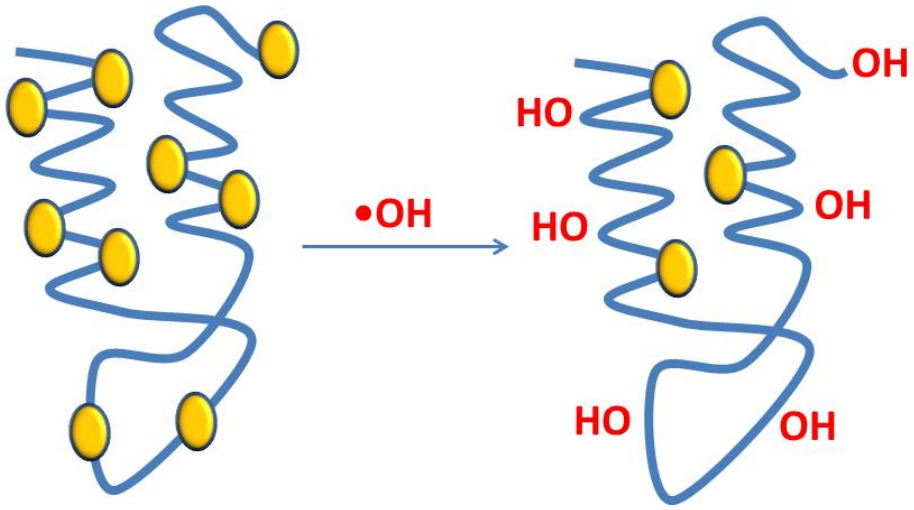

Figure 1-6: Schematic representation of a covalent labelling experiment. Solvent accessible reactive residues become modified (in this case via oxidation) while protected residues remain unlabeled

Hydroxyl radical ($^{\bullet}$OH) is a widely used covalent label because it is reactive and capable of labeling many types of residues. $^{\bullet}$OH labeling occurs very rapidly with an estimated time scale of ~1 µs under properly optimized conditions which is useful for monitoring short lived folding intermediates.[57] Quantitative analyses of oxidation patterns (or solvent accessibility) are usually conducted at the peptide level by subjecting the protein to enzymatic digestion prior to MS. Single residue resolution has also been reported using LC-

MS/MS methods.[58-60] Covalent labeling has been applied to the study of protein-protein interactions,[61-62] protein-DNA complexes,[63] integral membrane proteins binding studies[64] and some in vivo experiments.[65]

Although covalent labeling generates labels that are highly stable and relatively easy to detect, the analysis is complicated by the fact that differentially labeled peptides do not coelute during LC. Also, the introduction of covalent labels may alter the protein structure. This problem can be minimized by ensuring that the number of labels per protein is very low.[66-67]

1.5.2. Covalent Cross Linking

Covalent cross linking relies on the ability of two protein side chains, at an appropriate distance from each other, to undergo coupling upon exposure to a suitable cross-linking agent (Figure 1-7). A variety of cross-linkers have been made, most of consist of two reactive sites (commonly alkyl chain). Lysines represent the most widely targeted type of cross-linking site. Cysteine and other residues can be used as well.[68] The cross-linking agent can either be functionalized to probe Lys-Lys distances (homo-bifunctional linkers) or Lys-Cys distances (hetero-bifunctional linkers).

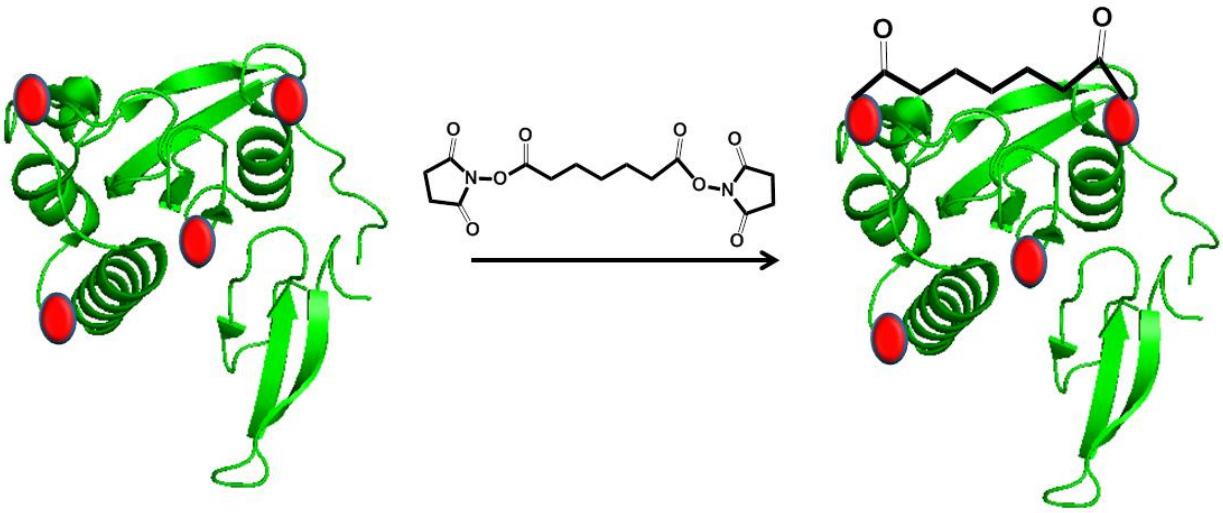

Figure 1-7: A schematic depiction of a crosslinking reaction, with Lysine residues shown in red.

Cross-linking agents can also have variable spacer lengths.[69] Similar to covalent labeling, an enzymatic cleavage step is almost always incorporated into the analysis. The analysis is complicated by the need to separate a small modified peptide fraction from a largely unmodified digest. This is even more challenging when protein interactions are being studied because the linker can react in a number of different ways.[70]

1.5.3. Hydrogen Deuterium Exchange Mass Spectrometry

Hydrogen deuterium exchange (HDX) is a powerful tool for probing the higher order structures and dynamics of protein.[71] HDX coupled with ESI-MS has evolved as a useful technique for studying the conformation, dynamics and interactions of proteins in solution.[72-73] HDX measurements can be used to locate binding sites, identify structural changes, and for distinguishing the populations of protein structures present during exchange.[74-75] Different

studies have used HDX to examine protein-protein and protein-ligand interactions.[76-80] HDX also allows the study of the conformation, dynamics and function of proteins larger than 40 kDa. [81-83]

In HDX, protein is exposed to a solvent containing D_2O or a fully deuterated protein is exposed to H_2O. The former is known as exchange-in and the latter is referred to as exchange-out, with both experiments giving identical information. Regions of the protein that are not involved in hydrogen bonding exhibit a burst phase exchange kinetic, whereas regions that are in the interior of the protein or involved in hydrogen bonds, exchange at much slower rates.[84] Depending on solvent accessibility and hydrogen bonding strength, different backbone amide (N-H) hydrogens undergo isotopic exchange at different rates.[85] Exchange can also occur at O-H, N-H and S-H sites on the side chains, but these deuteriums are lost during the LC step due to back-exchange. Thus, the side chains do not contribute to the measured mass shifts.[86] The overall backbone HDX exchange mechanism for native proteins under continuous labelling conditions can be described as

$$N-H_{(closed)} \underset{k_{cl}}{\overset{k_{op}}{\rightleftarrows}} N-H_{(opened)} \underset{D_2O}{\overset{k_{ch}}{\rightleftarrows}} N-D_{(opened)} \underset{k_{op}}{\overset{k_{cl}}{\rightleftarrows}} N-D_{(closed)} \qquad (1.10)$$

where k_{op}, k_{cl}, and k_{ch} are the opening, closing and chemical exchange rates constants respectively. Each amide hydrogens in a protein can exhibit a unique combination of k_{op}, k_{cl} and $k_{ch.}$ For exchange to occur in a protected region of the protein, the amide hydrogen of

interest has to be solvent accessible which means the hydrogen bonds have to be transiently broken.[87]

1.5.4. EX1 and EX2

Two limiting regimes are seen in HDX kinetics for a protein in the native state. They are

EX1 and EX2: EX1 is not common at physiological pH. In this scenario, the chemical exchange rate is faster than the closing rate ($k_{ch} >> k_{cl}$) (Figure 1-8). The regime can be promoted in the presence of denaturants and high temperatures. The resulting exchange rate constant is simply

$$k_{ex} = k_{op} \quad (1.11)$$

The EX1 regime is characterized by bimodal mass distribution (Figure 1-8)

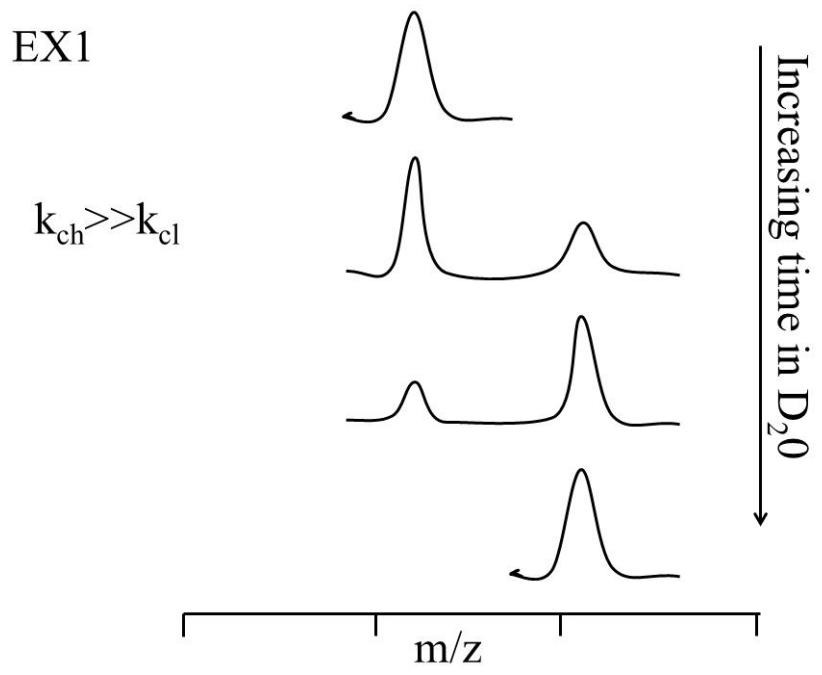

Figure 1-8: Deuterium uptake in the EX1 regime

The EX2 exchange regime is usually observed for native proteins at physiological pH where most labeling experiments take place with $k_{cl}>>k_{ch}$. The exchange rate constant is given by

$$k_{\mathrm{HDX}} = \frac{k_{\mathrm{op}}}{k_{\mathrm{cl}}} k_{\mathrm{ch}} = K_{\mathrm{op}} k_{\mathrm{ch}} \qquad (1.12)$$

where K_{op} is the equilibrium constant for the opening and closing events. This exchange regime is manifested via peak envelopes that shift to higher m/z values as the exposure time increases (Figure 1-9).

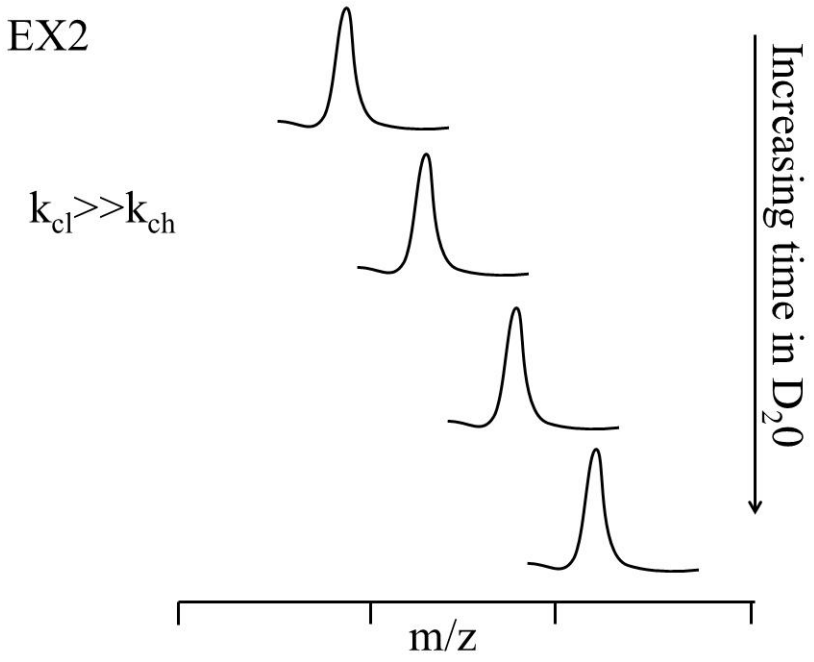

Figure 1-9: Deuterium uptake in the EX2 regime

Finally, for an unfolded protein, the exchange kinetics is only dependent on the chemical exchange rate constant i.e.

$$k_{\mathrm{HDX}} = k_{\mathrm{ch}} \tag{1.13}$$

1.5.5. Effects of Temperature, pH and Composition on Exchange Rate

The exchange rate of N-H hydrogens is dictated by the pH, temperature, solvent accessibility and hydrogen bonding. As noted, hydrogens in side chain as well as those in the

backbone can be exchanged with deuterium. Deuterium in the backbone is retained during HDX analysis, while side chains back to hydrogen during analysis.[88] N-H groups are catalyzed by acid and base. The rate constant for chemical exchange can be expressed as:

$$k_{ch} = k_H [H^+] + k_{OH} [OH^-] \quad (1.14)$$

where k_H and k_{OH} are rates of acid and base catalyzed exchange respectively. The exchange rate has a minimum at pH 2.5 - 3. The exchange kinetics are also dependent on temperature as dictated by the Arrhenius equation as shown below.

$$ln\, k_{ch} = lnA - {E_a}/{(RT)} \quad (1.15)$$

1.5.6. General Workflow of HDX-MS Experiments

The general procedure used in HDX-MS is illustrated in Figure 1-10. The experiment can be conducted at the intact protein level, or in a spatially-resolved manner with protease digestion.

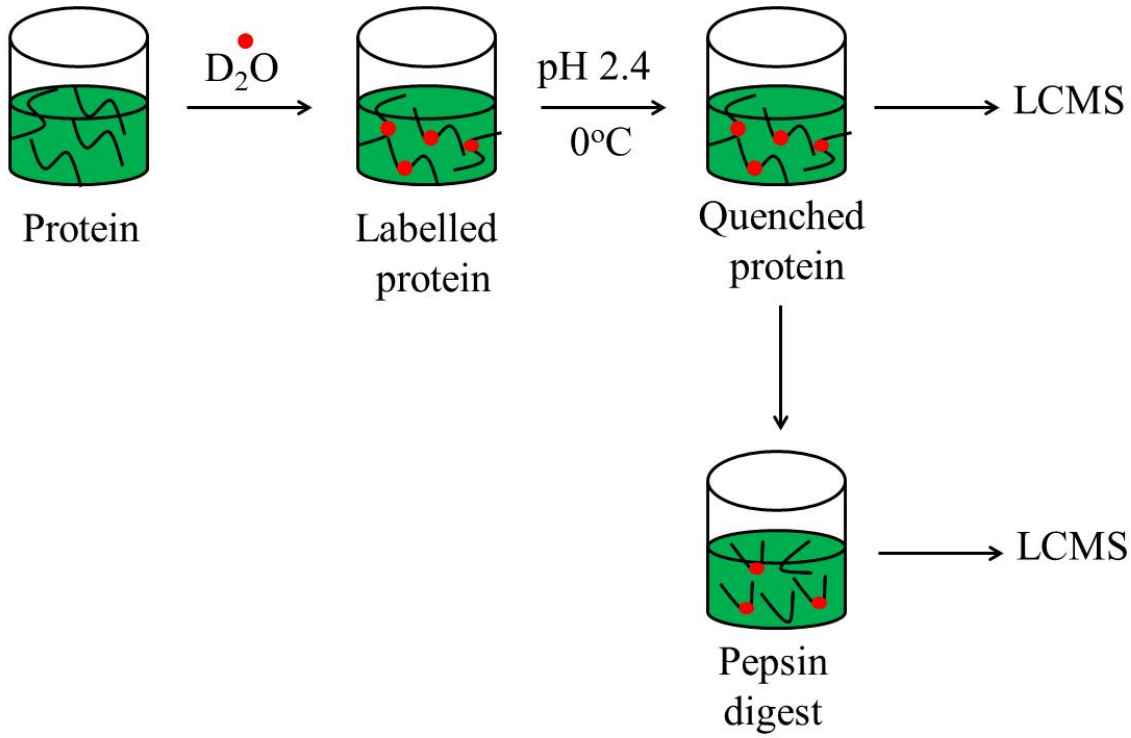

Figure 1-10: General protocol for an exchange-in HDX-MS experiment

Isotopic exchange is initiated with the folded protein incubated in D_2O buffered to the desired pH. Aliquots are removed at selected labelling times ranging from a few seconds to several days. After the deuterium exchange-in step, HDX is quenched by decreasing the pH to 2.4 and the temperature to 0^oC. The intact protein can then be analyzed for global exchange kinetics. The LCMS analysis is usually carried out within a short time to prevent back exchange.

To obtain HDX kinetics information on small regions of the protein, the protein is subjected to proteolysis using an immobilized pepsin column or other acid-active protease under quench conditions. The use of high pressure during proteolysis can enhance digestion efficiency.[89-90] The resulting peptides are retained on a trapping column before being

transferred to an analytical column for reverse phase LC to determine the level of deuterium incorporated in the different segments.[88,91] A schematic representation of a state-of-the-art digestion/desalting and separation fluidic unit for HDX-MS is shown in Figure 1-11.

To avoid carryover in the experiments, washing steps between injections are usually incorporated into the protocol.[92-93] For peptide analysis, MS/MS experiments have to be carried out first to identify peptides before the actual deuteration experiments. This is because pepsin is a nonspecific protease which complicates the identification of peptides after deuteration. The introduction of software packages have helped in minimizing the problem of peptide analysis in HDX workflows.[94-99] Nepenthesin is another acidic protease that has been used in HDX protocols.[100]

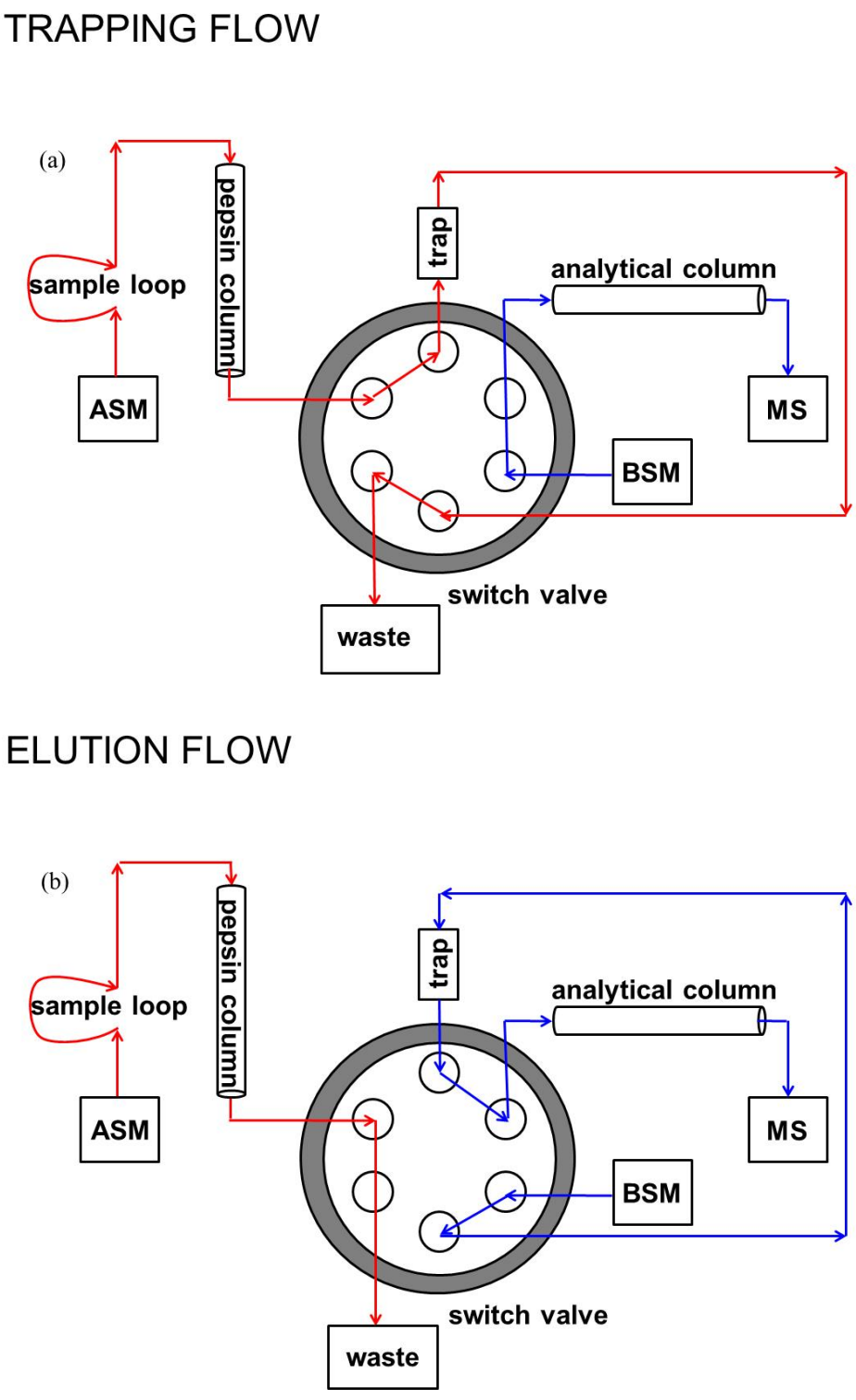

Figure 1-2: Layout of a typical fluidics unit for "bottom-up" proteolytic digestion HDX/MS experiments. (A) Isocratic flow (red) delivered by an auxiliary solvent module (ASM) moves the protein from the sample loop to a pepsin column for digestion. The resulting peptides are retained on a short trapping column. (B) Switching of the six-port valve allows the

proteolysis products to be washed off the trapping column via flow from a binary solvent module (BSM) which delivers a water/acetonitrile gradient (blue). The peptides are separated on a reversed-phase analytical column that is coupled to the ESI source of a mass spectrometer (MS). Reprinted with permission from Konermann et. al (2014) ACS.[97]

Back exchange still remains a major problem in HDX-MS experimental protocols. Back exchange washes out the deuterium pattern incorporated into the protein during the labelling process.[101] This can be mitigated by conducting the digestion and LC workflow in a short period of time at 0^{o}C. Recent studies have also shown that the use of freezing point depressants can significantly reduce the amount of back exchange.[102,91]

1.6. Scope of Thesis

Proteins are not static structures but dynamic systems that undergo fluctuations in which hydrogen bonds are constantly opened and reclosed. The degree of fluctuation can be modulated by external stimuli stabilize or destabilize the proteins. Protein-ligand interactions in HDX experiments usually induce a reduction in the measured HDX rates, and this is usually ascribed to stabilization of the protein structure.[103-104,77]

The objective of this research is to improve the understanding of changes in HDX patterns that are associated with protein-ligand binding. Ultimately, these efforts should provide insights into protein conformational dynamics, structures, and ultimately function.

Oxy-Hb and aquomet-Hb represent widely used MS test analytes and previous MS studies have paid little attention to the differences between them by assuming that they both

share the same solution phase properties. In Chapter 2, the structural dynamics in oxy-Hb and aquomet-Hb were compared using HDX-MS. The results indicate a global stabilization in Oxy-Hb with some destabilization in the heme binding pocket which is a possible explanation for heme release in aquomet-hemoglobin.

HDX experiments are usually carried out with the expectation that ligand binding will induce a reduction in the deuteration rates of the protein. In Chapter 3, the effect of ligands binding to hemoglobin and myoglobin was studied using HDX-MS. This chapter explores the different scenarios that can be encountered in an HDX experiment upon ligand binding. The experiments in this chapter suggest that proteins can be globally stabilized or destabilized after ligand binding. The results further show that it is possible to have both scenarios in a single protein after ligand binding while some regions of the protein experience no appreciable change at all.

ClpP is a protease complex responsible for the degradation of substrate proteins in bacteria. The mechanism of pore opening in ClpP has been a topic of debate in literature with different views. In Chapter 4, HDX-MS was used to study the interaction between Caseinolytic Protease (ClpP) an antibacterial drug target and its ligand ADEP. The findings from this chapter demonstrate that binding of a ligand can trigger conformational changes both at the binding site and at allosteric sites far from it with hydrophobic interactions playing a major role at the opening of the ClpP axial pore.

Peptidyl-prolyl isomerases (PPIase) catalyze the cis-trans conversion of X-pro bonds. Pin 1 is a PPIase involved in cell cycle regulation making it a promising anticancer target. In Chapter 5, the binding of a cyclic peptide to Pin1 isomerase was monitored using HDX-MS.

The experiments in this chapter were able to identify a loop region of residues which may have been responsible for the inability of researchers to crystalize Pin 1 with its ligands. The results also indicate that protein ligand interactions can result in both stabilization and destabilization of the protein structure.

1.7. References

1. Marcsisin, S. R.; Engen, J. R., Hydrogen exchange mass spectrometry: what is it and what can it tell us? *Anal. Bioanal. Chem.* **2010,** *397*, 967-972.

2. Dill, K. A.; Ozkan, S. B.; Shell, M. S.; Weikl, T. R., The Protein Folding Problem. *Annu. Rev. Biophys. Biomol. Struct.* **2008,** *37*, 289-316.

3. Prusiner, S. B., A Unifying Role for Prions in Neurodegenerative Diseases. *Science* **2012,** *336*, 1511-1513.

4. Kiefhaber, T.; Bachmann, A.; Jensen, K. S., Dynamics and mechanisms of coupled protein folding and binding reactions. *Curr. Op. Struct. Biol.* **2012,** *22*, 21-29.

5. Boehr, D. D.; Nussinov, R.; Wright, P. E., The role of dynamic conformational ensembles in biomolecular recognition. *Nat. Chem. Biol.* **2009,** *5*, 789-796.

6. Robinson, C. V.; Sali, A.; Baumeister, W., The molecular sociology of the cell. *Nature* **2007,** *450*, 973-982.

7. Kendrew, J. C.; Bodo, G.; Dintzis, H. M.; Parrish, R. G.; Wyckoff, H.; Phillips, D. C., A Three-Dimensional Model of the Myoglobin Molecule Obtained by X-Ray Analysis. *Nature* **1958,** *181* (4610), 662-666.

8. Frauenfelder, H.; Petsko, G. A.; Tsernoglou, D., Temperature-dependent X-ray diffraction as a probe of protein structural dynamics. *Nature* **1979,** *280*, 558-563.

9. Frauenfelder, H.; Sligar, S. G.; Wolynes, P. G., The Energy Landscape and Motions of Proteins. *Science* **1991,** *254*, 1598-1603.

10. Frauenfelder, H.; Chen, G.; Berendzen, J.; Fenimore, P. W.; Jansson, H.; McMahon, B. H.; Stroe, I. R.; Swenson, J.; Young, R. D., A unified model of protein dynamics. *Proc. Natl. Acad. Sci. U.S.A.* **2009,** *106*, 5129-5134.

11. DePristo, M. A.; de Bakker, P. I.; Blundell, T. L., Heterogeneity and inaccuracy in protein structures solved by X-ray crystallography. *Structure* **2004,** *12*, 831-838.

12. Woodward, C., Is the slow-exchange core the protein folding core? *Trends Biochem. Sci.* **1993,** *18*, 359-360.

13. Li, R.; Woodward, C., The hydrogen exchange core and protein folding. *Protein Science* **1999,** *8* (8), 1571-1590.

14. Wuthrich, K., NMR Studies of Structure and Function of Biological Macromolecules (Nobel Lecture). *Angew. Chem. Int. Ed.* **2003,** *42* 3340 –3363.

15. Wand, A. J., Dynamic activation of protein function: A view emerging from NMR spectroscopy. *Nat. Struct. Biol.* **2001,** *8*, 926-931.

16. Brahms, S.; Brahms, J., Determination of Protein Secondary Structure in Solution by Vacuum Ultraviolet Circular Dichroism. *J. Mol. Biol.* **1980,** *138*, 149-178.

17. Kelly, S. W.; Jess, T. J.; Price, N. C., How to Study Protein by Circular Dichroism. *Biochim. Biophys. Acta* **2005,** *1751*, 119-139.

18. Antonini, E.; Brunori, M., *Hemoglobin and Myoglobin in Their Reactions With Ligands*. North-Holland Publishing Company: Amsterdam, London, **1971**; Vol. 21.

19. Skoog, D. A., *Principles of Instrumental Analysis*. Brooks/Cole Thomson Learning: Toronto, **1998**.

20. Pan, Y.; Brown, L.; Konermann, L., Mapping the Structure of an Integral Membrane Protein under Semi-Denaturing Conditions by Laser-Induced Oxidative Labeling and Mass Spectrometry. *J. Mol. Biol.* **2009,** *394*, 968-981.

21. Förster, T., *Ann. Phys.* **1948,** *2*, 55-75.

22. Munoz, V., Conformational Dynamics and Ensembles in Protein Folding. *Annu. Rev. Biophys. Biomol. Struct.* **2007,** *36*, 395-412.

23. Schuler, B.; Lipman, E. A.; Eaton, W. A., Probing the free-energy surface for protein folding with single-molecule fluorescence spectroscopy. *Nature* **2002,** *419*, 743-747.

24. Elöve, G. A.; Bhuyan, A. K.; Roder, H., Kinetic Mechanism of Cytochrome c Folding: Involvement of the Heme and Its Ligands. *Biochemistry* **1994,** *33*, 6925-6935.

25. Lee, S. P.; Engman, K. C.; Tezcan, F. A.; Gray, H. B.; Winkler, J. R., Structural features of cytochrome c' folding intermediates revealed by fluorescence energy-transfer kinetics. *Proc. Natl. Acad. Sci. U.S.A.* **2002,** *99*, 14778-14782.

26. Kawamura-Konishi, Y.; Kihara, H.; Suzuki, H., Reconstitution of myoglobin from apoprotein and heme, monitored by stopped-flow absorption, fluorescence and circular dichroism. *Eur. J. Biochem.* **1988,** *170*, 589-595.

27. Shen, L. L.; Hermans, J., Kinetics of Conformation Change of Sperm-Whale Myoglobin. I. Folding and Unfolding of Metmyoglobin following pH jump. *Biochemistry* **1972,** *11*, 1836-1841.

28. Kaltashov, I. A.; Eyles, S. J., *Mass Spectrometry in Structural Biology and Biophysics: Architecture, Dynamics, and Interactions of Biomolecules*. 2nd ed.; Wiley: Hoboken, NJ, **2012**.

29. Heck, A. J. R.; Van den Heuvel, R. H. H., Investigation of intact protein complexes by mass spectrometry. *Mass Spectrom. Rev.* **2004,** *23*, 368-389.

30. Berkenkamp, S.; Kirpekar, F.; Hillenkamp, F., Infrared MALDI Mass Spectrometry of Large Nucleic Acids. *Science* **1998,** *281*, 260-262.

31. Karas, M.; Bachmann, D.; Hillenkamp, F., Influence of the wavelength in high-irradiance ultraviolet laser desorption mass spectrometry of organic molecules. *Anal. Chem.* **1985,** *57*, 2935-2939.

32. Fenn, J. B., Electrospray Wings for Molecular Elephants (Nobel Lecture). *Angew. Chem. Int. Ed.* **2003,** *42*, 3871-3894.

33. Kebarle, P.; Verkerk, U. H., Electrospray: From Ions in Solutions to Ions in the Gas Phase, What We Know Now. *Mass Spectrom. Rev.* **2009,** *28*, 898-917.

34. Wu, X.; Oleschuk, R. D.; Cann, N. M., Characterization of microstructured fibre emitters: in pursuit of improved nano electrospray ionization performance. *Analyst* **2012,** *137*, 4150-4161.

35. Rayleigh, L., On the Equilibrium of Liquid Conducting Masses charged with Electricity. *Phil. Mag.* **1882,** *14*, 184-186.

36. Cech, N. B.; Enke, C. G., Practical Implication of Some Recent Studies in Electrospray Ionization Fundamentals. *Mass Spectrom. Rev.* **2001,** *20*, 362-387.

37. Nguyen, S.; Fenn, J. B., Gas-phase ions of solute species from charged droplets of solutions. *Proc. Natl. Acad. Sci. U.S.A.* **2007,** *104*, 1111-1117.

38. Covey, T. R.; Thomson, B. A.; Schneider, B. B., Atmospheric Pressure Ion Sources. *Mass Spectrom. Rev.* **2009,** *28*, 870-897.

39. Juraschek, R.; Dulcks, T.; Karas, M., Nanoelectrospray - More than just a Minimized-Flow Electrospray Ionization Source. *J. Am. Soc. Mass Spectrom.* **1999,** *10*, 300-308.

40. Hogan, C. J.; Carroll, J. A.; Rohrs, H. W.; Biswas, P.; Gross, M. L., Combined Charged Residue-Field Emission Model of Macromolecular Electrospray Ionization. *Anal. Chem.* **2009,** *81*, 369-377.

41. Konermann, L.; Ahadi, E.; Rodriguez, A. D.; Vahidi, S., Unraveling the Mechanism of Electrospray Ionization. *Anal. Chem.* **2013,** *85*, 2-9.

42. Sciuto, S. V.; Liu, J.; Konermann, L., An Electrostatic Charge Partitioning Model for the Dissociation of Protein Complexes in the Gas Phase. *J. Am. Soc. Mass Spectrom.* **2011,** *22*, 1679-1689.

43. Watson, J. T., *Introduction to Mass Spectrometry*. third ed.; Lippincott - Raven: Philadelphia, New York, **1997**.

44. Roboz, J., *Mass Spectrometry: Instrumentation and Techniques*. Wiley: New York, **1968**.

45. Douglas, D. J.; Frank, A. J.; Mao, D., Linear Ion Traps in Mass Spectrometry. *Mass Spectrom. Rev.* **2005,** *24*, 1-29.

46. Makarov, A., Electrostatic Axially Harmonic Orbital Trapping: A High-Performance Technique of Mass Analysis. *Anal. Chem.* **2000,** *72*, 1156-1162.

47. Scigelova, M.; Makarov, A., Orbitrap Mass Analyzer - Overview and Applications in Proteomics. *Proteomics* **2006,** *6 Suppl. 2*, 16-21.

48. Zubarev, A. R.; Makarov, A., Orbitrap Mass Spectrometry. *Anal. Chem.* **2013,** *85*, 5288-5296.

49. Marshall, A. G.; Hendrickson, C. L.; Jackson, G. S., Fourier Transform Ion Cyclotron Resonance Mass Spectrometry: A Primer. *Mass Spectrom. Rev.* **1998,** *17*, 1-35.

50. Iribarne, J. V.; Dziedzic, P. J.; Thomson, B. A., Atmospheric pressure ion evaporation - mass spectrometry. *Int. J. Mass. Spectrom.* **1983,** *50*, 331-347.

51. Yamashita, M.; Fenn, J. B., Electrospray Ion Source. Another variation on the Free-Jet Theme. *J. Phys. Chem.* **1984,** *88*, 4451-4459.

52. Fenn, J. B.; Mann, M.; Meng, C. K.; Wong, S. F.; Whitehouse, C. M., Electrospray ionization-principles and practice. *Mass Spectrom Rev.* **1990,** *9*, 37-70.

53. Smith, R. D.; Loo, J. A.; Baringa, C. J.; Edmonds, C. G.; Udseth, H. R., Collisional Activation and Collision-Activated Dissociation of Large Multiply Charged Polypeptides and Proteins Produced by Electrospray Ionization. *J. Am. Soc. Mass Spectrom.* **1990,** *1*, 53-65.

54. Mirza, U. A.; Cohen, S. L.; Chait, B. T., Heat-Induced Conformational Changes in Proteins Studied by Electrospray Ionisation Mass Spectrometry. *Anal. Chem.* **1993,** *65*, 1-6.

55. Verentchikov, A. N.; Ens, W.; Standing, K. G., REFLECTING TIME-OF-FLIGHT MASS-SPECTROMETER WITH AN ELECTROSPRAY ION-SOURCE AND ORTHOGONAL EXTRACTION. *Anal. Chem.* **1994,** *66* (1), 126-133.

56. Mendoza, V. L.; Vachet, R. W., Probing Protein Structure by Amino Acid-specific Covalent Labeling and Mass Spectrometry. *Mass Spectrom. Rev.* **2009,** *28*, 785-815.

57. Gau, B. C.; Sharp, J. S.; Rempel, D. L.; Gross, M. L., Fast Photochemical Oxidation of Protein Footprints Faster than Protein Unfolding. *Anal. Chem.* **2009,** *81*, 6563–6571.

58. Gau, B. C.; Chen, J. W.; Gross, M. L., Fast photochemical oxidation of proteins for comparing solvent-accessibility accompanying protein folding: Data processing and application to barstar. *BBA-Proteins Proteomics* **2013,** *1834* (6), 1230-1238.

59. Li, X.; Li, Z.; Xie, B.; Sharp, J. S., Improved Identification and Relative Quantification of Sites of Peptide and Protein Oxidation for Hydroxyl Radical Footprinting. *J. Am. Soc. Mass Spectrom.* **2013,** *24* (11), 1767-1776.

60. Jumper, C. C.; Bomgarden, R.; Rogers, J.; Etienne, C.; Schriemer, D. C., High-Resolution Mapping of Carbene-Based Protein Footprints. *Anal. Chem.* **2012,** *84*, 4411-4418.

61. Zhang, H.; Gau, B. C.; Jones, L. M.; Vidavsky, I.; Gross, M. L., Fast Photochemical Oxidation of Proteins for Comparing Structures of Protein-Ligand Complexes: The Calmodulin-Peptide Model System. *Anal. Chem.* **2011,** *83*, 311-318.

62. Jones, L. M.; Sperry, J. B.; Carroll, J. A.; Gross, M. L., Fast Photochemical Oxidation of Proteins for Epitope Mapping. *Anal. Chem.* **2011,** *83*, 7657-7661.

63. Schorzman, A. N.; Perera, L.; Cutalo-Patterson, J. M.; Pedersen, L. C.; Pedersen, L. G.; Kunkel, T. A.; Tomer, K. B., Modeling of the DNA-binding site of yeast Pms1 by mass spectrometry. *DNA Repair* **2011,** *10*, 454-465.

64. Orban, T.; Jastrzebska, B.; Gupta, S.; Wang, B.; Miyagi, M.; Chance, M. R.; Palczewski, K., Conformational dynamics of activation for the pentameric complex of dimeric g protein-coupled receptor and heterotrimeric G protein. *Structure* **2012,** *20*, 826-840.

65. Clatterbuck Soper, S. F.; Dator, R. P.; Limbach, P. A.; Woodson, S. A., In Vivo X-Ray Footprinting of Pre-30S Ribosomes Reveals Chaperone-Dependent Remodeling of Late Assembly Intermediates. *Mol. Cell* **2013,** *52*, 506-516.

66. Xu, Y.; Falk, I. N.; Hallen, M. A.; Fitzgerald, M. C., Mass Spectrometry- and Lysine Amidination-Based Protocol for Thermodynamic Analysis of Protein Folding and Ligand Binding Interactions. *Anal. Chem.* **2011,** *83*, 3555-3562.

67. Zhou, Y. P.; Vachet, R. W., Covalent Labeling with Isotopically Encoded Reagents for Faster Structural Analysis of Proteins by Mass Spectrometry. *Analytical Chemistry* **2013,** *85* (20), 9664-9670.

68. Klockenbusch, C.; O'Hara, J. E.; Kast, J., Advancing formaldehyde cross-linking towards quantitative proteomic applications. *Anal. Bioanal. Chem.* **2012,** *404* (4), 1057-1067.

69. Fischer, L.; Chen, Z. A.; Rappsilber, J., Quantitative cross-linking/mass spectrometry using isotope-labelled cross-linkers. *J. Proteomics* **2013,** *88*, 120-128.

70. Leitner, A.; Walzthoeni, T.; Kahraman, A.; Herzog, F.; Rinner, O.; Beck, M.; Aebersold, R., Probing Native Protein Structures by Chemical Cross-linking, Mass Spectrometry, and Bioinformatics. *Mol. Cell. Proteomics* **2010,** *9* (8), 1634-1649.

71. Woodward, C.; Simon, I.; Tüchsen, E., Hydrogen exchange and the dynamic structure of proteins. *Mol. Cell. Biochem.* **1982,** *48*, 135-160.

72. Chalmers, M. J.; Busby, S. A.; Pascal, B. D.; Southern, M. R.; Griffin, P. R., A Two-Stage Differential Hydrogen Deuterium Exchange Method for the Rapid Characterization of Protein/Ligand Interactions. *J. Biomol. Techniques* **2007,** *18*, 194-204.

73. Rand, K. D.; Adams, C. M.; Zubarev, R. A.; Jørgensen, T. J. D., Electron Capture Dissociation Proceeds with a Low Degree of Intramolecular Migration of Peptide Amide Hydrogens. *J. Am. Chem. Soc.* **2008,** *130*, 1341-1349.

74. Miranker, A.; Robinson, C. V.; Radford, S. E.; Aplin, R.; Dobson, C. M., Detection of Transient Protein Folding Populations by Mass Spectrometry. *Science* **1993,** *262*, 896-900.

75. Liu, Y.; Belcheva, A.; Konermann, L.; Golemi-Kotra, D., Phosphorylation-Induced Activation of the Response Regulator VraR from Staphylococcus aureus: Insights from Hydrogen Exchange Mass Spectrometry. *J. Mol. Biol.* **2009,** *391*, 149-163.

76. Sperry, J. B.; Shi, X.; Rempel, D. L.; Nishimura, Y.; Akashi, S.; Gross, M. L., A Mass Spectrometric Approach to the Study of DNA-Binding Proteins: Interaction of Human TRF2 with Telomeric DNA. *Biochemistry* **2008,** *47*, 1797-1807.

77. Zhu, M. M.; Rempel, D. L.; Du, Z. H.; Gross, M. L., Quantification of protein-ligand interactions by mass spectrometry, titration, and H/D exchange: PLIMSTEX. *J. Am. Chem. Soc.* **2003,** *125* (18), 5252-5253.

78. Hopper, E. D.; Pittman, A. M. C.; Tucker, C. L.; Campa, M. J.; Patz, E. F.; Fitzgerald, M. C., Hydrogen/Deuterium Exchange- and Protease Digestion-Based Screening Assay for Protein-Ligand Binding Detection. *Anal. Chem.* **2009,** *81*, 6860-6867.

79. Hopper, E. D.; Roulhac, P. L.; Campa, M. J.; Patz, E. F.; Fitzgerald, M. C., Throughput and Efficiency of a Mass Spectrometry-Based Screening Assay for Protein–Ligand Binding Detection. *J. Am. Soc. Mass Spectrom.* **2008,** *19*, 1303-1311.

80. Rodriguez, A. D.; Dunn, S. D.; Konermann, L., ATP-Induced Dimerization of the FOF1 Epsilon Subunit from Bacillus PS3: A Hydrogen Exchange/Mass Spectrometry Study. *Biochemistry* **2014,** *53*, 4072-4080.

81. Uzawa, T.; Nishimura, C.; Akiyama, S.; Ishimori, K.; Takahashi, S.; Dyson, H. J.; Wright, P. E., Hierarchical folding mechanism of apomyoglobin revealed by ultra-fast H/D exchange coupled with 2D NMR. *Proc. Natl. Acad. Sci. U.S.A.* **2008,** *105*, 13859-13864.

82. Krishna, M. M. G.; Lin, Y.; Englander, S. W., Protein Misfolding: Optional Barriers, Misfolded Intermediates, and Pathway Heterogeneity. *J. Mol. Biol.* **2004,** *343*, 1095-1109.

83. Hughson, F. M.; Wright, P. E.; Baldwin, R. L., Structural Characterisation of a Partly Folded Apomyoglobin Intermediate. *Science* **1990,** *249*, 1544-1548.

84. Woodward, C., Advances in Protein Hydrogen Exchange by Mass Spectrometry. *J. Am. Soc. Mass Spectrom.* **1999,** *10*, 672-674.

85. Mitra, G.; Muralidharan, M.; Pinto, J.; Srinivasan, K.; Mandal, A. K., Structural Perturbation of Human Hemoglobin on Glutathionylation Probed by Hydrogen-Deuterium Exchange and MALDI Mass Spectrometry. *Bioconjugate Chem.* **2011,** *22*, 785-793.

86. Rand, K. D.; Lund, F. W.; Amon, S.; Jorgensen, T. J. D., Investigation of amide hydrogen back-exchange in Asp and His repeats measured by hydrogen (1H/2H) exchange mass spectrometry. *Int. J. Mass Spectrom.* **2011,** *302*, 110-115.

87. Skinner, J. J.; Lim, W. K.; Bédard, S.; Black, B. E.; Englander, S. W., Protein dynamics viewed by hydrogen exchange. *Protein Sci.* **2012,** *21*, 996-1005.

88. Englander, J. J.; Rogero, J. R.; Englander, S. W., Protein Hydrogen Exchange Studied by the Fragment Separation Method. *Anal. Biochem.* **1985,** *147*, 234-244.

89. Ahn, J.; Jung, M. C.; Wyndham, K.; Yu, Y. Q.; Engen, J. R., Pepsin Immobilized on High-Strength Hybrid Particles for Continuous Flow Online Digestion at 10 000 psi. *Anal. Chem.* **2012,** *84* (16), 7256-7262.

90. Jones, L. M.; Zhang, H.; Vidavsky, I.; Gross, M. L., Online, High-Pressure Digestion System for Protein Characterization by Hydrogen/Deuterium Exchange and Mass Spectrometry. *Anal. Chem.* **2010,** *82*, 1171-1174.

91. Venable, J. D.; Scuba, W.; Brock, A., Feature Based Retention Time Alignment for Improved HDX MS Analysis. *J. Am. Soc. Mass Spectrom.* **2013,** *24*, 642-645.

92. Majumdar, R.; Manikwar, P.; Hickey, J. M.; Arora, J.; Middaugh, C. R.; Volkin, D. B.; Weis, D. D., Minimizing Carry-Over in an Online Pepsin Digestion System used for the H/D Exchange Mass Spectrometric Analysis of an IgG1 Monoclonal Antibody. *J. Am. Soc. Mass Spectrom.* **2012,** *23*, 2140-2148.

93. Fang, J.; Rand, K. D.; Beuning, P. J.; Engen, J. R., False EX1 signatures caused by sample carryover during HX MS analyses. *Int. J. Mass Spectrom.* **2011,** *302*, 19-25.

94. Iacob, R. E.; Engen, J. R., Hydrogen Exchange Mass Spectrometry: Are We Out of the Quicksand? *J. Am. Soc. Mass Spectrom.* **2012,** *23*, 1003-1010.

95. Fajer, P. G.; Bou-Assaf, G. M.; Marshall, A. G., Improved Sequence Resolution by Global Analysis of Overlapped Peptides in Hydrogen/Deuterium Exchange Mass Spectrometry. *J. Am. Soc. Mass Spectrom.* **2012,** *23*, 1202-1208.

96. Kreshuk, A.; Stankiewicz, M.; Lou, X.; Kirchner, M.; Hamprecht, F. A.; Mayer, M. P., Automated detection and analysis of bimodal isotope peak distributions in H/D exchange mass spectrometry using HeXicon. *Int. J. Mass Spectrom.* **2011,** *302*, 125-131.

97. Kan, Z.-Y.; Mayne, L.; Chetty, P. S.; Englander, S. W., ExMS: Data Analysis for HX-MS Experiments. *J. Am. Soc. Mass Spectrom.* **2011,** *22*, 1906-1915.

98. Zhang, Z. Q.; Zhang, A.; Xiao, G., Improved Protein Hydrogen/Deuterium Exchange Mass Spectrometry Platform with Fully Automated Data Processing. *Anal. Chem.* **2012,** *84* (11), 4942-4949.

99. Guttman, M.; Weis, D. D.; Engen, J. R.; Lee, K. K., Analysis of Overlapped and Noisy Hydrogen/Deuterium Exchange Mass Spectra. *J. Am. Soc. Mass Spectrom.* **2013,** *24*, 1906-1912.

100. Rey, M.; Yang, M. L.; Burns, K. M.; Yu, Y. P.; Lees-Miller, S. P.; Schriemer, D. C., Nepenthesin from Monkey Cups for Hydrogen/Deuterium Exchange Mass Spectrometry. *Mol. Cell. Proteomics* **2013,** *12* (2), 464-472.

101. Sheff, J. G.; Rey, M.; Schriemer, D. C., Peptide-Column Interactions and Their Influence on Back Exchange Rates in Hydrogen/Deuterium Exchange-MS. *J. Am. Soc. Mass Spectrom.* **2013,** *24* (7), 1006-15.

102. Amon, S.; Trelle, M. B.; Jensen, O. N.; Jorgensen, T. J. D., Spatially Resolved Protein Hydrogen Exchange Measured by Subzero-Cooled Chip-Based Nanoelectrospray Ionization Tandem Mass Spectrometry. *Anal. Chem.* **2012,** *84*, 4467-4473.

103. Konermann, L.; Pan, J.; Liu, Y., Hydrogen Exchange Mass Spectrometry for Studying Protein Structure and Dynamics. *Chem. Soc. Rev.* **2011,** *40*, 1224-1234.

104. Powell, K. D.; Ghaemmaghami, S.; Wang, M. Z.; Ma, L.; Oas, T. G.; Fitzgerald, M. C., A General Mass Spectrometry-Based Assay for the Quantitation of Protein-Ligand Binding Interactions in Solution. *J. Am. Chem. Soc.* **2002,** *124*, 10256-10257.

Chapter 2. Comparative Analysis of Oxy-Hemoglobin and Aquomet-Hemoglobin by Hydrogen/Deuterium Exchange Mass Spectrometry

2.1. Introduction

Hemoglobin A (Hb), the oxygen carrier in red blood cells, is among the most thoroughly studied proteins.[1-4] Hereditary Hb defects are associated with anemia and other pathological symptoms.[5] Efforts are currently underway to design chemically modified Hbs for blood transfusions.[6]

Hb has a $(\alpha\beta)_2$ quaternary structure (Figure 2-1). Each α subunit is closely linked to one β subunit via a "packing" interface, resulting in two symmetrical heterodimers that are referred to as α1β1 and α2β2. In comparison, the contacts between α1 and β2 (as well as α2 and β1) are weaker, forming the so-called "sliding" interface.[5] O_2 transport is mediated by allosteric switching between the oxy (R) and deoxy (T) states. In oxy-Hb the distal coordination sites of all four heme iron centers are occupied by O_2, whereas in the deoxy state these sites are vacant. During the R-T transition α1β1 rotates by 15° relative to α2β2. Interactions across the sliding interface are less extensive in R, whereas T is stabilized by additional salt bridges.[1-5] O_2 binding is only possible if the heme iron is in the 2+ state. Autooxidation to Fe(3+) can take place under physiological stress, but also during protein isolation and storage. The aquomet-Hb generated in this way is dysfunctional and has the distal iron coordination sites occupied by water.[7] Aquomet-Hb formation *in vivo* causes a weakening of the heme-protein interactions. This facilitates release of Fe(3+) heme from the

protein and diffusion of the porphyrin into lipid membranes where it can trigger oxidative damage. Existing data provide little insights as to why heme dissociation from aquomet-Hb is more facile than from oxy-Hb.[8]

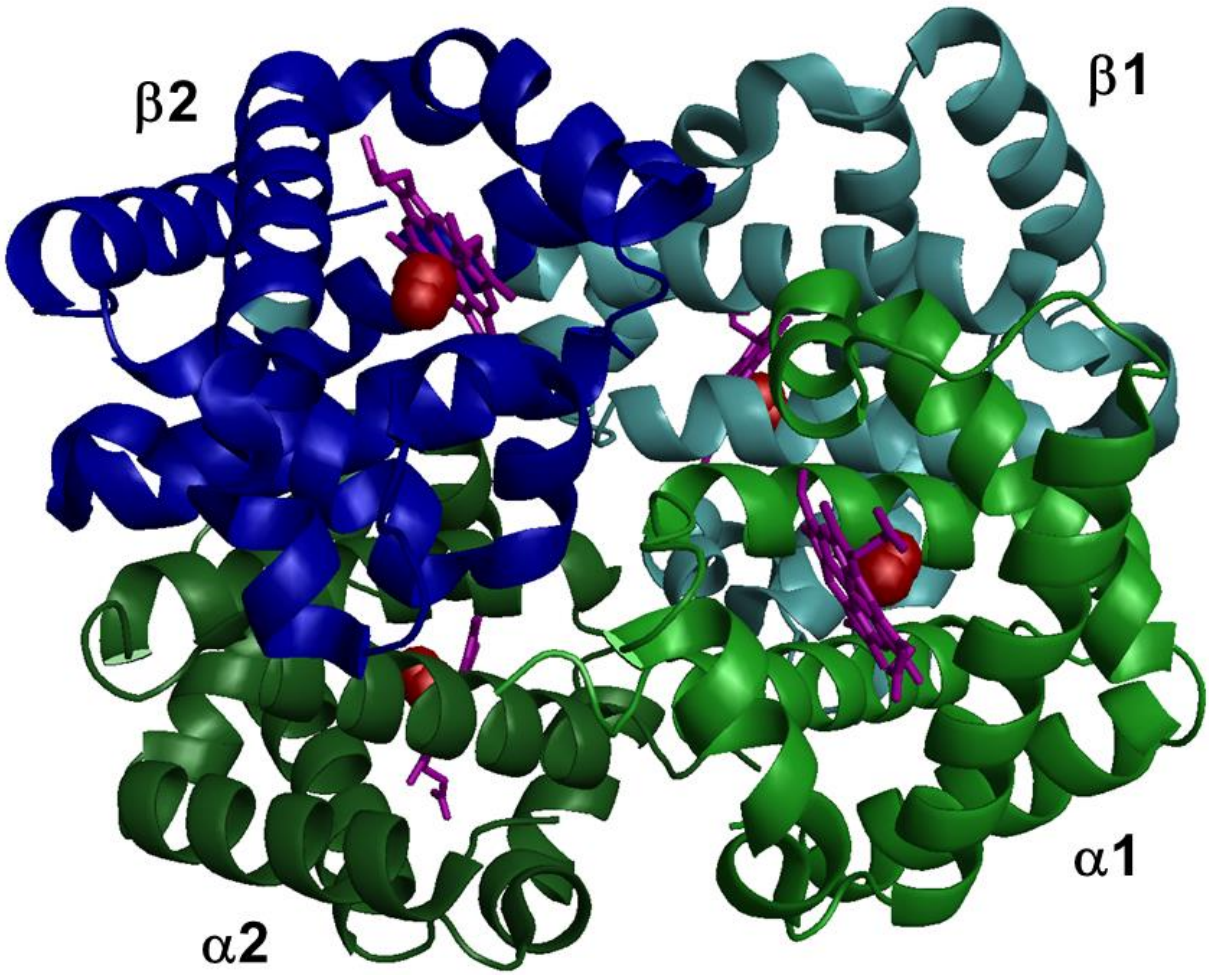

Figure 2-1: X-ray structure of bovine Hb (carbon monoxide-bound Fe(2+) state, pdb file 2qss 8). The subunit numbering follows the commonly used notation 1. Heme groups are shown in magenta. The sites of distal ligand binding to the heme iron (oxygen in oxy-Hb, and water in aquomet-Hb) are highlighted in red.

Although the properties of Hb have been explored in great detail, [1-5] there are still major gaps in the general understanding of this protein.[4-9] New X-ray investigations revealed a host of conformations that differ from the canonical T and R states. The functional significance of these newly discovered conformers remains unclear.[9-12] Wide-angle X-ray solution scattering[13] and NMR spectroscopy[14-15] point to marked differences between Hb in solution and in the crystallized state. As a result, many aspects related to Hb structure and function are more controversial today than they were 30 years ago.[13]

In addition to its central biomedical role, Hb represents an important test system for the development of novel bioanalytical techniques. Mass spectrometry (MS), in particular, relies heavily on Hb as model protein.[16-17] A key milestone was the development of "native" electrospray ionization (ESI)-MS for studies on intact Hb[18-20] and other protein complexes.[21-23] Those early successes[18-20] paved the way for subsequent Hb dissociation experiments, ion mobility studies, and gas phase isotope exchange investigations.[24-29] On-line ESI-MS has been used for probing Hb subunit interactions, highlighting the potential of this approach for monitoring self-assembly processes in solution.[30-33] Desorption ESI (DESI)-MS[34] and matrix-assisted laser desorption/ionization (MALDI)-MS [35] investigations routinely use Hb for benchmarking purposes. The prevalence of Hb as a MS model system is due to the fact that the protein is readily available at low cost. Also, existing X-ray data [1-5,12] provide a comprehensive reference base for the development of MS-based structural biology tools.

Backbone amide hydrogen/deuterium exchange (HDX) coupled with ESI-MS has become a widely used method for studying protein behavior in solution.[36-38] Polypeptide regions that exhibit a high degree of conformational dynamics undergo rapid exchange, whereas HDX in rigid hydrogen-bonded segments is much slower. HDX/MS measurements

commence with protein exposure to a D_2O-containing solvent. Aliquots taken at selected labeling times are quenched at acidic pH. Pepsin digestion and subsequent peptide analysis by liquid chromatography (LC)/ESI-MS are carried out at low temperature. Spatially-resolved HDX kinetics can then be obtained by tracking the mass shifts of individual peptides.

Of the three Hb forms mentioned above, only oxy-Hb and aquomet-Hb represent widely used MS test analytes.[16-20,24-26,28-35] In contrast, MS investigations on deoxy-Hb are rare because they require an O_2-free environment.[39] Previous MS studies paid little attention to possible differences between oxy-Hb and aquomet-Hb, implicitly assuming that both share the same solution phase properties. This view is consistent with X-ray data, according to which oxy-Hb and aquomet-Hb crystallize in virtually identical conformations. Depending on the conditions, this common structure can be either the R state,[5,40-41] or a conformation that is referred to as R2.[42-43] Close examination of oxy and aquomet-Hb crystal structures reveals only small differences related to the iron positioning within the heme.[5-44] Nonetheless, it remains unclear in how far those X-ray data [5,40-44] provide solid evidence for the notion that oxy-Hb and aquomet-Hb exhibit the same structural and dynamic behavior in solution. It is also noted that there are no crystallographic investigations that employed dilute ammonium acetate which serves as *de facto* standard solvent for MS studies on Hb.[18-19,24-25,28-35]

HDX/MS represents an obvious strategy for probing possible differences in the solution phase properties of the various Hb forms. Earlier HDX work examined the relationship between the oxy and deoxy states.[39,45-46] The latter exhibits a higher degree of protection, consistent with the more rigid structure of the T conformation.[1-4] Surprisingly,

there appear to be no prior HDX/MS-based comparative analyses of oxy-Hb and aquomet-Hb. The goal of the current work is to close this gap. Despite the fact that oxy-Hb and aquomet-Hb adopt virtually the same crystal structures [5,40-44], our HDX/MS data reveal that their solution phase behavior exhibits significant differences.

2.2. Experimental Procedures

2.2.1. Materials

Porcine pepsin and potassium ferricyanide were purchased from Sigma (St. Louis, MO, USA). Ammonium acetate was obtained from Fluka (St. Louis, MO, USA). D_2O was from Cambridge Isotope Laboratories (Andover, MA). All chemicals were used as received. Oxy-Hb was isolated from fresh bovine blood following established procedures,[7-32] and stored at -80 °C until further use. Protein concentrations are reported on a per-tetramer basis throughout this work. Hb solutions for all experiments contained 10 mM ammonium acetate. Aquomet-Hb was produced by exposing oxy-Hb to excess potassium ferricyanide, followed by desalting on a size exclusion column.[32] The level of covalent modifications due to side chain oxidation was found to be negligible for the protein samples used here, as reported previously[32] (data not shown). The measured mass values of the two subunits were consistent with those calculated from the sequence of bovine Hb[8], i.e., (15,053 ± 1) Da for α and (15,954 ± 1) Da for β. UV-Vis absorption spectra were recorded on a Cary 100 instrument (Varian, Mississauga, ON, Canada). pH values were measured using a Fisher (Waltham, MA) AB15 pH meter; these values are reported without isotope correction.

2.2.2. Hydrogen/Deuterium Exchange Mass Spectrometry

150 μM Hb (in the oxy or aquomet states) in 10 mM ammonium acetate was mixed with 4 volumes of D_2O containing 10 mM ammonium acetate, resulting in a protein concentration of 30 μM with a measured pH of 7.2 at room temperature. 30 μL aliquots were removed at various time points ranging from 1 to 360 min after initiating labeling. The aliquots were quenched at pH 2.4 by addition of HCl on ice, followed by flash freezing in liquid nitrogen and storage at -80 ^{o}C. For digestion, the aliquots were rapidly thawed to ~0 ^{o}C and mixed with 5 μL pepsin stock solution (1 mM in aqueous acetic acid, pH 4.1) at pH 2.4 for 1 min on ice. The final Hb concentration was 20 μM. The resulting peptic fragments were desalted and separated within 15 min on an equilibrated reversed phase column (Jupiter 4 μ Proteo, C12, 50 × 1 mm; Phenomenex, Torrance, CA) with an online prefilter (KrudKatcher; Phenomenex) coupled to a Waters UPLC pump at a flow rate of 100 μL min^{-1}, using a water/acetonitrile gradient in the presence of 0.1% formic acid. The injection loop volume was 20 μL and the total amount of protein per injection was 400 pmol. The injection syringe, column, injector and solvent delivery lines were kept at ~0 °C. Mass analysis of peptides was performed on a Synapt HDMS instrument (Waters, Milford, MA) with source and desolvation temperatures of 80 and 300 °C respectively, a cone voltage of 30 V, and an ESI voltage of 3 kV. The identity of each peptide was confirmed by tandem MS based on the known sequence of bovine Hb (pdb code 2QSS [8]). Zero time point controls (m_0) for the correction of artifactual in-exchange were performed by exposing Hb to a mixture of D_2O and quenching buffer, using the solutions described above. Controls for fully exchanged Hb (m_{100}, for the correction of artifactual back exchange) were prepared by incubating 30 μM Hb in labeling solution at pH 2.4 for 9 h. Intact protein HDX measurements were performed

using a procedure similar to that described above, but by using a different column (Jupiter 5 μm Proteo, C4, 50 mm × 1mm; Phenomenex) without pepsin digestion. Biolynx 4.1 (Waters), HX-Express [47] and manual inspection were employed to analyze the centroid mass of all peptides as a function of labeling time. Deuteration levels were determined as

$$\% \; Deuteration = \frac{(m - m_0)}{(m_{100} - m_0)} \tag{2.1}$$

All HDX measurements were conducted in triplicate; error bars shown in the figures below correspond to standard deviations.

2.3. Results and Discussion

2.3.1. Optical Characterization of Hb Samples

Prior to conducting MS experiments it is important to verify the properties of the protein samples. The UV-Vis absorption spectrum of Hb represents a sensitive probe of the heme oxidation and ligation state (Figure 2-2). After thawing, Hb samples obtained from fresh bovine blood exhibit an absorption spectrum with a dominant Soret signal at 415 nm, along with bands at 541 and 577 nm. The presence of these so-called γ, β, and α signals represents the hallmark of oxy-Hb.[7]

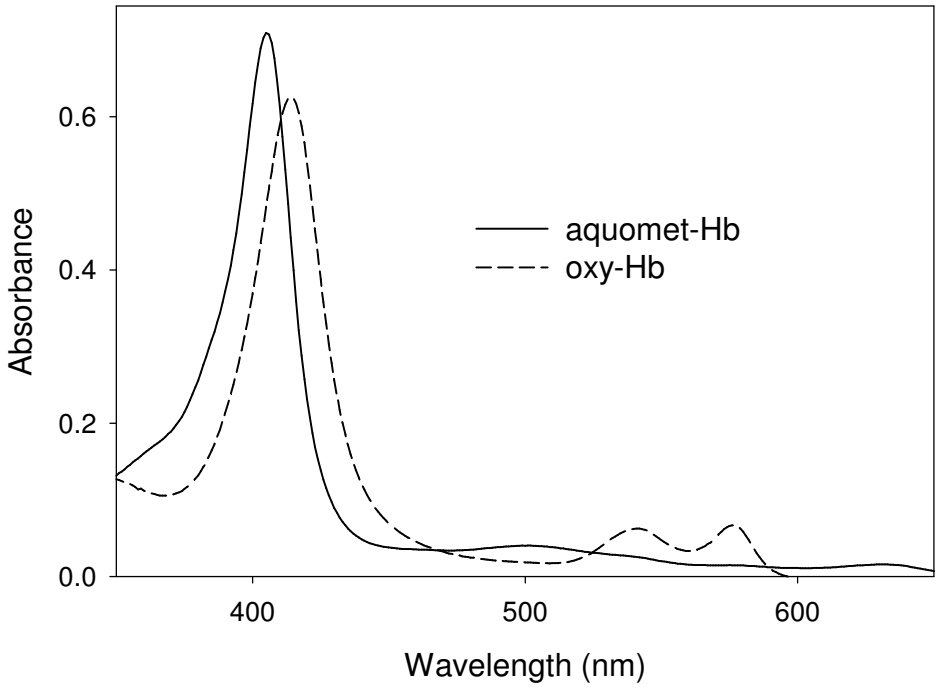

Figure 2-2: UV-Vis absorption spectra of oxy-Hb and aquomet-Hb in 10 mM ammonium acetate. The protein concentration was 3 μM for both samples. Differences in the intensity of the Soret peak are caused by the different molar absorption coefficients of the two forms [7].

After ferricyanide treatment the bands at 541 and 577 nm disappear and the Soret maximum shifts to 405 nm, as expected for Fe(3+) with distal iron coordination by water.[7,32] These spectral data confirm the authenticity of the oxy-Hb and aquomet-Hb samples used in this work.

2.3.2. Global HDX Kinetics

For comparing the solution phase behavior of oxy-Hb and aquomet-Hb, HDX/MS measurements were initially conducted on the intact subunits. Markedly different isotope exchange kinetics are observed for the oxy and aquomet forms (Figure 2-3). Throughout the

6 h experimental time window the deuteration levels of aquomet-Hb are higher (by up to 10%) than those of oxy-Hb. These differences extend to both subunits. Clearly, the oxy → aquomet transition induces a conformational destabilization, resulting in more pronounced conformational dynamics for aquomet-Hb than for oxy-Hb. This is despite the fact that both forms crystallize in virtually the same conformation. [5,40-43]

As noted in the Introduction, previous investigations demonstrated that deoxy-Hb exhibits lower HDX levels than oxy-Hb [39,45-46]. That behavior is consistent with the presence of more extensive contacts across the sliding interface in deoxy-Hb relative to oxy-Hb.[1-5] Those different subunit interactions are reflected in the tetramer-dimer dissociation constant (K_d) which is 2×10^{-6} M for oxy-Hb, and $<10^{-10}$ M for deoxy-Hb [8,48]. It might be expected that the enhancement of conformational dynamics seen in Figure 2-3 upon oxy → aquomet conversion is also related to changes in interaction strength at the sliding interface. However, the dissociation constants of aquomet-Hb and oxy-Hb are indistinguishable.[32] We therefore conclude that the enhanced dynamics seen for aquomet-Hb relative to oxy-Hb must be caused by an internal destabilization of the $\alpha 1\beta 1$ and $\alpha 2\beta 2$ units, rather than additional weakening of the sliding interface.

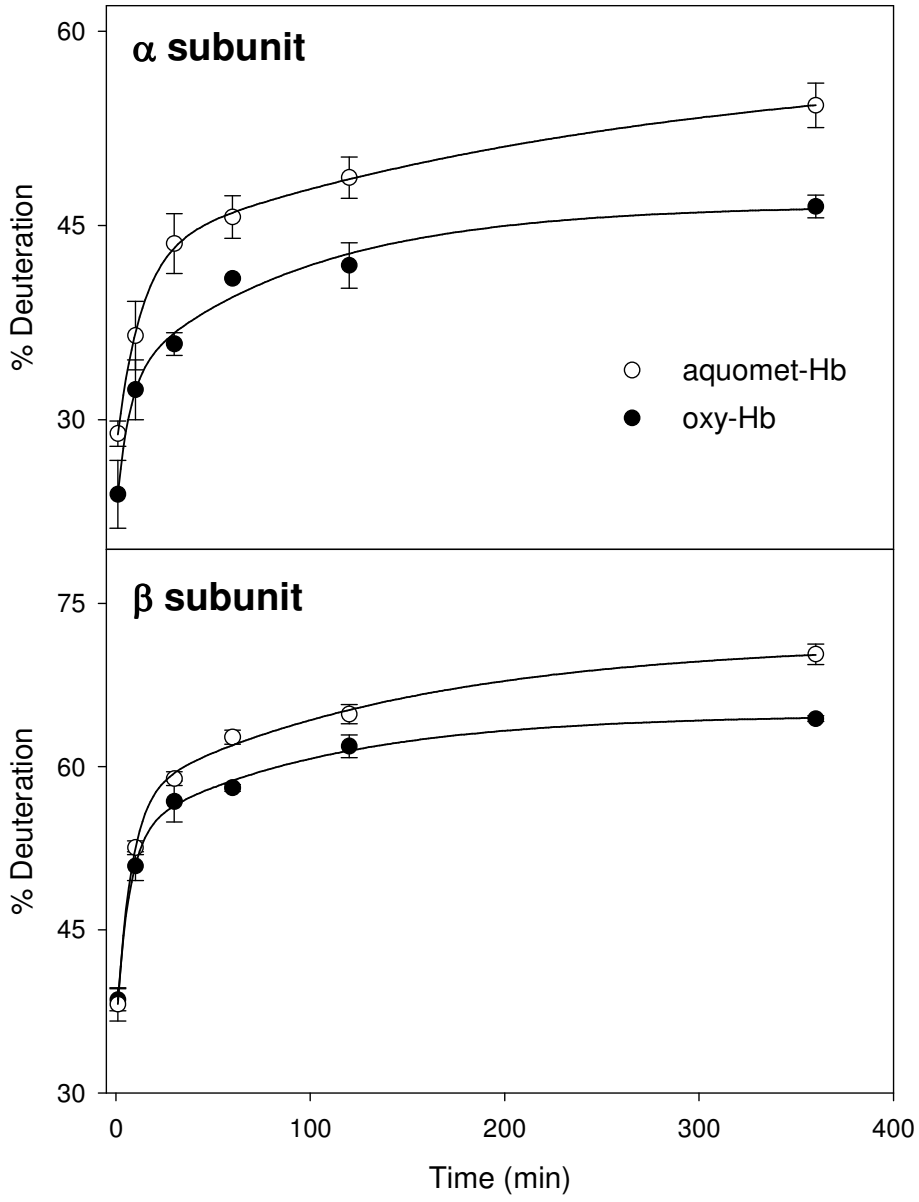

Figure 2-3: HDX kinetics of aquomet-Hb (open symbols) and oxy-Hb (filled symbols). The two panels show data for the intact α (top) and β subunits (bottom) of the tetramer. Lines represent biexponential fits according to eq. 2.2.

2.3.3. Spatially-Resolved HDX/MS Measurements

A more detailed view of the protein dynamics in the oxy and aquomet states is obtained when analyzing the HDX kinetics at the peptide level. Peptic digestion of Hb yielded 30 fragments that had a sufficiently high signal-to-noise ratio for reliable deuteration measurements. The overall sequence coverage obtained in this way is 82% (Figure 2-4). Exchange occurs in the EX2 regime, evident from a lack of peak splitting in the isotope envelopes (data not shown). As expected from the intact protein data (Figure 2-3), most peptides exhibit higher HDX levels for aquomet-Hb than for oxy-Hb throughout the experimental time window (Figure 2-5). However, there are several regions that display almost the same kinetics in both states (such as $\beta_{7\text{-}13}$); a few peptides even show the opposite trend ($\alpha_{1\text{-}23}$, $\alpha_{67\text{-}80}$, $\alpha_{110\text{-}125}$, and $\alpha_{129\text{-}136}$). This pattern reveals that the overall destabilization accompanying the oxy → aquomet transition does not affect all regions of the Hb tetramer to the same extent.

Many features of the measured HDX kinetics in Figure 2-5 are consistent with crystallographic data.[8] Peptides that comprise helical regions generally show significant protection. For example, $\alpha_{99\text{-}106}$ and $\beta_{102\text{-}109}$ exhibit the lowest deuteration levels, in line with their positioning in the central regions of helices αG and βG, respectively. By the same token, some of the most highly deuterated peptides such as $\alpha_{47\text{-}53}$, $\alpha_{135\text{-}141}$, $\beta_{1\text{-}8}$, and $\beta_{41\text{-}47}$ correspond to loops and termini that are expected to be relatively mobile. Interestingly, several other peptides show very limited protection, despite being located in regions that appear to be tightly folded in crystallized Hb.[8] One of these is $\alpha_{119\text{-}125}$, suggesting that the αG-αH loop comprises more residues than seen in the X-ray structure.

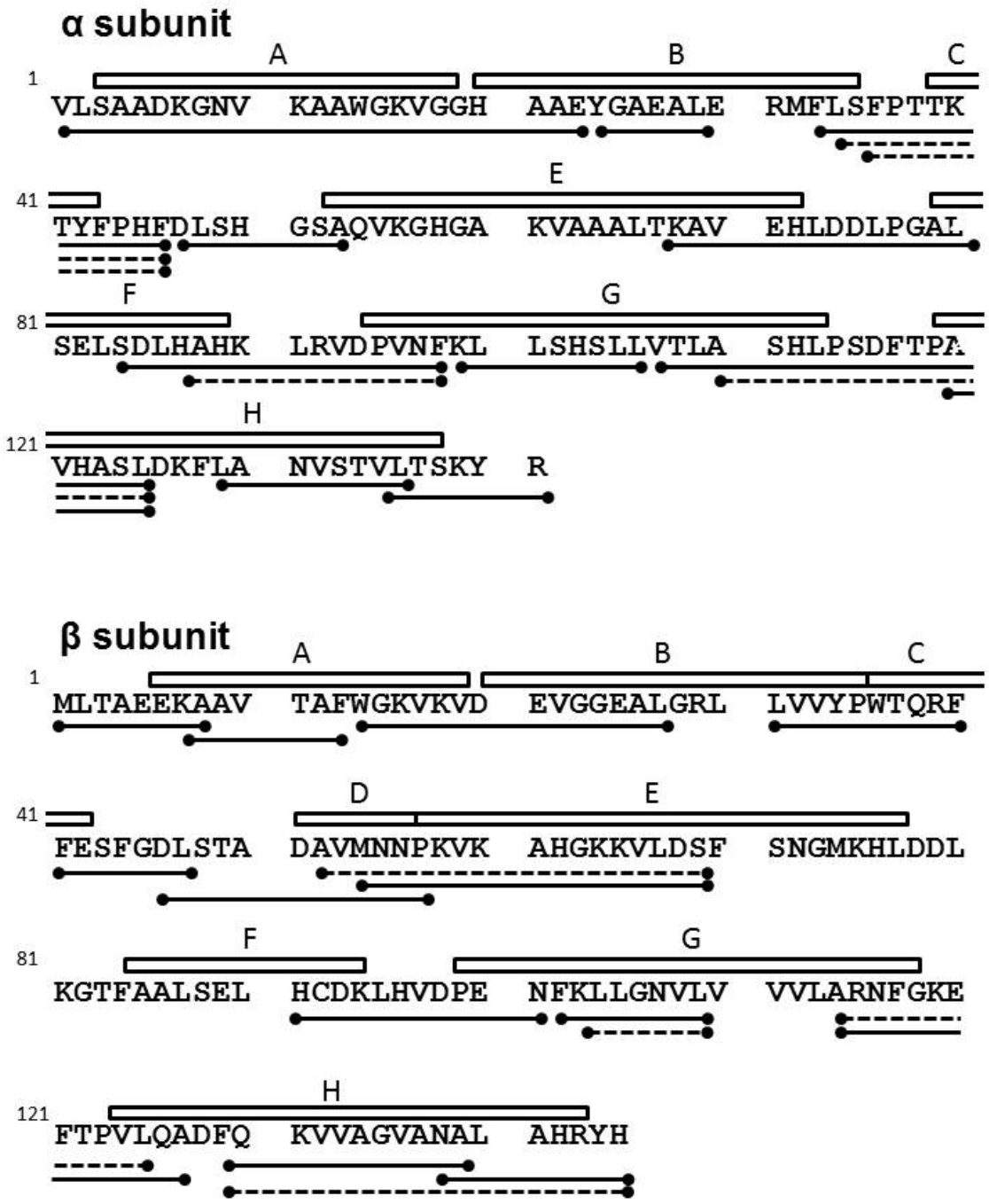

Figure 2-4: Sequence of the Hb α and β subunits. Helices are denoted as rectangles. Peptic fragments are indicated below the sequence. Solid lines represent peptides used for data analysis, whereas dashed lines represent redundant fragments. Boxes above the sequence indicate helices.

Similarly, the high HDX levels of $\beta_{7\text{-}13}$ indicate considerable fraying at the N-terminus of helix βA. Our data therefore support the view [13-15] that not all of the structural features seen in crystallized Hb adequately reflect the solution-phase behavior.

To facilitate the discussion of the measured HDX data, deuteration percentages were mapped to the X-ray structure of the Hb subunits for t = 120 min (Figure 2-6a-d). Overlapping peptides can be used to approximate the HDX behavior of segments that do not directly correspond to proteolysis products.[49] This case applies to peptides $\alpha_{107\text{-}125}$ and $\alpha_{119\text{-}125}$ that exhibit 41% and 99% deuteration, respectively, in oxy-Hb.

Thus, the average deuteration percentage of $\alpha_{107–118}$ can be estimated as [16×41% - 5×99%] / 10 = 16%. This calculation takes into account the presence of prolines, as well as deuterium loss on the first two residues of each peptide.[50] The adjacent peptide $\alpha_{99–106}$ shows an even lower deuteration level of 7%, thereby pinpointing helix αG as the most protected element in the α subunit (residues 99 – 118, blue in Figure 2-6a). Similarly, βG represents the most protected helix in the β subunit (green, Figure 2-6b). The four G helices retain high protection even after the oxy → aquomet transition (Figure 2-6c, d). The low deuteration levels are consistent with the role of αG and βG as deeply buried elements that

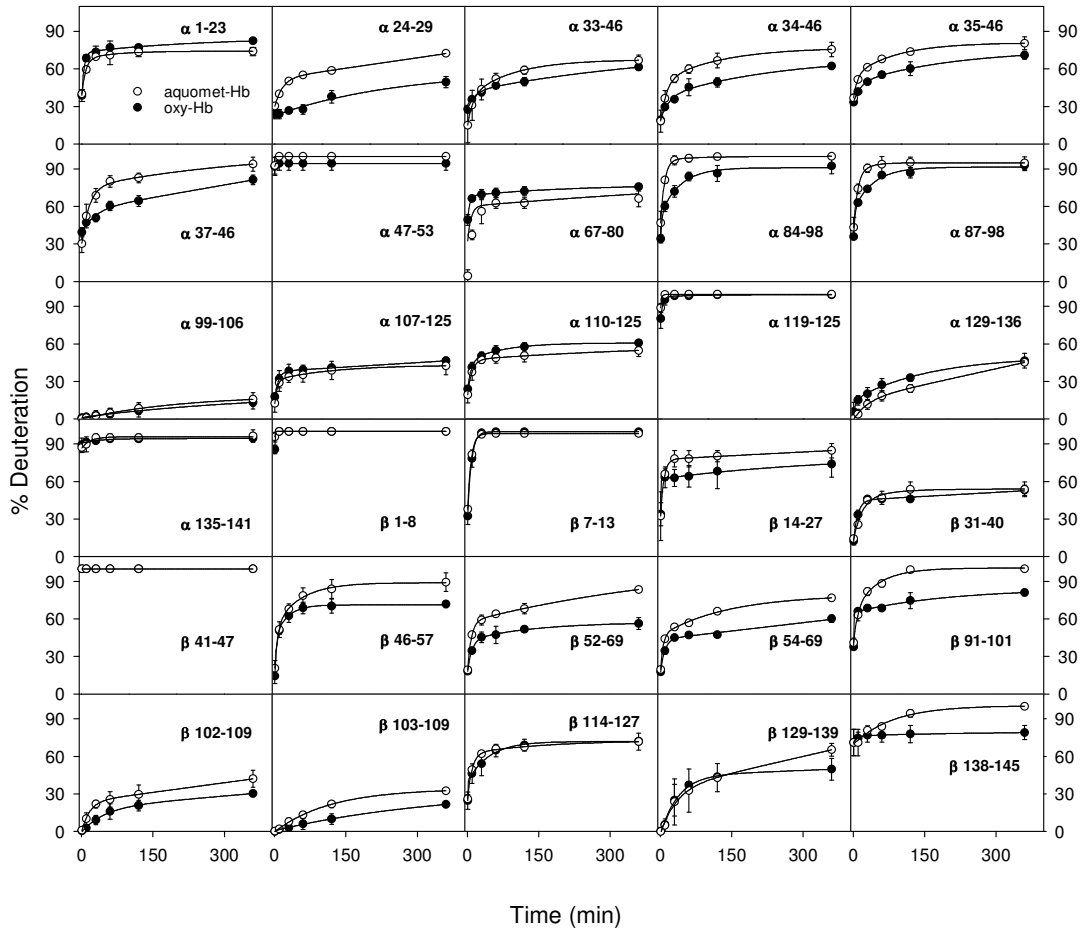

Figure 2-5: HDX kinetics of peptides covering the α and β subunits of aquomet-Hb (open symbols) and oxy-Hb (filled symbols). Residue numbers of the individual peptides are indicated in each panel. Lines are biexponential fits of the form $\%\ Deuteration = A_0 + A_1(1-e^{-k_1 t}) + A_2(1-e^{-k_2 t})$ where A_0 is the fraction of amide backbone groups that undergoes burst phase labeling, and A_1 and A_2 are the fractions that undergo deuteration with apparent rate constants k_1 and k_2, respectively.

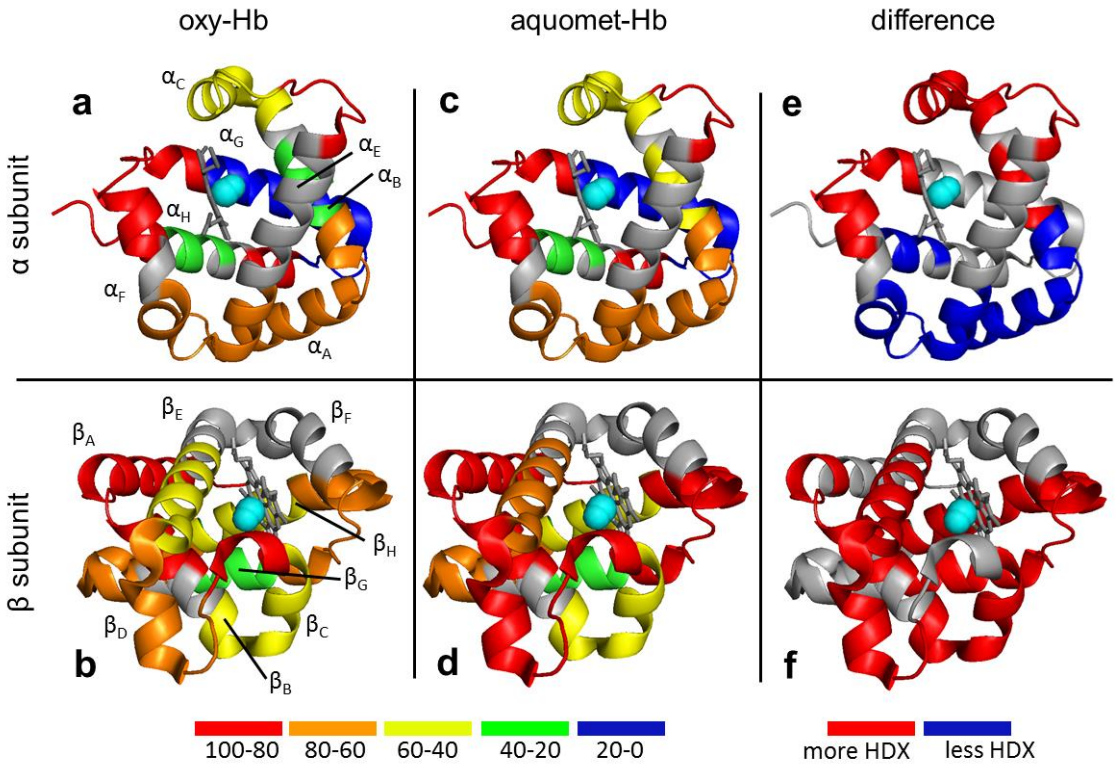

Figure 2-6: Mapping the HDX data of Figure 2-5 to the X-ray structure of bovine Hb [8] for *t* = 120 min. Using the orientation of Figure 2.1 as reference, the top row of panels in this Figure corresponds to α1, the bottom row represents β2. Colors in (a) - (d) represent deuteration percentages, as defined in the legend along the bottom. Gray elements in (a) - (d) were not covered by peptide mapping. Panels (e), (f): Deuteration differences, calculated as [aquomet - oxy] for *t* = 120 min. Colored regions correspond to |difference| > 5%. Segments that show elevated deuteration after oxy → aquomet conversion are depicted in red. Segments with reduced deuteration are shown in blue. In all six panels the ligand binding site on the heme is highlighted in cyan.

form key anchoring points at the packing interface.[8] Two other regions are quite highly protected in oxy-Hb, i.e., the central portions of αB and αH (green, Figure 2-6a).

The last two panels of Figure 2-6 highlight the deuteration differences upon oxy → aquomet conversion. Segments that show enhanced conformational dynamics are depicted in red, those that undergo rigidification are shown in blue. It is seen that changes in the β

subunit are not restricted to specific regions. Instead, the whole polypeptide chain experiences a global destabilization (Figure 2-6f). In contrast, α globin shows a more intricate behavior where enhancements in structural dynamics are largely confined to the vicinity of the heme (Figure 2-6e, red). The location of these red elements in Figure 2-6e is consistent with the expectation that the heme binding pocket should be the epicenter of any structural changes that accompany the transition from the $Fe(2+)\cdots O_2$ state to the $Fe(3+)\cdots H_2O$ form. Interestingly, helix αA as well as a number of adjoining regions become stabilized after aquomet formation (Figure 2-6e, blue). These stabilized regions in the α subunit are more remote from the heme, and they are not heavily involved in inter-subunit contacts. Overall, Figures 2-6e and 2-6f reveal that α and β globin respond to the oxy → aquomet conversion in a very different fashion. This behavior is surprising, when considering the very similar average conformations of α and β, their symmetrical positioning within the Hb tetramer, and their high sequence homology.[8]

2.4. Conclusions

To the best of our knowledge, this is the first HDX/MS investigation that compares the conformational dynamics of oxy-Hb and aquomet-Hb. The two forms adopt virtually the same crystal structures, yet they exhibit solution-phase dynamics that are clearly different. Our findings are consistent with earlier studies that noted limitations in the predictive power of crystallographic data for protein behavior in solution. [13-15,51]

Aquomet-Hb is known to show elevated rates of heme loss relative to oxy-Hb, although the reasons underlying this behavior remain incompletely understood. Heme loss is

of biomedical significance, because free Fe(3+) heme can incorporate into lipid membranes, thereby triggering oxidative damage.[8] This process is of particular relevance after hemolysis, where oxy-Hb or deoxy-Hb are released from red blood cells. Binding to haptoglobin is a mechanism for sequestering free Hb in the blood plasma, thereby counteracting aquomet-Hb formation and heme release.[52] Nonetheless, under some conditions there can still be free Hb molecules that undergo autooxidation to the Fe(3+) state.[53] We propose that the enhanced structural dynamics observed here for aquomet-Hb are a key factor that facilitates Fe(3+) heme dissociation from the protein. It is likely that the enhanced structural dynamics in the heme binding pocket of α globin (red in Figure 2-6e) directly reflect the adverse effects of aquomet formation on the stability of the heme-protein interactions.

Finally, we note that one of the most intriguing questions in biological MS is to what extent supramolecular solution phase structures can be preserved upon transfer into the gas phase.[54-57] Investigations targeting this issue typically rely on crystallographic data as surrogate for the actual solution phase structure of the system under investigation. As discussed above, this strategy is not always adequate.[13-15,51] The special role of oxy-Hb and aquomet-Hb as widely used model analytes in MS [16-20,24-35] warrants a close examination of their solution phase properties. In contrast to information provided by static X-ray data,[5,40-43] our HDX/MS results demonstrate that the solution phase dynamics of the two forms exhibits marked differences. It is hoped that the observations of this work will benefit future investigations on the relationship between Hb behavior in solution and in the gas phase.

2.5. References

1. Eaton, W. A.; Henry, E. R.; Hofrichter, J.; Mozzarelli, A., Is cooperative oxygen binding by hemoglobin really understood. *Nat. Struct. Biol.* **1999,** *6* (4), 351 - 358.

2. Bellelli, A.; Brunori, M., Hemoglobin allostery: Variations on the theme. *Biochim. Biophys. Acta* **2011,** *1807* (10), 1262-1272.

3. Perutz, M. F.; Wilkinson, A. J.; Paoli, M.; Dodson, G. G., The stereochemical mechanism of the cooperative effects in hemoglobin revisited. *Annu. Rev. Biophys. Biomolec. Struct.* **1998,** *27*, 1-34.

4. Yonetani, T.; Laberge, M., Protein dynamics explain the allosteric behaviors of hemoglobin. *Biochim. Biophys. Acta* **2008,** *1784* (9), 1146-1158.

5. Dickerson, R. E.; Geis, I., *Hemoglobin: Structure, Function, Evolution, and Pathology*. The Benjamin/Cummings Publishing Company, Inc.: Menlo Park, CA, **1983**.

6. Kluger, R., Red cell substitutes from hemoglobin - Do we start all over again? *Curr. Op. Chem. Biol.* **2010,** *14* (4), 538-543.

7. Antonini, E.; Brunori, M., *Hemoglobin and Myoglobin in Their Reactions With Ligands*. North-Holland Publishing Company: Amsterdam, London, **1971**; Vol. 21.

8. Aranda IV, R.; Cai, H.; Worley, C. E.; Levin, E. J.; Li, R.; Olson, J. S.; Phillips Jr, G. N.; Richard, M. P., Structural analysis of fish versus mammalian hemoglobins: Effect of the heme pocket enviornment on autooxidation and hemin loss. *Proteins* **2009,** *75*, 217-230.

9. Kim, K. H.; Muniyappan, S.; Oang, K. Y.; Kim, J. G.; Nozawa, S.; Sato, T.; Koshihara, S. Y.; Henning, R.; Kosheleva, I.; Ki, H.; Kim, Y.; Kim, T. W.; Kim, J.; Adachi, S.; Ihee, H., Direct Observation of Cooperative Protein Structural Dynamics of Homodimeric

Hemoglobin from 100 ps to 10 ms with Pump-Probe X-ray Solution Scattering. *J. Am. Chem. Soc.* **2012,** *134* (16), 7001-7008.

10. Fischer, S.; Olsen, K. W.; Nam, K.; Karplus, M., Unsuspected pathway of the allosteric transition in hemoglobin. *Proc. Nat. Acad. Sci. U.S.A.* **2011,** *108*, 5608-5613.

11. Safo, M. K.; Abraham, D. J., The enigma of the liganded hemoglobin end state: A novel quaternary structure of human carbonmonoxy hemoglobin. *Biochemistry* **2005,** *44* (23), 8347-8359.

12. Dey, S.; Chakrabarti, P.; Janin, J., A survey of hemoglobin quaternary structures. *Proteins* **2011,** *79* (10), 2861-2870.

13. Makowski, L.; Bardhan, J.; Gore, D.; LaI, J.; Mandava, S.; Park, S.; Rodi, D. J.; Ho, N. T.; Ho, C.; Fischetti, R. F., WAXS Studies of the Structural Diversity of Hemoglobin in Solution. *J. Mol Biol.* **2011,** *408*, 909-921.

14. Lukin, J. A.; Ho, C., The structure-function relationship of hemoglobin in solution at atomic resolution. *Chemical Reviews* **2004,** *104* (3), 1219-1230.

15. Song, X. J.; Yuan, Y.; Simplaceanu, V.; Sahu, S. C.; Ho, N. T.; Ho, C., A comparative NMR study of the polypeptide backbone dynamics of hemoglobin in the deoxy and carbonmonoxy forms. *Biochemistry* **2007,** *46* (23), 6795-6803.

16. Chernushevich, I. V.; Loboda, A. V.; Thomson, B. A., An introduction to quadrupole time-of-flight mass spectrometry. *J. Mass Spectrom.* **2001,** *36*, 849 - 865.

17. Edwards, R. L.; Creese, A. J.; Baumert, M.; Griffiths, P.; Bunch, J.; Cooper, H. J., Hemoglobin Variant Analysis via Direct Surface Sampling of Dried Blood Spots Coupled with High-Resolution Mass Spectrometry. *Anal. Chem.* **2011,** *83* (2265-2270).

18. Li, Y.-T.; Hsieh, Y.-L.; Henion, J. D.; Ganem, B., Studies on Heme Binding in Myoglobin, Hemoglobin, and Cytochrome c by Ion Spray Mass Spectrometry. *J. Am. Soc. Mass Spectrom.* **1993,** *4*, 631-637.

19. Light-Wahl, K. J.; Schwartz, B. L.; Smith, R. D., Observation of the Noncovalent Quaternary Association of Proteins by Electrospray Ionization Mass Spectrometry. *J. Am. Chem. Soc.* **1994,** *116*, 5271-5278.

20. Lemaire, D.; Marie, G.; Serani, L.; Larprevote, O., Stabilization of Gas-Phase Noncovlanet Macromolecular Complexes in Electrospray Mass Spectrometry Using Aqueous Triethylammonium Bicarbonate Buffer. *Anal. Chem.* **2001,** *73*, 1699-1706.

21. Loo, J. A., Electrospray Ionization Mass Spectrometry: a Technology for Studying Noncovalent Macromolecular Complexes. *Int. J. Mass Spectrom.* **2000,** *200*, 175-186.

22. Heck, A. J. R., Native mass spectrometry: a bridge between interactomics and structural biology. *Nat. Methods* **2008,** *5*, 927 - 933.

23. Benesch, J. L. P.; Ruotolo, B. T.; Simmons, D. A.; Robinson, C. V., Protein Complexes in the Gas Phase: Technology for Structural Genomics and Proteomics. *Chem. Rev.* **2007,** *107*, 3544-3567.

24. Versluis, C.; Heck, A. J. R., Gas-phase dissociation of hemoglobin. *Int. J. Mass Spectrom.* **2001,** *210/211*, 637-649.

25. Schmidt, A.; Karas, M., The Influence of Electrostatic Interactions on the Detection of Heme-Globin Complexes in ESI-MS. *J. Am. Soc. Mass Spectrom.* **2001,** *12*, 1092-1098.

26. Sciuto, S. V.; Liu, J.; Konermann, L., An Electrostatic Charge Partitioning Model for the Dissociation of Protein Complexes in the Gas Phase. *J. Am. Soc. Mass Spectrom.* **2011,** *22*, 1679-1689.

27. Kang, Y.; Terrier, P.; Douglas, D. J., Mass Spectra and Ion Collision Cross Sections of Hemoglobin. *J. Am. Soc. Mass Spectrom.* **2011,** *22*, 290-299.

28. Kang, Y.; Douglas, D. J., Gas-Phase Ions of Human Hemoglobin A, F, and S. *J. Am. Soc. Mass Spectrom.* **2011,** *22*, 1187-1196.

29. Scarff, C. A.; Patel, V. J.; Thalassinos, K.; Scrivens, J. H., Probing Hemoglobin Structure by Means of Traveling-Wave Ion Mobility Mass Spectrometry. *J. Am. Soc. Mass Spectrom.* **2009,** *20*, 625-631.

30. Griffith, W. P.; Kaltashov, I. A., Highly asymmetric interactions between globin chains during hemoglobin assembly revealed by electrospray ionization mass spectrometry. *Biochemistry* **2003,** *42*, 10024 - 10033.

31. Griffith, W. P.; Kaltashov, I. A., Protein Conformational Heterogeneity as a Binding Catalyst: ESI-MS Study of Hemoglobin H Formation. *Biochemistry* **2007,** *46*, 2020-2026.

32. Boys, B. L.; Kuprowski, M. C.; Konermann, L., Symmetric Behavior of Hemoglobin a- and b- Subunits during Acid-Induced Denaturation Observed by Electrospray Mass Spectrometry. *Biochemistry* **2007,** *46*, 10675-10684.

33. Apostol, I., Assessing the relative stabilities of engineered hemoglobins using electrospray mass spectrometry. *Anal. Biochem.* **1999,** *272*, 8 - 18.

34. Ferguson, C. N.; Benchaar, S. A.; Miao, Z. X.; Loo, J. A.; Chen, H., Direct Ionization of Large Proteins and Protein Complexes by Desorption Electrospray Ionization-Mass Spectrometry. *Anal. Chem.* **2011,** *83* (17), 6468-6473.

35. Zehl, M.; Allmaier, G., Ultraviolet matrix-assisted laser desorption/ionization time-of-flight mass spectrometry of intact hemoglobin complex from whole human blood. *Rapid Commun. Mass Spectrom.* **2004,** *18*, 1932-1938.

36. Iacob, R. E.; Engen, J. R., Hydrogen Exchange Mass Spectrometry: Are We Out of the Quicksand? *J. Am. Soc. Mass Spectrom.* **2012,** *23*, 1003-1010.

37. Percy, A. J.; Rey, M.; Burns, K. M.; Schriemer, D. C., Probing protein interactions with hydrogen/deuterium exchange and mass spectrometry-A review. *Anal. Chim. Acta* **2012,** *721*, 7-21.

38. Englander, S. W., Hydrogen Exchange and Mass Spectrometry: A Historical Perspective. *J. Am. Soc. Mass Spectrom.* **2006,** *17*, 1481-1489.

39. Englander, J. J.; Del Mar, C.; Li, W.; Englander, S. W.; Kim, J. S.; Stranz, D. D.; Hamuro, Y.; Woods, V. L., Protein structure change studied by hydrogen-deuterium exchange, functional labeling, and mass spectrometry. *Proc. Natl. Acad. Sci. U.S.A.* **2003,** *100* (12), 7057 - 7062.

40. Bunn, H. F.; Forget, B. G., *Hemoglobin: Molecular, Genetic and Clinical Aspects*. W.B. Saunders Company: Philadelphia, **1986**; p 690.

41. Perutz, M. F., Stereochemistry of Cooperative Effects in Haemoglobin. *Nature* **1970,** *228*, 726-739.

42. Smith, F. R.; Simmons, K. C., Cyanomet Human Hemoglobin Crystallized under Physiological Conditions Exhibits the Y-Quaternary Structure. *Proteins* **1994,** *18* (3), 295-300.

43. Silva, M. M.; Rogers, P. H.; Arnone, A., A 3rd Quaternary Structure of Human Hemoglobin-A at 1.7A Resolution. *J. Biol. Chem.* **1992,** *267* (24), 17248-17256.

44. Perutz, M. F.; Fersht, A. R.; Simon, S. R.; Roberts, G. C. K., Influence of Globin Structure on the State of the Heme.II. Allosteric Transitions in Methemoglobin. *Biochemistry* **1974,** *13*, 2174-2186.

45. Mitra, G.; Muralidharan, M.; Narayanan, S.; Pinto, J.; Srinivasan, K.; Mandal, A. K., Glutathionylation Induced Structural Changes in Oxy Human Hemoglobin Analyzed by Backbone Amide Hydrogen/Deuterium Exchange and MALDI-Mass Spectrometry. *Bioconjugate Chem.* **2012,** *23* (12), 2344-2353.

46. Abaturov, L. V.; Nosova, N. G.; Shlyapnicov, S. V.; Faizullin, D. A., The conformational dynamic of the tetramer hemoglobin molecule as revealed by hydrogen exchange. I. Influence of pH, temperature and ligand binding. *Mol. Biol.* **2006,** *40* (2), 326-340.

47. Weis, D. D.; Engen, J. R.; Kass, I. J., Semi-Automated Data Processing of Hydrogen Exchange Mass Spectra Using HX-Express. *J. Am. Soc. Mass Spectrom.* **2006,** *17*, 1700-1703.

48. Liu, J.; Konermann, L., Protein-Protein Binding Affinities In Solution Determined by Electrospray Mass Spectrometry. *J. Am. Soc. Mass Spectrom.* **2011,** *22*, 408-417.

49. Mayne, L.; Kan, Z.-Y.; Chetty, P. S.; Ricciuti, A.; Walters, B. T.; Englander, S. W., Many Overlapping Peptides for Protein Hydrogen Exchange Experiments by the Fragment Separation-Mass Spectrometry Method. *J. Am. Soc. Mass Spectrom.* **2011,** *22*, 1898-1905.

50. Wang, L.; Smith, D. L., Downsizing improves sensitivity 100-fold for hydrogen exchange-mass spectrometry. *Anal. Biochem.* **2003,** *314*, 46-53.

51. Milne, J. S.; Mayne, L.; Roder, H.; Wand, A. J.; Englander, S. W., Determinants of protein hydrogen exchange studied in equine cytochrome c. *Protein Sci.* **1998,** *7*, 739-745.

52. Andersen, C. B. F.; Torvund-Jensen, M.; Nielsen, M. J.; de Oliveira, C. L. P.; Hersleth, H. P.; Andersen, N. H.; Pedersen, J. S.; Andersen, G. R.; Moestrup, S. K., Structure of the haptoglobin-haemoglobin complex. *Nature* **2012,** *489* (7416), 456-U150.

53. Bamm, V. V.; Tsemakhovich, V. A.; Shaklai, M.; Shaklai, N., Haptoglobin Phenotypes Differ in Their Ability To Inhibit Heme Transfer from Hemoglobin to LDL. *Biochemistry* **2004,** *43*, 3899-3906.

54. Ruotolo, B. T.; Robinson, C. V., Aspects of native proteins are retained in vacuum. *Curr. Op. Chem. Biol.* **2006,** *10*, 402-408.

55. Hamdy, O. M.; Julian, R. R., Reflections on Charge State Distributions, Protein Structure, and the Mystical Mechanism of Electrospray Ionization. *J. Am. Soc. Mass Spectrom.* **2012,** *23*, 1-6.

56. Breuker, K.; McLafferty, F. W., Stepwise evolution of protein native structure with electrospray into the gas phase, 10^{-12} to 10^{2} s. *Proc. Natl. Acad. Sci. U.S.A.* **2008,** *105*, 18145-18152.

57. Deng, L.; Broom, A.; Kitova, E. N.; Richards, M. R.; Zheng, R. B.; Shoemaker, G. K.; Meiering, E. M.; Klassen, J. S., Kinetic Stability of the Streptavidin-Biotin Interaction Enhanced in the Gas Phase. *J. Am. Chem. Soc.* **2012,** *134* (40), 16586-16596

Chapter 3. Effects of Protein-Ligand Interactions on Hydrogen/Deuterium Exchange Kinetics: Canonical and Non-Canonical Scenarios

3.1. Introduction

Hydrogen/deuterium exchange (HDX) methods are widely used for monitoring protein-ligand interactions. This approach relies on the fact that ligand binding can modulate the extent of protein structural fluctuations that transiently disrupt hydrogen bonds and expose backbone amides to the solvent. It is commonly observed that ligand binding causes a reduction of HDX rates. This reduction may be restricted to elements adjacent to the binding site, but other regions can be affected as well. Qualitatively, ligand-induced HDX protection can be rationalized on the basis of two-state models that equate structural dynamics with global unfolding/refolding. Unfortunately, such models tend to be unrealistic because the dynamics of native proteins are dominated by sub-global transitions and local fluctuations. Ligand binding lowers the ground state free energy. It is not obvious why this should necessarily be accompanied by a depletion of excited state occupancies, which would be required for a reduction of HDX rates. Here, we propose a framework which implies that ligand binding can either slow down or accelerate amide deuteration throughout the protein. These scenarios are referred to as “type 1” and “type 2”, respectively. Evidence for type 1 binding is abundant in the literature, whereas the viability of type 2 interactions is less clear. Using HDX mass spectrometry (MS) we demonstrate that the oxygenation of hemoglobin (Hb) provides a dramatic example of a type 2 scenario. The observed behavior is consistent

with cooperative T $\rightarrow$ R switching, where part of the intrinsic O_2 binding energy is reinvested for destabilizing the ground state. This destabilization increases the Boltzmann occupancy of unfolded conformers, thereby enhancing HDX rates. Surprisingly, O_2 binding to myoglobin (Mb) also induces elevated HDX rates. These Mb data reveal that type 2 behavior is not limited to cooperative multi-subunit systems. Although enhanced protection from deuteration is widely considered to be a hallmark of protein-ligand interactions, this work establishes that an overall deuteration increase also represents a viable outcome. HDX-based ligand screening assays, therefore, have to allow for canonical as well as non-canonical effects.

Numerous biological processes and drug action mechanisms are mediated by noncovalent protein-ligand binding. The affinity of these interactions ranges from millimolar to sub-picomolar K_d values, with dissociation free energies that are given by $\Delta_d G^\circ = -RT \ln K_d$. For a protein P and its ligand L the dissociation constant is defined as K_d = [P][L]/[PL]. The magnitude of $\Delta_d G^\circ$ is governed by a complex interplay of entropic and enthalpic factors, with contributions originating from the protein, the ligand, and the solvent.[1-3] Methods for predicting protein-ligand affinities are still in their infancy,[4-5] largely because enthalpy-entropy compensation effects and related issues remain poorly understood.[6-11]

Isothermal titration calorimetry (ITC) is widely used for exploring thermodynamic aspects of protein-ligand interactions.[2] Binding can also be explored in titration studies with optical, NMR,[12] or mass spectrometric detection.[13-14] Nonetheless, there remains a need for improved strategies that are capable of probing thermodynamic and structural aspects of protein-ligand systems. Areas that will benefit from such initiatives include the screening of drug candidates, as well as epitope mapping applications.[15-16]

Hydrogen/deuterium exchange measurements (HDX) with mass spectrometry (MS)[17-22] or nuclear magnetic resonance (NMR) spectroscopic detection[23-32] have gained a strong foothold for protein-ligand binding studies. Exposure of a protein to a D_2O-based solvent induces the replacement of backbone amide hydrogens with deuterium. Most backbone N-H groups in natively folded proteins are engaged in hydrogen bonds. Deuteration at these sites is mediated by thermally activated opening/closing fluctuations that transiently rupture hydrogen bonds and expose N-H groups to the solvent.[33] The exchange mechanism can be expressed as[34]

$$N-H_{closed} \underset{k_{cl}}{\overset{k_{op}}{\rightleftharpoons}} N-H_{open} \xrightarrow[D_2O]{k_{ch}} exchanged \qquad (3.1)$$

where the opening and closing rate constants are designated as k_{op} and k_{cl}, respectively, and where k_{ch} is the chemical rate constant.[35]

HDX experiments are generally conducted with the expectation that ligand binding will induce a *reduction* in deuteration rates, a view that is based on a large body of prior MS[17-22] and NMR[23-32] work. This widely held paradigm implies that ligand-bound systems will tend to be "more tightly folded", and hence more resilient towards structural fluctuations of the type described in eq 2.1. A multitude of protein-ligand systems behave in accordance with this canonical scenario,[17-20,22-32,36-37] consistent with the fact that intermolecular binding is often accompanied by the formation or the strengthening of intramolecular bonds.[38-39] In favorable cases this ligand-induced HDX protection is most pronounced for regions that directly interact with the ligand. However, this is not always the case,[40-41] e.g., when the binding mechanism involves allosteric elements.[17-18,26,42]

Interestingly, it appears that ligand binding can have stabilizing as well as destabilizing effects on the protein structure.[43] For example, there are instances where ligand binding decreases deuteration rates only in some regions of the protein, whereas other regions display more extensive HDX.[42,44-46] Related differential effects have been reported on the basis of neutron scattering experiments,[47] computer simulations,[48] and NMR spin relaxation measurements.[3,9] *J*-coupling experiments have highlighted the possibility that ligand binding can induce a buildup of strain in some regions of a protein, evident from an elongation of certain backbone hydrogen-bonds.[49]

The preceding considerations call into question the view that protein-ligand interactions are generally associated with reduced deuteration rates. The current work goes one step further, and asks if it is possible that ligand binding can sometimes cause an *overall HDX acceleration*. We show that such a scenario is indeed feasible. Using hemoglobin (Hb) and myoglobin (Mb) as examples, we illustrate the entire range of possible outcomes – from strongly reduced ("type 1") to strongly increased deuteration rates ("type 2"). We propose a model that links the different types of ligand binding effects to alterations in the Boltzmann occupancy of partially unfolded conformers.

3.2. Materials and Methods

3.2.1. Proteins and Reagents.

Horse heart met-(FeIII)-Mb and sodium dithionite (NaS_2O_4) were purchased from Sigma (St. Louis, MO). Na_2HPO_4, NaH_2PO4, and NaCl were from Caledon (Georgetown, ON, Canada), and D_2O was procured from Cambridge Isotope Laboratories (Andover, MA). Protein solutions for all experiments contained 50 mM phosphate buffer, as well as 20 mM NaCl or

10 mM sodium dithionite. Apo-Mb was prepared using butanone extraction.[50] Deoxy-(FeII)-Mb was prepared by exposing met-Mb to 10 mM dithionite under nitrogen at neutral pH.[51] Deoxy-Mb was then converted to oxy-Mb by the introduction of air followed by dithionite removal on a G-25 Sephadex size exclusion column (Sigma) that was eluted with 10 mM aqueous ammonium acetate. Subsequently, the protein was dialyzed against 50 mM phosphate buffer containing 20 mM NaCl. Oxy-Hb was isolated from fresh bovine blood as described previously.[52] Deoxy-Hb was prepared by exposing oxy-Hb to 10 mM sodium dithionite and deoxygenation under nitrogen.[53] UV-Vis absorption spectra were recorded on a Cary 100 instrument (Varian, Mississauga, ON, Canada). The different heme oxidation and ligation states produced by the procedures outlined above give rise to characteristic UV-Vis absorption spectra that are consistent with reference data from the literature (Figure 3-1).[54] pH values were measured using a Fisher (Waltham, MA) AB15 pH meter, these values are reported without isotope correction.

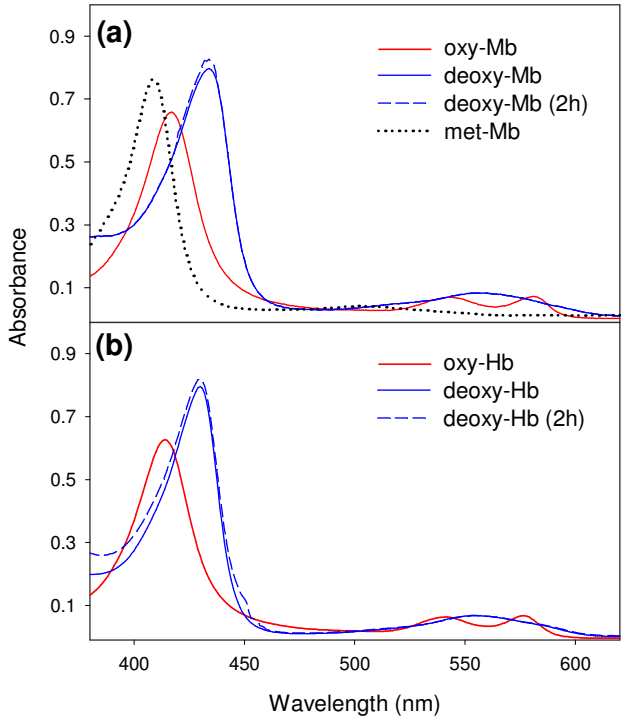

Figure 3-1: (a) UV-Vis absorption spectra of different Mb derivatives (oxy, deoxy, and met) at pH 7. (b) UV-Vis spectra of oxy- and deoxy-Hb. Also shown in both panels are spectra of the deoxy proteins after 2h of HDX with repeated removal of aliquots.

3.2.2. Hydrogen/Deuterium Exchange Mass Spectrometry.

50 µM protein (in the apo, oxy or deoxy states) in 50 mM sodium phosphate buffer containing 20 mM NaCl or 10 mM sodium dithionite was mixed with 9 volumes of D_2O containing the same buffer and salt concentrations as the stock, resulting in a protein concentration of 5 µM with a measured pH of 7.2 at room temperature (22 °C). 30 µL aliquots were removed at various time points ranging from 1 to 120 minutes after initiation of labeling. UV-Vis experiments confirmed that the deoxy-samples remained de-oxygenated throughout the experiment (Figure 3-1). The aliquots were quenched at pH 2.4 by addition of HCl on ice, followed by flash freezing in liquid nitrogen and storage at -80 °C. The aliquots

were rapidly thawed to ~0 °C and manually injected into a nanoACQUITY UPLC with HDX technology (Waters, Milford, MA)[55] for desalting and peptide separation within 15 min on an equilibrated reversed phase column (BEH C18 1.7 μm, 1 mm × 100 mm) using a water/acetonitrile gradient in the presence of 0.1% formic acid at 35 μL min^{-1}. Online digestion was performed using a POROS pepsin column (2.1 mm × 30 mm) from Life Technologies/Applied Biosystems (Carlsbad, CA) at 15 °C. The temperature for peptide trapping and reversed phase separation was set to 0 °C. Blank (water) injections were performed in-between protein injections to eliminate carryover. Peptide mass analysis was performed on a Waters Synapt HDMS instrument with source and desolvation temperatures of 80 and 300 °C, respectively, a cone voltage of 30 V, and an electrospray voltage of 2.8 kV. The identity of each peptide was confirmed by tandem MS based on the known sequences (Figure 3-2 and 3-3).

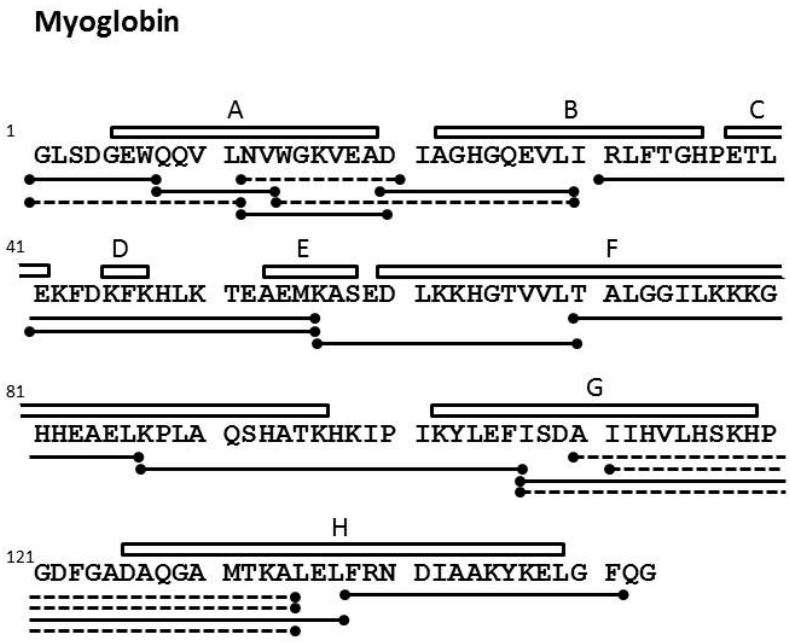

Figure 3-2: Peptic cleavage map of Mb. Solid lines represent peptides used for data analysis, and dashed lines represent redundant fragments. Helices are indicated by boxes

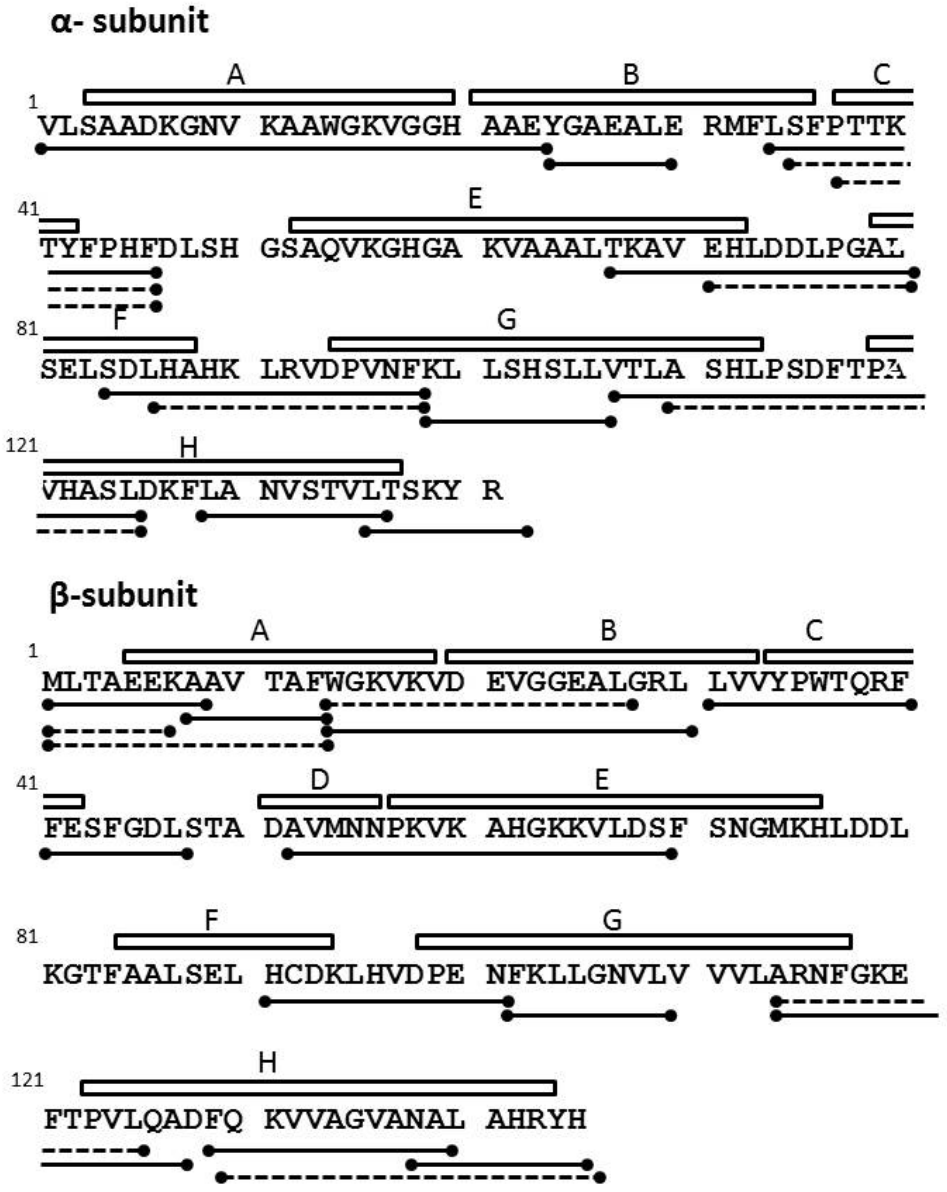

Figure 3-3: Sequence of the Hb α and β subunits. Solid lines represent peptides used for data analysis, and dashed lines represent redundant fragments. Helices are indicated by boxes.

Zero time point controls (m_0) for the correction of artifactual in-exchange were performed by exposing the proteins to premixed D_2O and quenching buffer, using the

solutions described above. Fully exchanged control samples (m_{100}, for the correction of artifactual back exchange) were prepared by incubating 5 μM protein in labeling solution at pH 2.4 for 9 h (Hb) or 48 h (Mb). For measuring HDX kinetic profiles the centroid mass of all peptides as a function of labeling time was determined using HX-Express(Figure 3-4 and 3-5).[56]

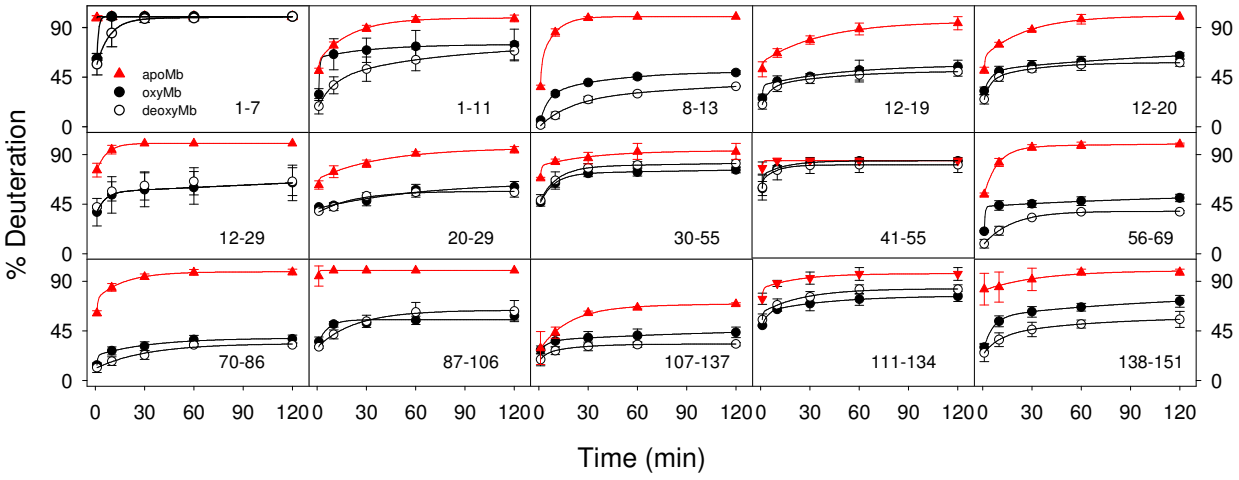

Figure 3-4: HDX kinetics of peptides covering the sequence of Mb showing deoxy-Mb (open black circles) and oxy-Mb (filled circles). Residue numbers of the individual peptides are indicated in each panel. Also shown are data acquired for apo-Mb (filled red triangles).

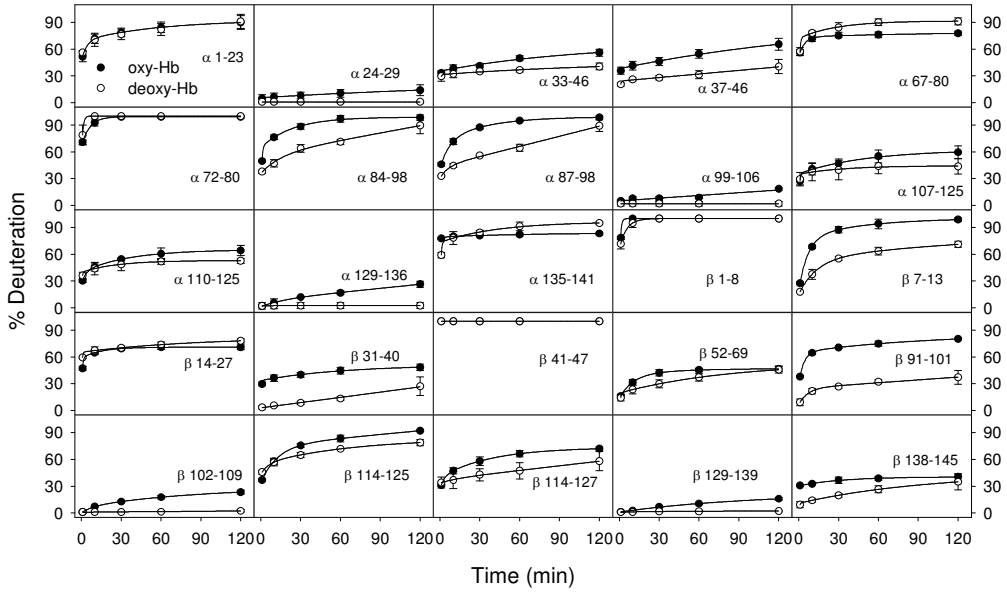

Figure 3-5: HDX kinetics of peptides covering the α and β subunits of oxy-Hb (filled symbols) and deoxy-Hb (open symbols). Residue numbers are indicated in each panel. Lines are biexponential fits.

The resulting data are reported as *% Deuteration* = $(m-m_0)/(m_{100}-m_0)$. Intact protein HDX/MS was conducted without using the integrated HDX module. Protein separation was performed on a C4 column (BEH300 C4 1.7 µm, 2.1 mm × 50 mm) at a flow rate of 200 μL min^{-1}. The injection loop volume was 20 μL and the total amount of protein per injection was 100 pmol. The injection syringe, column, injector and solvent delivery lines were kept at 0 °C in an ice bath. All measurements were conducted in triplicate; error bars represent standard deviations.

3.3. Results and Discussion

3.3.1. Thermodynamic Considerations.

Prior to discussing experimental data, it is necessary to examine the connection between ligand binding and HDX kinetics. Under EX2 conditions ($k_{cl} >> k_{ch}$) the deuteration rate constant k_{HDX} of a backbone N-H within the framework of eq 2.1 can be expressed as

$$k_{HDX} = p_{op}\, k_{ch} \tag{3.2}$$

where p_{op} is the fraction of time that the site spends in the open state.[33] A lowering of k_{HDX} does not necessarily imply that the protein becomes "more rigid" in the sense that it loses conformational entropy, has less extensive RMS fluctuations, or slows down its closed ↔ open interconversion. Instead, according to eq 2 the only unambiguous conclusion that can be drawn from a reduced EX2 rate is that amides spend less time in the open state.

Using Boltzmann statistics,[57] p_{op} can be calculated according to

$$p_{op} = \frac{e^{-\frac{\Delta_{op}G^\circ}{RT}}}{Z} \tag{3.3}$$

where $\Delta_{op}G^\circ$ is the opening free energy and $Z = 1 + \exp(-\Delta_{op}G^\circ/RT)$ is the partition function.[58] For a stable protein $k_{cl} >> k_{op}$, such that $\Delta_{op}G^\circ >> 0$ and $Z \approx 1$. [Note that One can define an opening equilibrium constant $K_{op} = \exp(-\Delta_{op}G^\circ/RT)$, such that eq 2.2 turns into the well-known expression $k_{HDX} = K_{op}\ k_{ch}$. For interpreting protein-ligand interactions it is advantageous to use an alternative approach that retains the exponential notation of eq 2.3.]

The occupancy of the closed state is $1/Z \approx 1$. When expressing free energy in *RT* units ($\Delta_{op}G° = \Delta j \times RT$) the excited state occupancy becomes $p_{op} = \exp(-\Delta j)$ such that

$$k_{HDX} = e^{-\Delta j} k_{ch} \qquad (3.4)$$

We will first discuss ligand binding effects for a hypothetical two-state protein that undergoes conformational fluctuations between its native (N) and unfolded conformation (U). This textbook approach (Figure 3.6)[22,59] envisions that N can form a complex NL, whereas U is incapable of ligand binding. Opening/closing transitions (eq 1) are equivalent to global unfolding/refolding for this two-state system. We arbitrarily assume that in the absence of ligand $\Delta_{op}G° = 4\ RT$, such that $p_{op} = e^{-4}$ (Figure 3-6A). Figure 3-6B illustrates what happens when ligand binding lowers the standard free energy of the ground state by $\Delta_d G° = 2\ RT$. This widening of the free energy gap changes p_{op} from e^{-4} to e^{-6}, thereby reducing k_{HDX} (eq 2.4). This example demonstrates that alterations of excited state occupancies are key to understanding ligand binding effects in HDX studies.

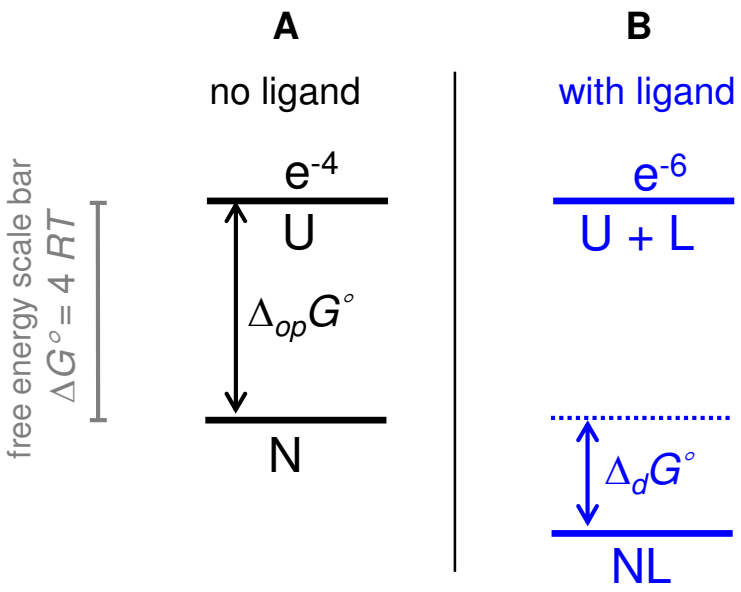

Figure 3-6: Free energy level diagram of a two-state protein that can bind a ligand L in the ground state only. (A) No ligand present. U (open) is separated from the ground state N (closed) by 4 *RT*, resulting in an excited state occupancy of e^{-4}. (B) Ligand binding widens the gap between U and the new ground state NL to 6 *RT*. The excited state occupancy drops to e^{-6} and k_{HDX} decreases according to eq 3.4.

Unfortunately, the two-state model of Figure 3-6 represents an oversimplification (except for special cases[33]). Under realistic conditions the opening/closing dynamics of proteins are dominated by a multitude of sub-global events such as foldon fluctuations, fraying, and local dynamics down to the individual amide level.[33,36,60-61] Most of these spatially confined events can proceed without dissociation of the PL complex. It is not obvious, therefore, why ligand binding should always widen the free energy gaps between the ground state and partially unfolded conformers. In other words, it seems unjustified to expect that binding will generally decrease k_{HDX}. A closer examination of this issue requires a refined model.

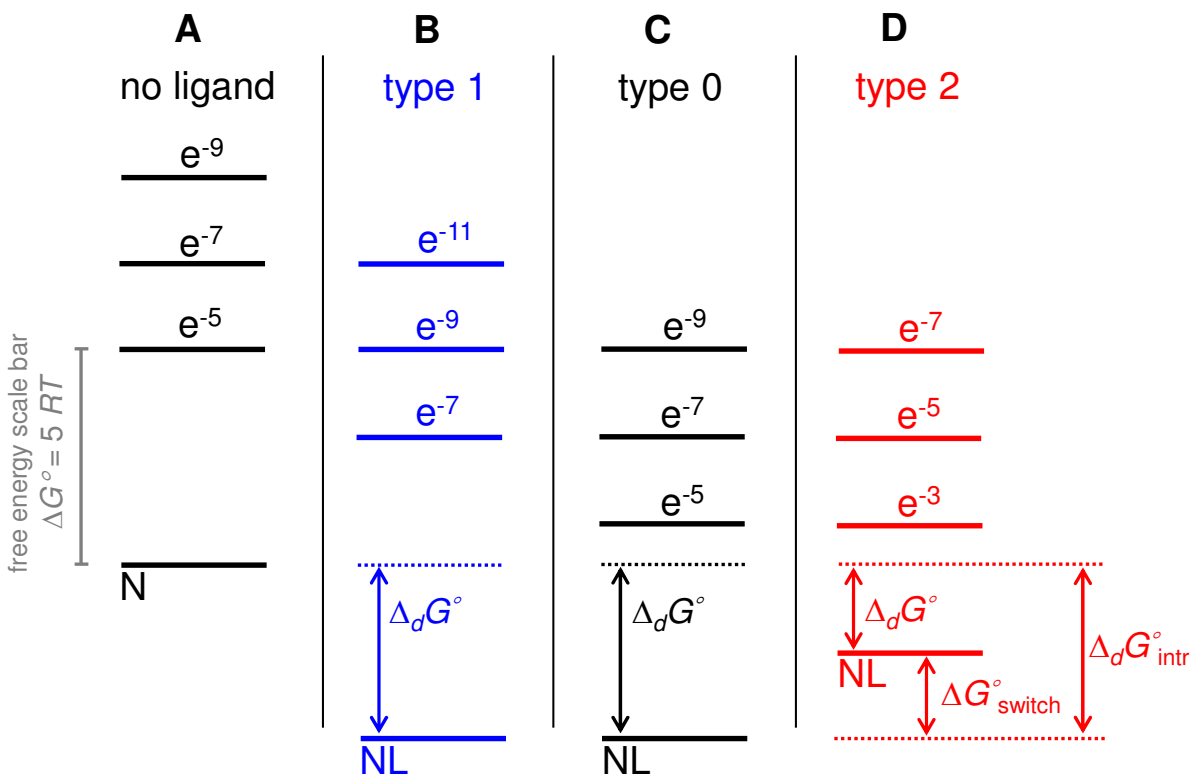

Figure 3-7: Free energy level diagram of a protein that can adopt many partially unfolded ligand-bound states. Only three of these are shown. The Boltzmann occupancy of each state is exp(-Δ*j*). Ligand binding lowers the free energy of the ground state by $\Delta_d G°$. (A) No ligand present. Excited states are assumed to be Δj = 5, 7, and 9 *RT* units above the ground state; (B) Type 1 scenario, where ligand binding lowers HDX rates. Excited state populations are reduced relative to (A), and k_{HDX} decreases. (C) Type 0 scenario, where excited state populations and HDX kinetics remain unchanged after binding. (D) Type 2 scenario, where excited state populations are increased such that deuteration proceeds more rapidly after binding. The overall binding affinity in (D) is determined by two competing contributions (eq 3.5).

Figure 3-7A schematically illustrates the many thermally excited states that are accessible to a ligand-free protein under native solvent conditions. Each of these excited levels (only three are shown to prevent clutter) represents a conformation where a certain subset of amides is open, whereas the ground state N is all-closed. The occupancy of each level is given by eq 3.3, with the caveat that the partition function now becomes $Z = 1 + \Sigma \exp(-\Delta j)$ where the sum extends over all possible conformers. Nonetheless, the

approximation $Z \approx 1$ still holds because $k_{cl} >> k_{op}$.[23,24] This implies that the occupancy of each excited state can still be expressed as $p = \exp(-\Delta j)$, and that eq3.4 remains valid. Ligand binding will shift the free energy levels of the ground state, as well as those of the partially open conformers. We will have a look at three conceivable types of outcomes, all of which are scaled such that the NL ground state corresponds to $\Delta j = 0$.

Type 1: Ligand binding lowers the free energy of NL by $\Delta_d G°$ (chosen to be 4 *RT* in Figure 3-7B). Protein-ligand contacts cause a strengthening of intramolecular bonds via entropic cooperativity and local concentration effects.[59] As a consequence, transitions to excited conformers are associated with wider free energy gaps (larger Δj values) than in the absence of ligand. The lower occupancy of partially unfolded conformers causes a *decrease* of HDX rates, as dictated by eq 3.4.

Type 0: A ligand binds with the same affinity as in the previous case ($\Delta_d G° = 4\ RT$), but in a fashion that has only very minor effects on the internal energy landscape of the protein. For example, the ligand might interact with a solvent-exposed side chain.[62] In this case all of the excited conformations will shift down by the same amount $\Delta_d G°$ as the NL ground state. The Δj values under these conditions will remain the same as for the ligand-free case. Hence, ligand binding will cause *no change* in the HDX kinetics (Figure 3-7C).

Type 2: We consider a protein with a binding site that possesses a large intrinsic affinity $\Delta_d G°_{\text{intr}}$. However, the ligand can only be accommodated in the NL ground state after an unfavorable structural change has taken place. This conformational switching event is associated with a free energy "penalty" termed $\Delta G°_{\text{switch}}$. The overall binding affinity in this scenario is the sum of two opposing contributions.

$$\Delta_d G^\circ = |\Delta_d G^\circ_{intr}| - |\Delta G^\circ_{switch}| \qquad (3.5)$$

The NL ground state remains thermodynamically favored as long as $\Delta_d G^\circ > 0$. Ligand-induced distortion of the protein implies that conformers with open N-H sites are more readily accessible than in the absence of L. Thus, ligand binding lowers Δj values, resulting in *increased* HDX rates throughout the protein (eq 3.4, Figure 3-7D).

The countless published examples[17-20,22-32,36-37] of HDX rate reduction following ligand binding demonstrate that Type 1 interactions represent by far the most common scenario. Reports of Type 0 behavior are more scarce, although the use of HDX/MS for verifying the absence of perturbations in antibody-drug conjugates is relevant in this context.[63] Type 2 behavior has been rarely, if ever, discussed. It remains unclear if (and under what conditions) the occurrence of globally accelerated HDX kinetics after ligand binding is a realistic scenario.

3.3.2. Oxygenation of Hemoglobin: Type 2 Binding.

Hb consists of two symmetric heterodimers, α1β1 and α2β2. The helical subunits within each dimer interact closely with one another, whereas contacts across the α1β1/α2β2 interfaces are less extensive.[64] Each subunit can bind O_2 at its Fe(2+) heme. The cooperative deoxy (T) → oxy (R) transition has been explored in great detail.[54,65-68] Oxygenation causes a ~15° rotation of α1β1 relative to α2β2,[65-66] thereby disrupting salt bridges between the Lys40(α1/2) side chains and the β2/1 C-termini.[67] Other α1β1/α2β2 contacts are weakened as well. The structural distortion upon O_2 binding carries a significant free energy penalty ΔG°_{switch},[68-70] making Hb a likely candidate for a type 2 scenario.

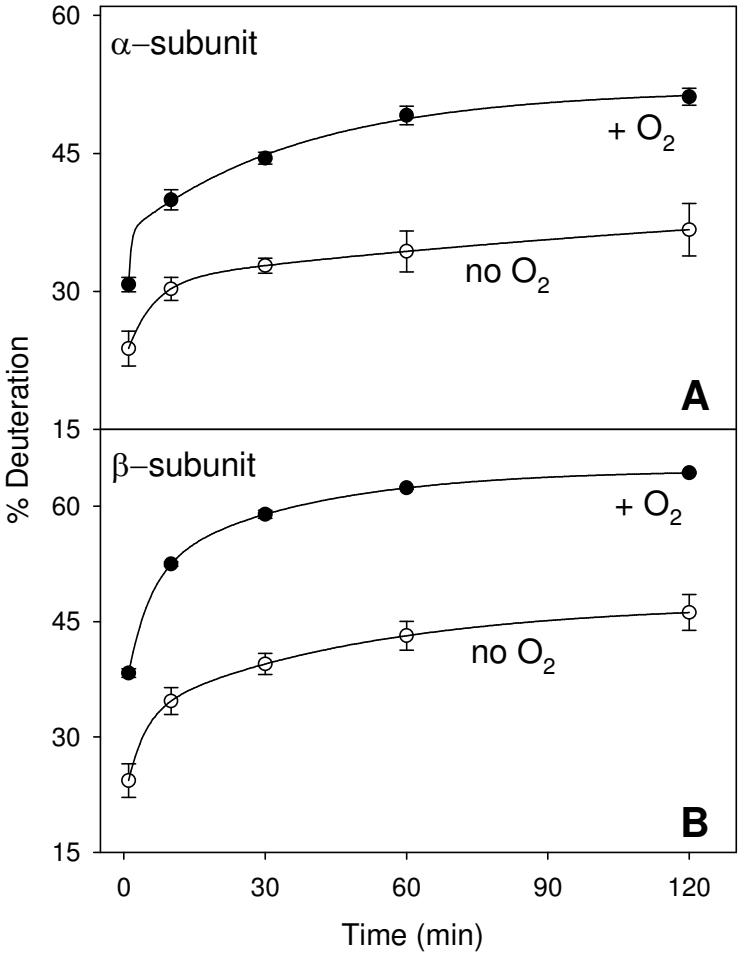

Figure 3-8: HDX kinetics of deoxy-Hb (open symbols) and oxy-Hb (filled symbols). The two panels show data for the intact α (A) and β subunits (B) of the tetramer. Solid lines are biexponential fits.

HDX/MS experiments on deoxy- and oxy-Hb were conducted in neutral solution. Intact subunit measurements reveal that deuteration is greatly elevated for oxy-Hb compared to deoxy-Hb. When averaged over the 2 h experimental time window, the deuteration increase for α- and β-globin after oxygenation is about 15% and 20%, respectively (Figure 3-8). These data reveal that Hb indeed represents a type 2 binder. Our findings are consistent

with earlier tritium labeling and HDX work.[71-72] However, those studies did not discuss the unusual nature of Hb-O_2 interactions, which are different from the type 1 binding behavior seen for most other proteins.[17-20,22,36-37]

Spatially-resolved HDX data were obtained using pepsin digestion and LC-MS. The resulting peptide deuteration kinetics reflect the opening/closing dynamics exhibited by individual Hb regions (Figures 3-3, 3-5). Deuteration percentages for t = 60 min were mapped onto Hb crystal structures (Figure 3-9A, B). Segments in the interior of the tetramer tend to be strongly protected (e.g., the center portions of helices G and H in both subunits, Figure 3-9A, B, blue). Peripheral elements such as helices αA and βA exchange quite rapidly (Figure 3-9B, red). The difference map of Figure 3-9C highlights the changes in deuteration after oxygen binding. More extensive HDX takes place predominantly for elements that contact the α1β1/α2β2 interfaces. Large deuteration increases are also seen for α87-98 and β91-101 (Figure 3-5, Figure 3-9C, red). These two peptides comprise the proximal iron ligands αHis87 and βHis91 which play a key role for transmitting movements of the iron centers to the F helices.[67] Thus, protein elements that directly participate in cooperative T → R switching are those for which type 2 behavior is most pronounced.

The type 2 behavior of Hb reflects free energy partitioning upon oxygenation, consistent with the model put forward in Figure 3-7D and eq 3.5. The intrinsic O_2 binding free energy is $\Delta_d G°_{intr}$ = 34 kJ mol^{-1} heme^{-1} when averaged over all four binding steps from the deoxy-T to oxy-R.[68] This intrinsic contribution arises from interactions of O_2 with the Fe(2+) center and hydrogen bonding with the distal His of helix E.[73] A significant fraction of this free energy ($\Delta G°_{switch}$ = 7 kJ mol^{-1} heme^{-1}) is used up for T → R switching of the protein

scaffold,[68] thereby destabilizing the ground state structure and enhancing HDX kinetics as dictated by eq 3.4. The resulting overall O_2 binding affinity is $\Delta_d G° = 34 - 7 = 27$ kJ mol^{-1} heme^{-1} (eq 3.5).[68]

On the basis of these Hb data it is tempting to speculate that type 2 HDX might be limited to cooperative multi-subunit systems. Interestingly, the observations discussed below reveal that this is not the case.

3.3.3. Type 2 Oxygen Binding to Myoglobin.

Mb is a monomeric protein with a fold very similar to that of α- and β-globin.[74] Mb-O_2 interactions are virtually identical to those in Hb, involving a Fe(2+) heme and a distal His.[54] However, protein structural changes upon Mb oxygenation are much less extensive than for Hb.[74] The average RMS displacement after O_2 binding is only 0.2 Å for Mb, whereas that of Hb is 1.1 Å.[75] Due to the lack of subunit cooperativity Mb exhibits a hyperbolic O_2 binding profile, while the Hb oxygenation curve is sigmoidal.[76] Thus, Mb represents an ideal model system for scrutinizing possible linkages between binding cooperativity and type 2 behavior.

Intact protein data reveal that oxy-Mb shows more extensive HDX than deoxy-Mb (Figure 3-10). The deuteration enhancement is roughly one third of that seen for Hb (Figure 3-8). Nonetheless, Figure 3-10 clearly demonstrates that O_2 binding to Mb also represents a type 2 scenario. In other words, type 2 effects are *not* limited to proteins with multi-subunit cooperativity.

Spatially-resolved HDX/MS measurements for Mb (Figure 3-2, 3-4) reveal extensive structural dynamics in the N-terminus, and in the B/C/D loop region (Figure 3-11A, B). O_2 binding significantly increases HDX levels in helices A and H (Figure 3-11C, red),

resembling the behavior seen for Hb (Figure 3-9C). In addition, oxygenated Mb shows strongly enhanced deuteration in helix E (Figure 3-11C, red) which participates in ligand binding via the distal His64. This accelerated deuteration of helix E is somewhat different from the behavior seen for Hb, where HDX enhancements are more pronounced on the proximal side of the heme (helix βF, Figure 3-9C).

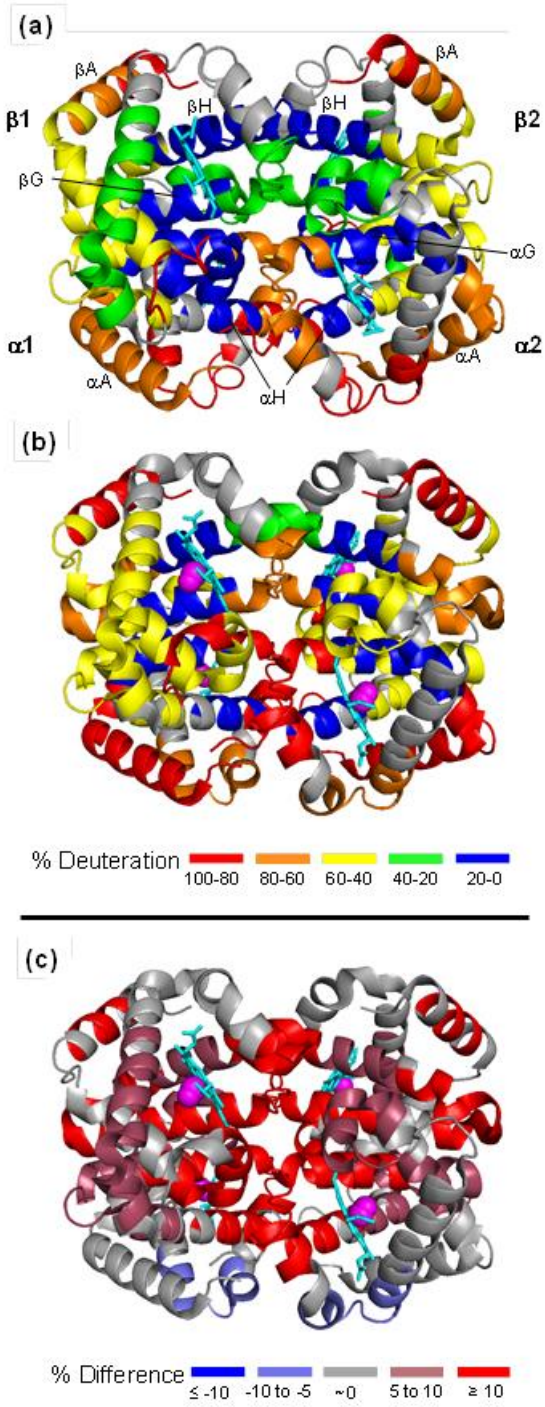

Figure 3-9: Spatially-resolved deuteration pattern of (A) deoxy-Hb and (B) oxy-Hb for t = 60 min (PDB files 1HDA[77] and 2QSS[78]). Complete time profiles are shown in Figure S3. (C) HDX difference map averaged over the 2h experimental time window; red represents segments that show most strongly elevated deuteration after O_2 binding.

The observation of type 2 behavior for Mb suggests that O_2 binding to this protein is also

associated with a free energy penalty $\Delta G°_{switch}$ (eq 3.5). However, this $\Delta G°_{switch}$ must be smaller than the corresponding Hb value (less than 7 kJ mol^{-1}),[68-69] as implied by two observations: (1) deuteration enhancements are less pronounced for Mb than for Hb (Figures 2.3, 2.5). (2) Although $\Delta_d G°_{intr}$ is virtually identical for the two proteins, the overall O_2 binding affinity of Mb ($\Delta_d G°$ = 35 kJ mol^{-1})[73] is larger than that of Hb (27 kJ mol^{-1} $heme^{-1}$).[68] In the case of Hb it is clear that $\Delta G°_{switch}$ is dissipated via the disruption of protein-protein contacts during T $\rightarrow$ R switching.[68] In the case of Mb the fate of this free energy contribution is not as clear. Our observations, as well as existing X-ray data[74-75] are consistent with the view that oxygenation-induced local changes on the heme build up conformational strain in the protein. The Mb elements affected by this phenomenon display elevated deuteration rates as a result of their increased p_{op} values (red in Figure 3-11C).

3.3.4. Heme Binding to Apo-Myoglobin: A Type 1 Event.

Heme binding to apo-Mb results in significant stabilization of the protein. This transition has been studied extensively,[79-80] but we include it here for completeness as an example of a type 1 scenario. Heme makes numerous contacts within the hydrophobic binding pocket of the protein, in addition to iron ligation by the proximal His93 in helix F.[81]

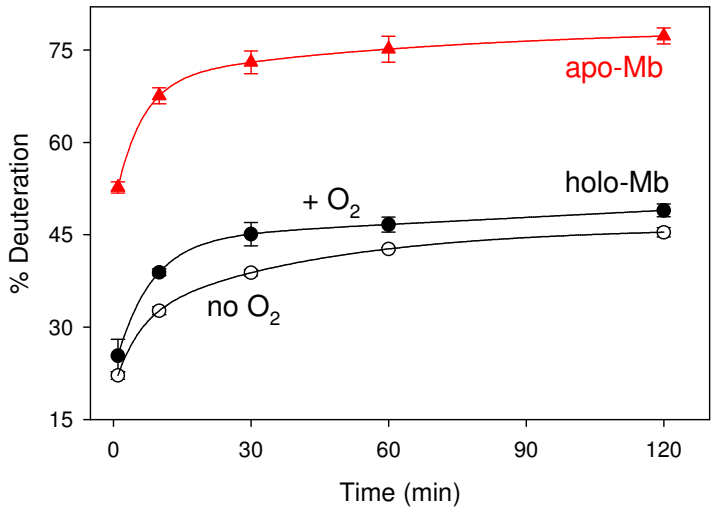

Figure 3-10: Intact protein HDX kinetics of holo-Mb in the oxy-state (filled symbols) and in the deoxy-state (open symbols). Also included are data for the heme-free protein (apo-Mb, red).

Heme-bound Mb exhibits dramatically lower deuteration values than the apo-state (Figure 3-10). Spatially resolved measurements (Figure 3-2) show that this stabilization affects all regions of the protein (Figure 3-12A, B). The largest changes are seen around helix F (Figure 3-2) which adopts a well-defined structure only in the presence of heme.[79] The type 1 character of the apo-Mb → holo-Mb transition is readily apparent from the HDX difference map of Figure 3-12C which is completely blue. This has to be contrasted with the red difference maps that apply to the oxygenation events discussed above (type 2 behavior, Figure 3-9C, 3-11C).

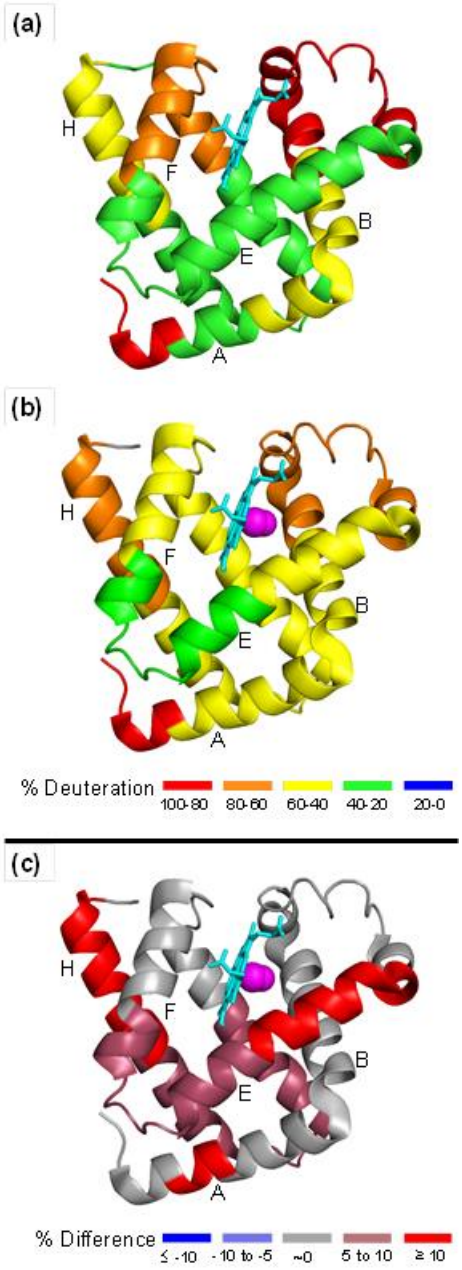

Figure 3-11: Spatially-resolved deuteration pattern of (A) deoxy-Mb and (B) oxy-Mb for t = 60 min (PDB files 2V1K[82] and 1DWR[83]). Complete time profiles are shown in Figure S5. (C) HDX difference map averaged over the 2h experimental time window; red represents segments that show most strongly elevated deuteration after O_2 binding.

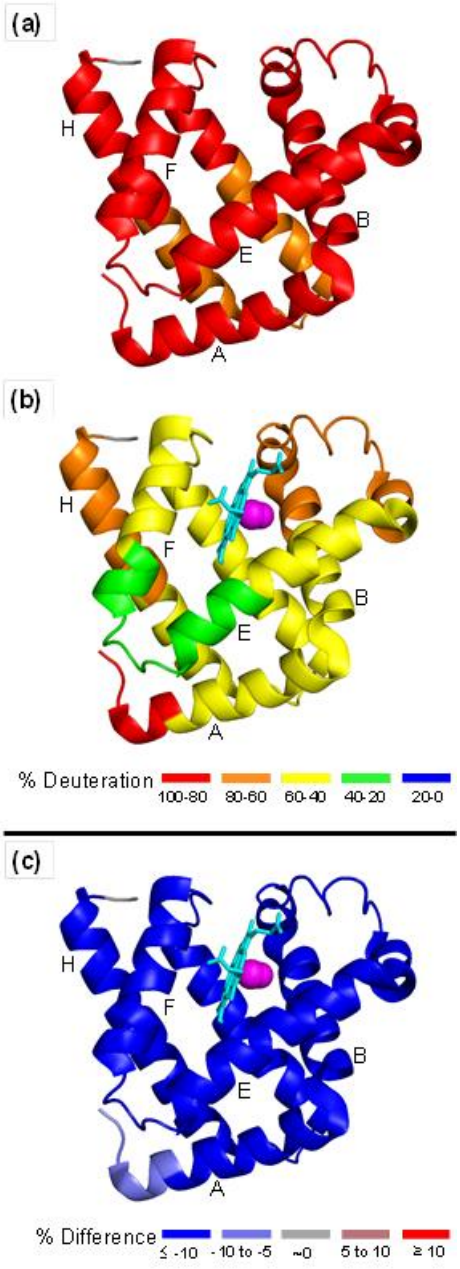

Figure 3-12: Spatially-resolved deuteration pattern of (A) apo-Mb and (B) oxy-Mb for t = 60 min. PDB file 1DWR[83] was used for both panels because high resolution X-ray data for apo-Mb are not available. (C) Difference map averaged over the 2h experimental time window; regions that show less extensive HDX in the presence of heme are highlighted in dark blue.

3.4. Conclusions

This work demonstrates that protein-ligand interactions can result in a wide range of HDX signatures. Binding can cause a global decrease of deuteration rates (type 1), or it may cause accelerated deuteration (type 2). Both of these extremes are thermodynamically feasible because the ensemble-averaged behavior of a protein is dominated by the ground state. Binding is a spontaneous process as long as the free energy of NL is lower than that of N (Figure 3-7). This criterion for spontaneity is irrespective of the excited state behavior, because the cumulative Boltzmann occupancy of the corresponding conformers is low.[33] Nonetheless, it is these sparsely populated open states that govern the HDX properties of the protein according to eqs 3.1, 3.4. The largely unpredictable ligand-induced changes of Δj values translate into a range of possible deuteration scenarios (Figure 3-7). Type 1 and 2 scenarios are both compatible with either induced fit or conformational selection modes of binding, whereas type 0 behavior may be more appropriately described as a lock-and-key interaction.[84-85]

The observation of type 2 behavior is, perhaps, not so surprising in the case of Hb due to the known interplay between $\Delta G°_{\text{switch}}$ and $\Delta_d G°_{\text{intr}}$ which is a common feature of cooperative multi-subunit proteins (Figure 3-7D).[68] However, the observation that oxygenation of Mb also represents a type 2 transition demonstrates that ligand-induced deuteration enhancements are not limited to cooperative systems with multiple binding sites.

The cartoon representation of Figure 3-7 depicts just three conceivable scenarios that might be encountered upon ligand binding. Other cases are certainly possible. For example, data consistent with mixed type 1/0/2 scenarios have been reported.[42,44-46] Also, individual amide N-H groups do not have to remain associated with a certain type of opening event.

Ligand-induced changes of the protein energy landscape may cause N-H sites to move within the excited state manifold, e.g., from a low level in Figure 3-7A to a higher one in Figure 3-7B. Such differential free energy shifts provide an opportunity for binding site mapping, keeping in mind that allosteric effects have to be considered for this type of experiment.[17-18,42]

The prevalence of type 1 binding in the literature tends to foster the view that reduced deuteration rates are a general hallmark of protein-ligand interactions.[17-20,22-32,36-37] Our findings demonstrate that it is easy to overlook biologically important interactions when using screening approaches that exclusively focus on such type 1 scenarios. The observation of type 2 behavior for two of the most "mundane" protein-ligand complexes (Hb-O_2 and Mb-O_2) suggests that non-canonical HDX scenarios may be more common than currently thought. In any case, practitioners have to be aware that biological interactions in different proteins may elicit very different types of HDX responses.

3.5. References

1. Bissantz, C.; Kuhn, B.; Stahl, M., A Medicinal Chemist's Guide to Molecular Interactions. *J. Med. Chem.* **2010,** *53*, 5061-5084.

2. Garbett, N. C.; Chaires, J. B., Thermodynamic studies for drug design and screening. *Expert. Opin. Drug Discov.* **2012,** *7* (4), 299-314.

3. Tzeng, S.-R.; Kalodimos, C. G., Dynamic activation of an allosteric regulatory protein. *Nature* **2009,** *462* (7271), 368-372.

4. Martin, S. F.; Clements, J. H., Correlating Structure and Energetics in Protein-Ligand Interactions: Paradigms and Paradoxes. *Annu. Rev. Biochem.* **2013,** *82*, 267-293.

5. Dill, K. A.; MacCallum, J. L., The Protein-Folding Problem, 50 Years On. *Science* **2012,** *338*, 1042-1046.

6. Breiten, B.; Lockett, M. R.; Sherman, W. V.; Fujita, S.; Al-Sayah, M.; Lange, H.; Bowers, C. M.; Heroux, A.; Krilov, G.; Whitesides, G. M., Water Networks Contribute to Enthalpy/Entropy Compensation in Protein–Ligand Binding. *J. Am. Chem. Soc.* **2013,** *135* (41), 15579-15584.

7. Chodera, J. D.; Mobley, D. L., Entropy-Enthalpy Compensation: Role and Ramifications in Biomolecular Ligand Recognition and Design. *Annu. Rev. Biophys.* **2013,** *42*, 121-142.

8. Ford, D. M., Enthalpy-Entropy Compensation is Not a General Feature of Weak Association. *J. Am. Chem. Soc.* **2005,** *127*, 16167-16170.

9. Diehl, C.; Engstrom, O.; Delaine, T.; Hakansson, M.; Genheden, S.; Modig, K.; Leffler, H.; Ryde, U.; Nilsson, U. J.; Akke, M., Protein Flexibility and Conformational

Entropy in Ligand Design Targeting the Carbohydrate Recognition Domain of Galectin-3. *J. Am. Chem. Soc.* **2010,** *132* (41), 14577-14589.

10. Fernandez, T. F.; Samal, A. B.; Bedwell, G. J.; Chen, Y. B.; Saad, J. S., Structural and Biophysical Characterization of the Interactions between the Death Domain of Fas Receptor and Calmodulin. *J. Biol. Chem.* **2013,** *288* (30), 21898-21908.

11. Skowronsky, R. A.; Schroeter, M.; Baxley, T.; Li, Y. M.; Chalovich, J. M.; Spuches, A. M., Thermodynamics and molecular dynamics simulations of calcium binding to the regulatory site of human cardiac troponin C: evidence for communication with the structural calcium binding sites. *J. Biol. Inorg. Chem.* **2013,** *18* (1), 49-58.

12. Duncan, K. E.; Dempsey, B. R.; Killip, L. E.; Adams, J.; Bailey, M. L.; Lajoie, G. A.; Litchfield, D. W.; Brandl, C. J.; Shaw, G. S.; Shilton, B. H., Discovery and Characterization of a Nonphosphorylated Cyclic Peptide Inhibitor of the Peptidylprolyl Isomerase, Pin1. *J. Med. Chem.* **2011,** *54* (11), 3854-3865.

13. Kitova, E. N.; El-Hawiet, A.; Schnier, P. D.; Klassen, J. S., Reliable Determinations of Protein–Ligand Interactions by Direct ESI-MS Measurements. Are We There Yet? *J. Am. Soc. Mass Spectrom.* **2012,** *23*, 431-441.

14. Daniel, J. M.; Friess, S. D.; Rajagopalan, S.; Wendt, S.; Zenobi, R., Quantitative determination of noncovalent binding interactions using soft ionization mass spectrometry. *Int. J. Mass Spectrom.* **2002,** *216*, 1-27.

15. Clementi, N.; Mancini, N.; Castelli, M.; Clementi, M.; Burioni, R., Characterization of epitopes recognized by monoclonal antibodies: experimental approaches supported by freely accessible bioinformatic tools. *Drug Discov. Today* **2013,** *18* (9-10), 464-471.

16. Pandit, D.; Tuske, S. J.; Coales, S. J.; Yen, S.; Liu, A.; Lee, J. E.; Morrow, J. A.; Nemeth, J. F.; Hamuro, Y., Mapping of discontinuous conformational epitopes by amide

hydrogen/deuterium exchange mass spectrometry and computational docking. *J. Mol. Recognit.* **2012,** *25* (3), 114-124.

17. Percy, A. J.; Rey, M.; Burns, K. M.; Schriemer, D. C., Probing protein interactions with hydrogen/deuterium exchange and mass spectrometry-A review. *Anal. Chim. Acta* **2012,** *721*, 7-21.

18. Chalmers, M. J.; Busby, S. A.; Pascal, B. D.; West, G. M.; Griffin, P. R., Differential hydrogen/deuterium exchange mass spectrometry analysis of protein-Ligand interactions. *Exp. Rev. Proteomics* **2011,** *8*, 43-59.

19. Wales, T. E.; Engen, J. R., Hydrogen Exchange Mass Spectrometry for the Analysis of Protein Dynamics. *Mass Spectrom. Rev.* **2006,** *25*, 158-170.

20. Zhu, M. M.; Rempel, D. L.; Du, Z. H.; Gross, M. L., Quantification of protein-ligand interactions by mass spectrometry, titration, and H/D exchange: PLIMSTEX. *J. Am. Chem. Soc.* **2003,** *125* (18), 5252-5253.

21. Powell, K. D.; Ghaemmaghami, S.; Wang, M. Z.; Ma, L.; Oas, T. G.; Fitzgerald, M. C., A General Mass Spectrometry-Based Assay for the Quantitation of Protein-Ligand Binding Interactions in Solution. *J. Am. Chem. Soc.* **2002,** *124*, 10256-10257.

22. Konermann, L.; Pan, J.; Liu, Y., Hydrogen Exchange Mass Spectrometry for Studying Protein Structure and Dynamics. *Chem. Soc. Rev.* **2011,** *40*, 1224-1234.

23. Paterson, Y.; Englander, S. W.; Roder, H., An Antibody-Binding Site on Cytochrome-C Defined by Hydrogen-Exchange and 2-Dimensional NMR. *Science* **1990,** *249* (4970), 755-759.

24. Mayne, L.; Paterson, Y.; Cerasoli, D.; Englander, S. W., Effect of Antibody Binding on Protein Motions Studied by Hydrogen-Exchange Labeling and 2-Dimensional NMR. *Biochemistry* **1992,** *31* (44), 10678-10685.

25. Werner, M. H.; Wemmer, D. E., Identification of a Protein-binding Surface by Differential Amide Hydrogen-Exchange Measurements - Application to Bowman-Birk Serine-Protease Inhibitor. *J. Mol. Biol.* **1992,** *225* (3), 873-889.

26. Benjamin, D. C.; Williams, D. C.; Smithgill, S. J.; Rule, G. S., Long-Range Changes in a Protein Antigen Due to Antigen-Antibody Interactions. *Biochemistry* **1992,** *31* (40), 9539-9545.

27. Orban, J.; Alexander, P.; Bryan, P., Hydrogen-Deuterium Exchange in the Free and Immunoglobulin G-Bound Protein-G B-Domain. *Biochemistry* **1994,** *33* (19), 5702-5710.

28. Yi, Q.; Erman, J. E.; Satterlee, J. D., Studies of Protein-Protein Association between Yeast Cytochrome-C Peroxidase and Yeast Iso-1 Ferricytochrome-C by Hydrogen-Deuterium Exchange Labeling and Proton NMR-Spectroscopy. *Biochemistry* **1994,** *33* (40), 12032-12041.

29. Wang, C. Y.; Pawley, N. H.; Nicholson, L. K., The role of backbone motions in ligand binding to the c-Src SH3 domain. *J. Mol. Biol.* **2001,** *313* (4), 873-887.

30. Williams, D. C.; Rule, G. S.; Poljak, R. J.; Benjamin, D. C., Reduction in the amide hydrogen exchange rates of an anti-lysozyme Fv fragment due to formation of the Fv-lysozyme complex. *J. Mol. Biol.* **1997,** *270* (5), 751-762.

31. Massiah, M. A.; Saraswat, V.; Azurmendi, H. F.; Mildvan, A. S., Solution structure and NH exchange studies of the MutT pyrophosphohydrolase complexed with Mg2+ and 8-oxo-dGMP, a tightly bound product. *Biochemistry* **2003,** *42* (34), 10140-10154.

32. Emerson, S. D.; Palermo, R.; Liu, C. M.; Tilley, J. W.; Chen, L.; Danho, W.; Madison, V. S.; Greeley, D. N.; Ju, G.; Fry, D. C., NMR characterization of interleukin-2 in

complexes with the IL-2R alpha receptor component, and with low molecular weight compounds that inhibit the IL-2/IL-R alpha interaction. *Protein Sci.* **2003,** *12* (4), 811-822.

33. Englander, S. W.; Mayne, L.; Krishna, M. M. G., Protein folding and misfolding: mechanism and principles. *Quart. Rev. Biophys.* **2007,** *40*, 287-326.

34. Hvidt, A.; Nielsen, S. O., Hydrogen exchange in proteins. *Adv. Protein Chem.* **1966,** *21*, 287-386.

35. Bai, Y.; Milne, J. S.; Mayne, L.; Englander, S. W., Primary Structure Effects on Peptide Group Hydrogen Exchange. *Proteins: Struct., Funct., Genet.* **1993,** *17*, 75-86.

36. Kaltashov, I. A.; Bobst, C. E.; Abzalimov, R. R., Mass spectrometry-based methods to study protein architecture and dynamics. *Protein Sci.* **2013,** *22* (5), 530-544.

37. Trelle, M. B.; Hirschberg, D.; Jansson, A.; Ploug, M.; Roepstorff, P.; Andreasen, P. A.; Jørgensen, T. J. D., Hydrogen/Deuterium Exchange Mass Spectrometry Reveals Specific Changes in the Local Flexibility of Plasminogen Activator Inhibitor 1 upon Binding to the Somatomedin B Domain of Vitronectin. *Biochemistry* **2012,** *51* (41), 8256-8266.

38. Levy, Y.; Onuchic, J. N.; Wolynes, P. G., Fly-Casting in Protein-DNA Binding: Frustration between Protein Folding and Electrostatics Facilitates Target Recognition. *J. Am. Chem. Soc.* **2007,** *129*, 738-739.

39. Keppel, T. R.; Howard, B. A.; Weis, D. D., Mapping Unstructured Regions and Synergistic Folding in Intrinsically Disordered Proteins with Amide H/D Exchange Mass Spectrometry. *Biochemistry* **2011,** *50* (40), 8722-8732.

40. Henkels, C. H.; Oas, T. G., Ligation-state hydrogen exchange: Coupled binding and folding equilibria in ribonuclease P protein. *J. Am. Chem. Soc.* **2006,** *128* (24), 7772-7781.

41. Wildes, D.; Marqusee, S., Hydrogen exchange and ligand binding: Ligand-dependent and ligand-independent protection in the Src SH3 domain. *Protein Sci.* **2005,** *14* (1), 81-88.

42. Sowole, M. A.; Alexopoulos, J. A.; Cheng, Y.-Q.; Ortega, J.; Konermann, L., Activation of ClpP Protease by ADEP Antibiotics: Insights from Hydrogen Exchange Mass Spectrometry. *J. Mol. Biol.* **2013,** *425* (22), 4508-4519.

43. Cooper, A.; Dryden, D. T. F., Allostery Without Conformational Change - A Plausible Model. *Eur. Biophys. J. Biophys. Lett.* **1984,** *11* (2), 103-109.

44. Bobst, C. E.; Zhang, M.; Kaltashov, I. A., Existence of a Noncanonical State of Iron-Bound Transferrin at Endosomal pH Revealed by Hydrogen Exchange and Mass Spectrometry. *J. Mol. Biol.* **2009,** *388* (5), 954-967.

45. Asuru, A. P.; An, M.; Busenlehner, L. S., Dissection of Porphyrin-Induced Conformational Dynamics in the Heme Biosynthesis Enzyme Ferrochelatase. *Biochemistry* **2012,** *51* (36), 7116-7127.

46. Burke, J. E.; Babakhani, A.; Gorfe, A. A.; Kokotos, G.; Li, S.; Woods, V. L.; McCammon, J. A.; Dennis, E. A., Location of Inhibitors Bound to Group IVA Phospholipase A(2) Determined by Molecular Dynamics and Deuterium Exchange Mass Spectrometry. *J. Am. Chem. Soc.* **2009,** *131* (23), 8083-8091.

47. Balog, E.; Becker, T.; Oettl, M.; Lechner, R.; Daniel, R.; Finney, J.; Smith, J. C., Direct determination of vibrational density of states change on ligand binding to a protein. *Phys. Rev. Lett.* **2004,** *93* (2), 0281031-0281034.

48. Balog, E.; Perahia, D.; Smith, J. C.; Merzel, F., Vibrational Softening of a Protein on Ligand Binding. *J. Phys. Chem. B* **2011,** *115* (21), 6811-6817.

49. Cordier, F.; Wang, C. Y.; Grzesiek, S.; Nicholson, L. K., Ligand-induced strain in hydrogen bonds of the c-Src SH3 domain detected by NMR. *J. Mol. Biol.* **2000,** *304* (4), 497-505.

50. Teale, F. W. J., Cleavage of the heme-protein link by acid methylethylketone. *Biochim. Biophys. Acta* **1959,** *35*, 543.

51. Bailey, J. A., An Undergraduate Laboratory Experiment in Bioinorganic Chemistry: Ligation States of Myoglobin. *J. Chem. Ed.* **2011,** *88*, 995-998.

52. Boys, B. L.; Kuprowski, M. C.; Konermann, L., Symmetric Behavior of Hemoglobin α- and β- Subunits during Acid-Induced Denaturation Observed by Electrospray Mass Spectrometry. *Biochemistry* **2007,** *46*, 10675-10684.

53. Mitra, G.; Muralidharan, M.; Pinto, J.; Srinivasan, K.; Mandal, A. K., Structural Perturbation of Human Hemoglobin on Glutathionylation Probed by Hydrogen-Deuterium Exchange and MALDI Mass Spectrometry. *Bioconjugate Chem.* **2011,** *22*, 785-793.

54. Antonini, E.; Brunori, M., *Hemoglobin and Myoglobin in Their Reactions With Ligands*. North-Holland Publishing Company: Amsterdam, London, **1971**; Vol. 21.

55. Wales, T. E.; Fadgen, K. E.; Gerhardt, G. C.; Engen, J. R., High-Speed and High-Resolution UPLC Separation at Zero Degree Celsius. *Anal. Chem.* **2008,** *80*, 6815-6820.

56. Weis, D. D.; Engen, J. R.; Kass, I. J., Semi-automated data processing of hydrogen exchange mass spectra using HX-Express. *J. Am. Soc. Mass Spectrom.* **2006,** *17* (12), 1700-1703.

57. Dill, K. A.; Bromberg, S., *Molecular Driving Forces*. Garland: New York, **2003**.

58. Hilser, V. J.; Freire, E., Structure-based calculation of the equilibrium folding pathway of proteins. Correlation with hydrogen exchange protection factors. *J. Mol. Biol.* **1996,** *262* (5), 756-772.

59. Creighton, T. E., *Proteins*. W. H. Freeman & Co: New York, **1993**.

60. Gu, Z. Y.; Zitzewitz, J. A.; Matthews, C. R., Mapping the structure of folding cores in TIM barrel proteins by hydrogen exchange mass spectrometry: The roles of motif and sequence for the indole-3-glycerol phosphate synthase from Sulfolobus solfataricus. *J. Mol. Biol.* **2007,** *368* (2), 582-594.

61. Weinkam, P.; Zimmermann, J.; Romesberg, F. E.; Wolynes, P. G., The Folding Energy Landscape and Free Energy Excitations of Cytochrome c. *Acc. Chem. Res.* **2010,** *43*, 652-660.

62. Ly, T.; Julian, R. R., Using ESI-MS to Probe Protein Structure by Site-Specific Noncovalent Attachment of 18-Crown-6. *J. Am. Soc. Mass Spectrom.* **2006,** *17*, 1209-1215.

63. Pan, L. Y.; Salas-Solano, O.; Valliere-Douglass, J. F., Conformation and Dynamics of Interchain Cysteine-Linked Antibody-Drug Conjugates as Revealed by Hydrogen/Deuterium Exchange Mass Spectrometry. *Anal. Chem.* **2014,** *86*, 2657-2664.

64. Dickerson, R. E.; Geis, I., *Hemoglobin: Structure, Function, Evolution, and Pathology*. The Benjamin/Cummings Publishing Company, Inc.: Menlo Park, CA, **1983**.

65. Eaton, W. A.; Henry, E. R.; Hofrichter, J.; Mozzarelli, A., Is cooperative oxygen binding by hemoglobin really understood. *Nat. Struct. Biol.* **1999,** *6* (4), 351 - 358.

66. Lukin, J. A.; Ho, C., The structure-function relationship of hemoglobin in solution at atomic resolution. *Chemical Reviews* **2004,** *104* (3), 1219-1230.

67. Perutz, M. F.; Wilkinson, A. J.; Paoli, M.; Dodson, G. G., The stereochemical mechanism of the cooperative effects in hemoglobin revisited. *Annu. Rev. Biophys. Biomolec. Struct.* **1998,** *27*, 1-34.

68. Ackers, G. K.; Doyle, M. L.; Myers, D.; Daugherty, M. A., Molecular Code for Cooperativity in Hemoglobin. *Science* **1992,** *255* (5040), 54-63.

69. Ackers, G. K.; Holt, J. M.; Burgie, E. S.; Yarian, C. S., Analyzing intermediate state cooperativity in hemoglobin. *Methods Enzymol.* **2004,** *379*, 3-28.

70. White, S. L., The molecular dissociation of ferrihemoglobin derivatives. *J. Biol. Chem.* **1975,** *250*, 1263-1268.

71. Englander, J. J.; Del Mar, C.; Li, W.; Englander, S. W.; Kim, J. S.; Stranz, D. D.; Hamuro, Y.; Woods, V. L., Protein structure change studied by hydrogen-deuterium exchange, functional labeling, and mass spectrometry. *Proct. Nat. Acad. Sci.* **2003,** *100*, 7057 - 7062

72. Mitra, G.; Muralidharan, M.; Narayanan, S.; Pinto, J.; Srinivasan, K.; Mandal, A. K., Glutathionylation Induced Structural Changes in Oxy Human Hemoglobin Analyzed by Backbone Amide Hydrogen/Deuterium Exchange and MALDI-Mass Spectrometry. *Bioconjugate Chem.* **2012,** *23* (12), 2344-2353.

73. Olson, J. S.; Phillips, G. N., Myoglobin discriminates between O-2, NO, and CO by electrostatic interactions with the bound ligand. *J. Biol. Inorg. Chem.* **1997,** *2* (4), 544-552.

74. Phillips, S. E. V., Structure and Refinement of Oxymyoglobin at l.6 A Resolution. *J. Mol Biol.* **1980,** *142*, 531-554.

75. Seno, Y.; Go, N., Deoxymyoglobin Studied by the Conformational Normal Mode Analysis. *J. Mol Biol.* **1990,** *216*, 111-126.

76. Fersht, A. R., *Structure and Mechanism in Protein Science*. W. H. Freeman & Co.: New York, **1999**.

77. Perutz, M. F.; Fermi, G.; Poyart, C.; Pagnier, J.; Kister, J., A novel allosteric mechanism in haemoglobin. Structure of bovine deoxyhaemoglobin, absence of specific chloride-binding sites and origin of the chloride-linked Bohr effect in bovine and human haemoglobin. *J. Mol. Biol.* **1993,** *233* (3), 536-545.

78. Aranda IV, R.; Cai, H.; Worley, C. E.; Levin, E. J.; Li, R.; Olson, J. S.; Phillips Jr, G. N.; Richard, M. P., Structural analysis of fish versus mammalian hemoglobins: Effect of the heme pocket enviornment on autooxidation and hemin loss. *Proteins* **2009,** *75*, 217-230.

79. Eliezer, D.; Yao, J.; Dyson, H. J.; Wright, P. E., Structural and dynamic characterization of partially folded states of apomyoglobin and implications for protein folding. *Nat. Struct. Biol.* **1998,** *5*, 148-155.

80. Johnson, R. S.; Walsh, K. A., Mass spectrometric measurement of protein amide hydrogen exchange rates of apo- and holo-myoglobin. *Protein Sci.* **1994,** *3*, 2411-2418.

81. Maurus, R.; Overall, C. M.; Bogumil, R.; Luo, Y.; Mauk, A. G.; Smith, M.; Brayer, G. D., A myoglobin variant with a polar substitution in a conserved hydrophobic cluster in the heme binding pocket. *Biochim. Biophys. Acta* **1997,** *1341*, 1-13.

82. Hersleth, H. P.; Uchida, T.; Rohr, A. K.; Teschner, T.; Schuenemann, V.; Kitagawa, T.; Trautwein, A. X.; Gorbitz, C. H.; Andersson, K. K., Crystallographic and spectroscopic studies of peroxide-derived myoglobin compound II and occurrence of protonated Fe(IV)-O. *J. Biol. Chem.* **2007,** *282* (32), 23372-23386.

83. Chu, K.; Vojtchovsky, J.; McMahon, B. H.; Sweet, R. M.; Berendzen, J.; Schlichting, I., Structure of a ligand-binding intermediate in wild-type carbonmonoxy myoglobin. *Nature* **2000,** *403*, 921-923.

84. Boehr, D. D.; Nussinov, R.; Wright, P. E., The role of dynamic conformational ensembles in biomolecular recognition. *Nat. Chem. Biol.* **2009,** *5*, 789-796.

85. Silva, D. A.; Bowman, G. R.; Sosa-Peinado, A.; Huang, X. H., A Role for Both Conformational Selection and Induced Fit in Ligand Binding by the LAO Protein. *PLoS Comput. Biol.* **2011,** *7* (5), e1002054.

Chapter 4. Activation of ClpP Protease by ADEP Antibiotics: Insights from Hydrogen Exchange Mass Spectrometry

4.1. Introduction

The ability to degrade damaged or misfolded proteins is a prerequisite for maintaining a healthy intracellular milieu.[1] In eukaryotic cells the dominant non-lysosomal degradation pathway proceeds via the ubiquitin-proteasome system.[2] Prokaryotes[3] and mitochondria[4] mainly rely on members of the caseinolytic protease (Clp) family for ATP-dependent degradation. ClpP is a member of this family that was initially discovered in *Escherichia coli*,[5] and that has become a paradigm for proteolytic degradation complexes in general.[3,6-8]

In ClpP fourteen identical subunits assemble into two stacked heptameric rings, forming a 300 kDa barrel. The hydrolytically active sites are located inside a central chamber that can be accessed via two axial pores.[6-7,9-15] Each of the subunits consists of an N-terminal region, a globular head domain, and a handle (Figure 4-1a-c).[13,16] Contacts between the two heptameric rings are mediated by intercalation of the handles from alternating subunits.[16] ClpP by itself cannot hydrolyze large substrates because the axial pores are blocked by the N-terminal regions of the seven subunits at both ends of the barrel (Fig. 4-1c).[6-7,15,17-18]

An active degradation complex that is capable of degrading full-length proteins is formed when ClpP binds to AAA+ proteins such as ClpX or ClpA.[3,6,19] These AAA+ proteins are ATP-dependent unfoldases that form hexameric rings. They interact with ClpP

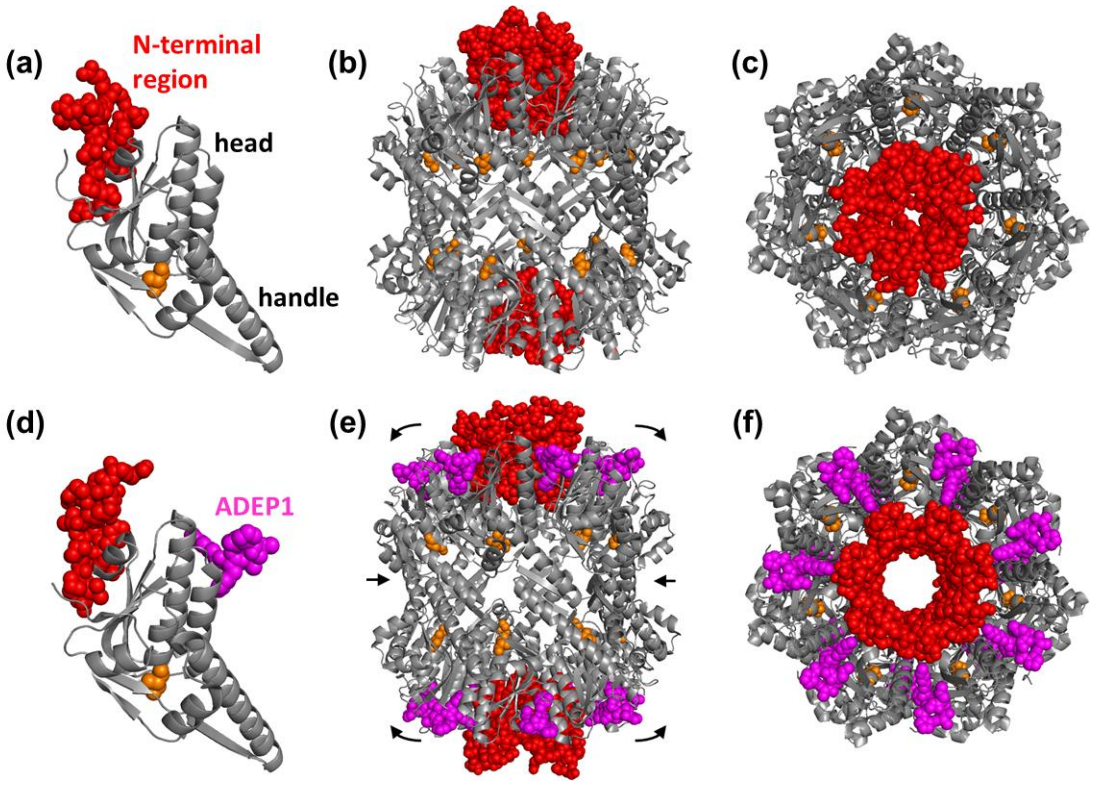

Figure 4-1: X-ray structural data for *E. coli* ClpP. (a) ClpP monomer in the absence of ADEP1. N-terminal region, head and handle regions are indicated. Residues 1-18 are highlighted in red, the active site nucleophile S97 is shown in orange. (b) Equatorial and (c) axial view of the ADEP1-free ClpP 14mer (pdb file 1YG6).[9] (d) Single monomer, (e) equatorial view, and (f) axial view of ClpP bound to ADEP1 (pdb file 3MT6).[14] ADEP1 molecules are highlighted in magenta. Arrows in (e) highlight a slight dilation of the apical (head) regions upon ADEP1 binding, as well as a subtle contraction in the equatorial plane.[14]

via insertion of hydrophobic loops into nonpolar clefts. These clefts are located between adjacent ClpP subunits, surrounding the axial pores. The function of AAA+ proteins is to recognize, bind, unfold, and translocate substrate proteins through the ClpP axial pores into the degradation chamber.[3,6,20-22] It has not been possible thus far to obtain X-ray structures of intact ClpP/AAA+ complexes. Crystallization of these systems is complicated by the peculiar symmetry mismatch, where heptameric ClpP rings are stacked against hexameric AAA+ rings.[6-7,9] Thus, many functional aspects of these degradation machines remain unclear. Cryo-

electron microscopy (EM)[22] revealed that binding to an AAA+ ring causes the corresponding ClpP axial pore to open up, implying major structural changes of the ClpP N-terminal regions. The open pore allows threading of unfolded substrates into the degradation chamber. Unfortunately, the limited structural resolution of cryo-EM does not provide detailed information on the nature of the pore opening transition.[7] Another unresolved question concerns the mechanism of product release, which may proceed via the ClpP axial pores,[13,23-24] or through openings that transiently form in the equatorial region.[10,25-27]

Acyldepsipeptides (ADEPs) are nonpolar antibacterial compounds.[7] The parent substance (ADEP1) has a lactone core derived from five amino acids, and an aliphatic C_7H_9 tail.[15] ADEPs bind ClpP in the hydrophobic clefts that would normally interact with AAA+ proteins.[7] Intriguingly, ADEP binding opens the ClpP axial pores (Figure 1d-f).[6-7] This transition allows ClpP to degrade a range of loosely folded proteins with high efficiency, bypassing the requirement for AAA+ participation. The resulting uncontrolled proteolysis is responsible for the antibiotic activity of ADEPs.[28-29] *Staphylococcus aureus* and other Gram-positive bacteria are susceptible to these compounds.[30] Gram-negative organisms are largely resistant because their outer membrane acts as protective barrier against ADEPs, and possibly because of the presence of specific efflux pumps.[31] Similar to the ADEP-bound state, a constitutively active form of ClpP is obtained by deleting the first 14 N-terminal residues.[32]

Deciphering the nature of ADEP-induced structural changes is complicated by the fact that ClpP can crystallize in various conformations, pointing to a malleable structure that is sensitive to crystal packing effects.[7,9-10,26] This is particularly true for the N-terminal regions which are key for gating the axial pores. Most of the available ClpP X-ray structures

provide incomplete information for the first 18 residues, suggesting considerable disorder and highly dynamic behavior. Nonetheless, it is clear that the N-terminal regions have a propensity to form loops or hairpins, with two strands termed β_{-1} and β_0.[9-10,12-13,15,21,26-27]

Recent X-ray studies led to two competing models for the ADEP-induced activation of ClpP.[7] According to one proposal,[15] the closed-pore conformation has relatively structured N-termini that are stabilized by hydrophobic clustering. Pore opening by ADEP was attributed to switching of the termini to a more disordered state.[15] This scenario has been questioned,[7] because the N-terminal regions in the open state of ref.[15] appear to be influenced by crystal packing. An alternative model[14] envisions that ADEP binding triggers formation of an "open collar", consisting of β_{-1}/β_0 loops that are oriented parallel to the ClpP symmetry axis (Figs. 4-1d-f).[14] Both models agree that ADEP binding causes a slight equatorial contraction, and a dilation of the axial regions (arrows in Fig. 4-1e).[14-15]

X-ray crystallography and cryo-EM provide static ground state structures that do not directly reflect biomolecular dynamics in solution.[7,33-34] For understanding protein behavior it is essential to perform complementary investigations that probe dynamic features in a physiologically relevant solvent environment. Relaxation dispersion NMR measurements represent one promising avenue,[25,35] but their application remains limited to very few laboratories. Hydrogen/deuterium exchange (HDX) coupled with mass spectrometry (MS) is a more accessible method.[36-44] Protein regions that are disordered and/or highly dynamic undergo rapid deuteration, whereas HDX in rigid segments is much slower. HDX rates primarily reflect the stability of amide backbone H-bonds, although solvent accessibility also plays a role.[45] The deuteration behavior of individual segments can be monitored by

subjecting the protein to peptic digestion after incubation in a D_2O-containing environment. This approach allows the tracking of time-dependent peptide mass shifts by MS.

Here, we employ HDX/MS for probing changes in the structure and dynamics of ClpP upon activation by ADEP1. Ligand binding causes rigidification of the equatorial belt, whereas the head regions undergo a slight destabilization. ADEP1-mediated switching to the open-pore state causes surprisingly small changes in the HDX behavior of the N-terminal regions. Our data suggest that gating of the axial pores is mainly based on alterations in the packing of N-terminal nonpolar residues. Such a mechanism helps reconcile the two competing proposals of the activation process.[7,14-15] To the best of our knowledge, this work represents the first HDX/MS study on the ADEP-mediated activation of ClpP.

4.2. Materials and Methods

4.2.1. Materials

HEPES and glycerol were from Sigma (St. Louis, MO, USA), and potassium chloride was from Caledon (Ontario, Canada). D_2O was from Cambridge Isotope Laboratories (Andover, MA). Magnesium chloride was purchased from Merck (Darmstadt, Germany). All chemicals were used as received. *E. coli* ClpP was overexpressed and purified from transformed *E. coli* cells as described,[46] and ADEP1 was purified from *Streptomyces hawaiiensis* fermentation broth following established procedures.[14]

4.2.2. Backbone Amide Hydrogen/Deuterium Exchange Mass Spectrometry

The experiments started with 300 µM ClpP (on a monomer basis) in 10 mM magnesium chloride, 100 mM KCl, 25 mM HEPES, and 10% glycerol (pH 7.5). ADEP1-bound samples were prepared by adding 2 µL of ADEP1 in DMSO to 20 µL of ClpP solution, resulting in a five-fold molar excess of ligand. These mixtures were pre-equilibrated for 24 h at 4 °C. Deuteration was conducted at room temperature. HDX was initiated by addition of 9 volumes of D_2O containing labeling buffer which had the same salt and glycerol concentration as the stock solution, for a final measured pH of 7.3. On the basis of previously measured dissociation constants,[47] the fraction of bound protein under labeling conditions was estimated to be 99%. 30 µL aliquots were removed at various time points ranging from 1 to 360 min after initiating of labeling. These aliquots were quenched at pH 2.4 by addition of HCl on ice, followed by flash freezing in liquid nitrogen and storage at -80 °C. For spatially-resolved HDX/MS experiments, the aliquots were rapidly thawed to ~0 °C and manually injected into a nanoACQUITY UPLC with HDX technology (Waters, Milford, MA)[48] for desalting and peptide separation within 15 min on an equilibrated reversed phase column (BEH C18 1.7 µm, 1 mm × 100 mm) using a water/acetonitrile gradient in the presence of 0.1% formic acid at 40 μL min^{-1} . Online digestion was performed using a POROS pepsin column (2.1 mm × 30 mm) from Life Technologies/Applied Biosystems (Carlsbad, CA) at room temperature. The temperature for peptide trapping and reversed phase separation was set to 1 °C. Blank (water) injections were performed in-between protein injections to eliminate carryover.

Mass analysis of peptides was performed on a Waters Synapt HDMS instrument with source and desolvation temperatures of 80 and 300 °C, respectively, a cone voltage of 30 V, and an electrospray voltage of 3 kV. The identity of each peptide was confirmed by tandem MS based on the known ClpP sequence.[9] Zero time point controls (m_0) for the correction of artifactual in-exchange were performed by first exposing ClpP to quenching buffer, followed by brief D_2O exposure, resulting in the same final solution composition as for all other samples. Controls for fully exchanged ClpP (m_{100}, for the correction of back exchange) were prepared by incubating 30 μM ClpP in labeling solution at pH 2.0 for 24 h. Biolynx 4.1 (Waters) and HX-Express[49] were employed to analyze the centroid mass of all peptides as a function of labeling time. Deuteration levels were determined as

$$\%\ Deuteration = \frac{(m - m_0)}{(m_{100} - m_0)} \times 100\% \qquad (4.1)$$

Intact protein deuteration measurements were performed using a procedure similar to that described above, but without using the integrated Waters HDX module. Protein separation was achieved using a C4 column (Jupiter 5 µm Proteo, 50 mm × 1 mm; Phenomenex) coupled to a UPLC pump at a flow rate of 100 μL min^{-1} without pepsin digestion. The injection loop volume was 20 μL and the total amount of protein per injection was 600 pmol. The injection syringe, column, injector and solvent delivery lines were kept at 0 °C in an ice bath. All measurements were performed in triplicate. Error bars represent standard deviations. Average deuteration differences for Figs. 4-6e, f were calculated as

$$average\ difference = \frac{1}{N}\sum (\%Deuteration_{ADEP1} - \%Deuteration_{free}) \qquad (4.2)$$

%Deuteration values were determined by using eq. 4.1. The sum extends over the $N = 6$ time points that were measured for each peptide.

4.3. Results and Discussion

4.3.1. Global HDX Kinetics

As a first step to understand the interaction of ADEP1 with ClpP, deuteration measurements were conducted at the level of intact subunits. Backbone amide HDX/MS data were recorded for labeling times ranging from one minute to six hours (Figure 4-2). ADEP1-free ClpP reaches a deuteration level of almost 60% at the end of the experimental time window. ADEP1 binding causes a dramatic reduction in the extent of labeling, resulting in a deuteration level that is ~20% lower after 6 h. This reduced deuterium uptake points to a stabilization of the overall ClpP structure upon ligand binding, resulting in a state that (on average) is less dynamic. Qualitatively similar ligand-induced stabilization effects have previously been observed by HDX/MS for many other proteins.[37,39,50-51]

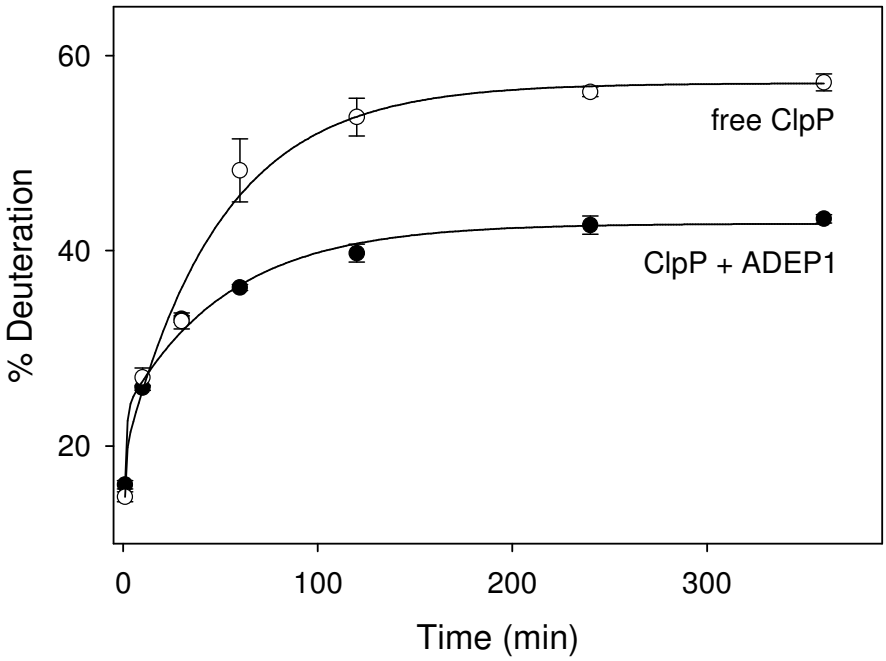

Figure 4-2: Global ClpP HDX/MS kinetics recorded in the absence (open symbols) and presence of ADEP1 (filled symbols). Lines represent biexponential fits.

4.3.2. Spatially-Resolved HDX/MS Measurements

A more detailed view of the ClpP conformational dynamics can be gained by analyzing the HDX kinetics in a spatially-resolved fashion. Peptic digestion yielded 32 peptides with signal-to-noise ratios that were adequate for deuteration measurements, with an overall sequence coverage of 95% (Figure 4-3). Even without detailed analyses, it can be seen that ADEP1 binding does not affect all ClpP regions in the same fashion (Figure 4-4). As expected from the intact protein data, many peptides exhibit reduced deuteration levels in the presence of ADEP1. Other peptides show virtually identical HDX behavior with and without ADEP1. Surprisingly, there are also some segments that show higher deuteration levels after ligand binding. These three scenarios are exemplified in Figure 4.4 for peptides 135-141, 50-61 and 82-89.

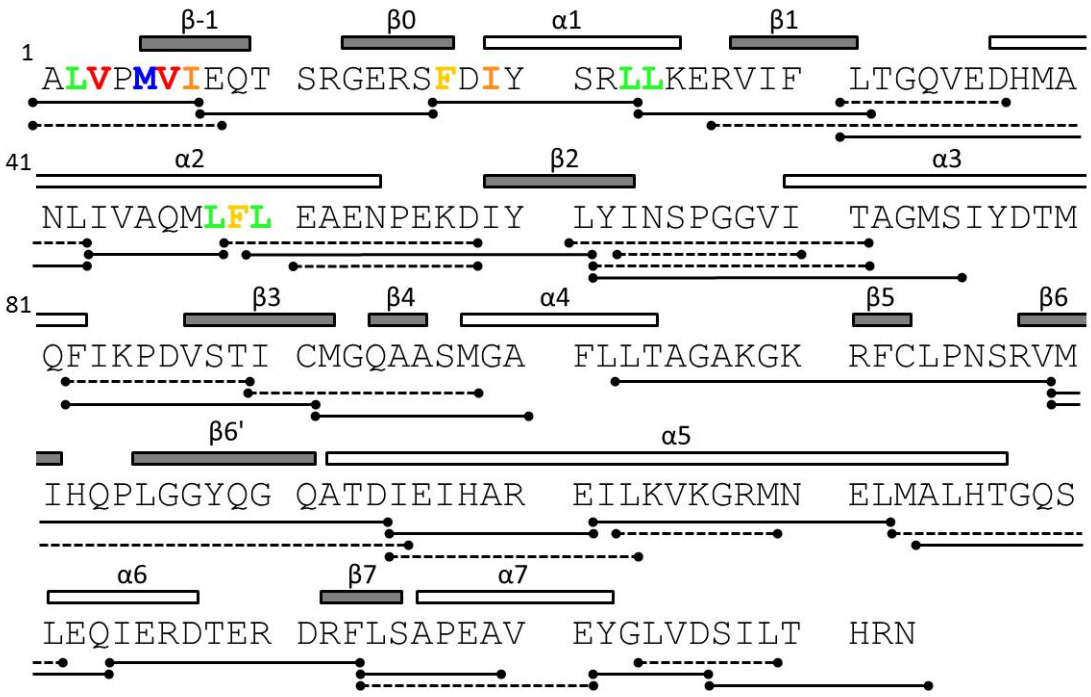

Figure 4-3: Sequence of *E. coli* ClpP.[9] Solid lines represent peptides used for HDX/MS data analyses, dashed lines represent redundant peptides. Secondary structure elements are indicated. Selected hydrophobic residues are highlighted, matching the color scheme used in Figs. 4-7b-d.

A summary of all peptide data is provided in the deuterium uptake curves of Figure 4.5. For the following discussion we will focus on a subset of peptides that cover the ClpP

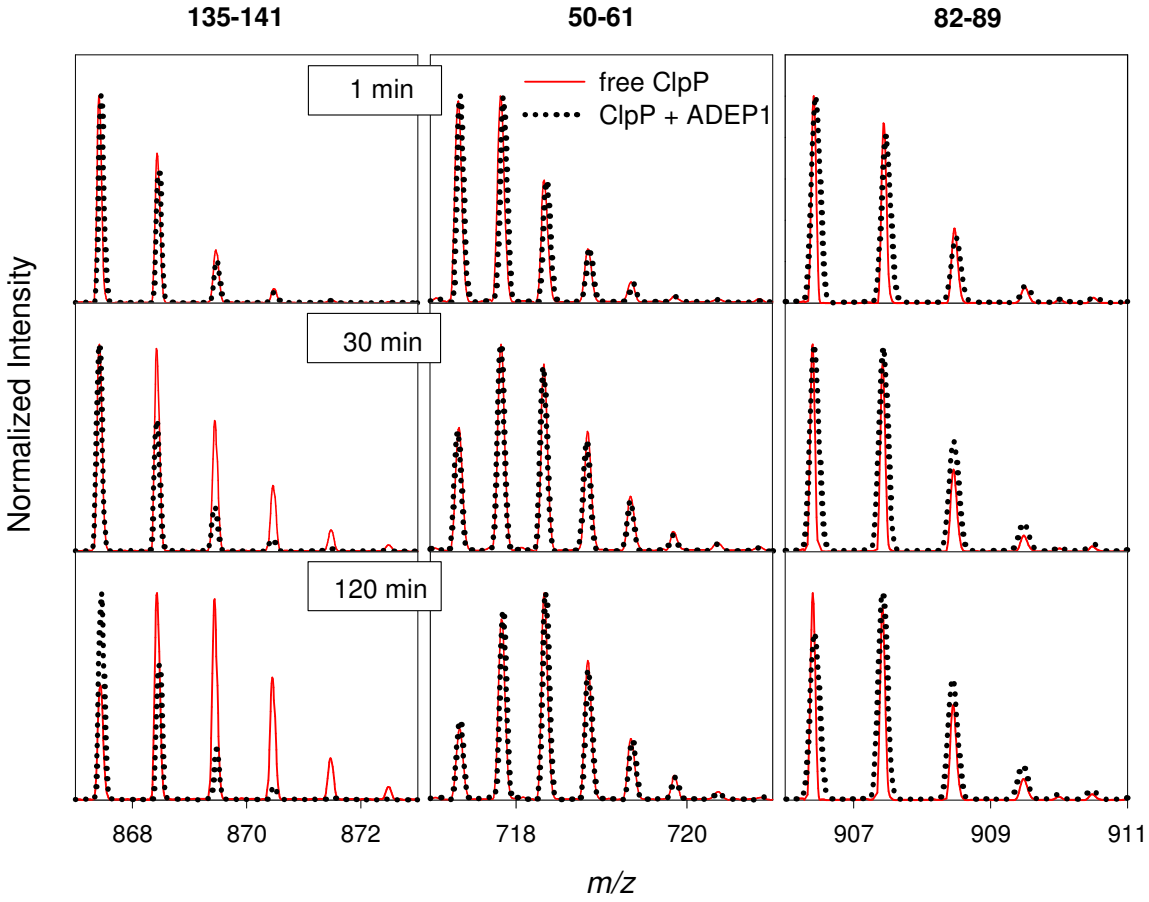

Figure 4-4: Unprocessed HDX/MS data for three ClpP peptic peptides recorded in the absence (red solid lines) and in the presence (black dotted lines) of ADEP1 for three HDX time points.

sequence in an almost contiguous fashion (solid lines in Figure 4-3). The availability of redundant data is nonetheless important, because it provides an internal consistency control. It is reassuring that peptides representing similar protein regions exhibit comparable kinetics (e.g., 50-61/51-58, 61-71/62-71/62-75, 82-89/82-91, 142-152/143-149, 184-189/187-193 in Fig. 4-5).

To facilitate the discussion of peptide-resolved HDX data, deuteration percentages were mapped onto the crystal structure of ClpP in the absence (Figure 4-6a, b) and presence

of ADEP1 (Figure 4-6c, d) for t = 60 min. The handle domain (α_5 and β_6', residues 120 to 152) shows the most dramatic changes upon binding. In the absence of ADEP1 this region is only

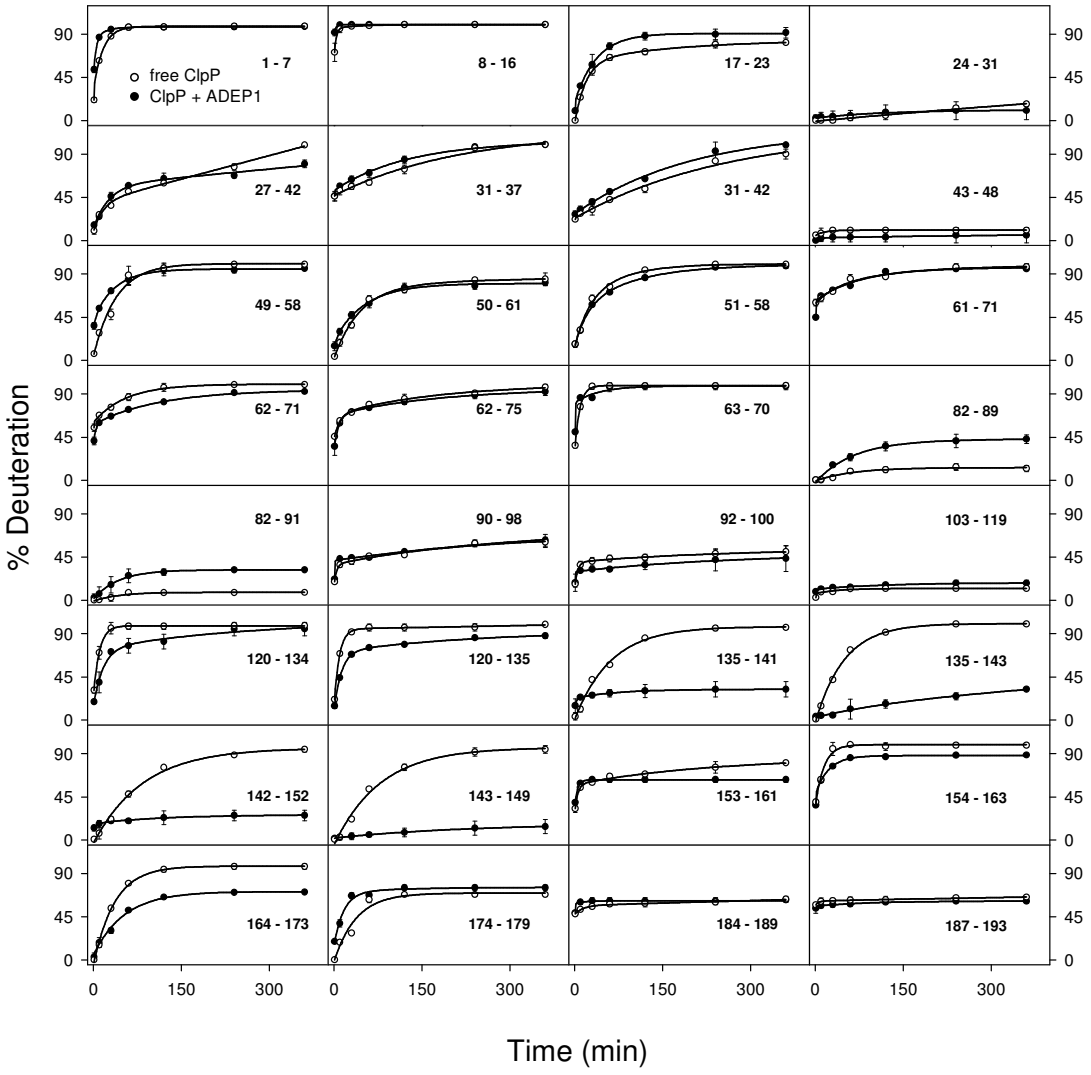

Figure 4-5: HDX kinetics of peptides in free ClpP (open symbols) and after ADEP1 binding (filled symbols). Residue numbers are indicated in each panel. Lines are biexponential fits. Error bars represent standard deviations of triplicate measurements.

marginally protected (β_6' is red and α_5 is yellow, Figure 4-6a, b). ADEP1 binding causes a major stabilization of the handle, particularly in the 135-152 range that covers much of α_5 (green, Figure 4-6c, d). β_6' gets stabilized as well (orange, Figure 4-6c, d).

Ligand-induced changes in the head domain are more subtle. Many elements in this region show high protection with and without ADEP1 (blue, Fig. 6a-d), such as 24-31 (β_1), 43-48 (center of α_2), and 103-119 (β_5, parts of α_4 and β_6). As already noted, there are several peptides in the head region that show *higher* HDX levels after ADEP1 binding.

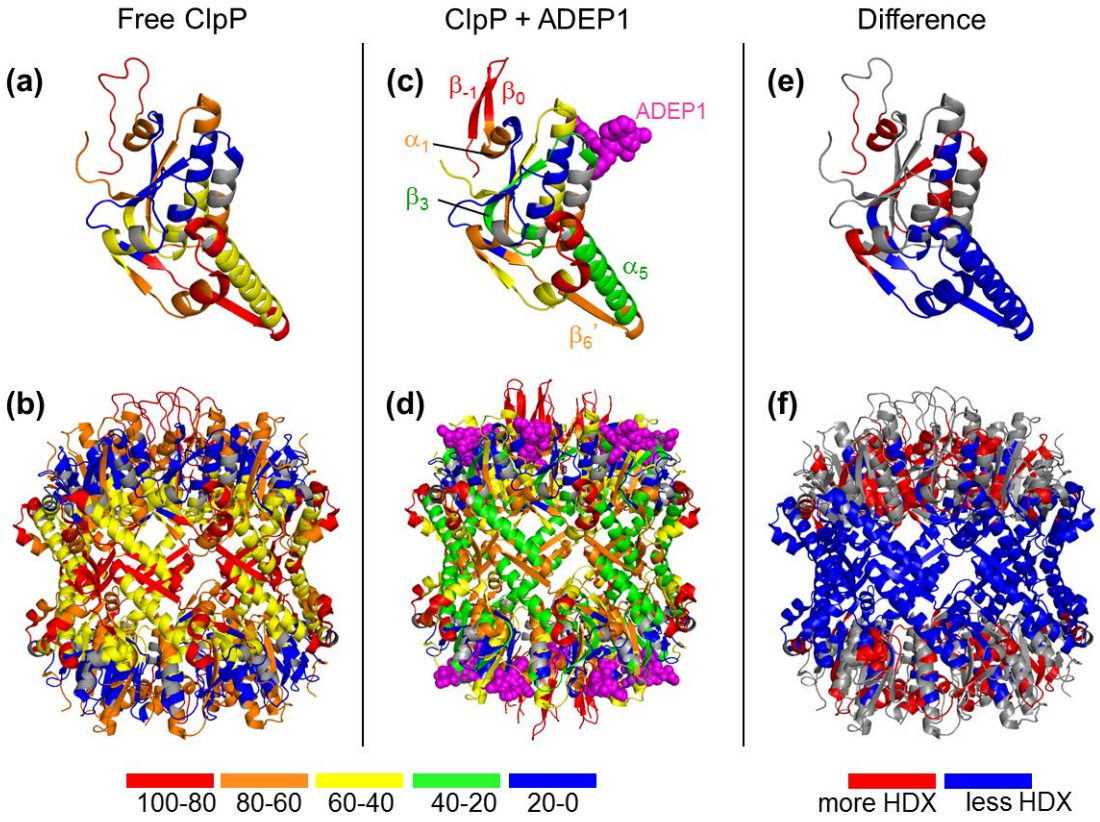

Figure 4-6: Mapping of the of Figure 4-5 HDX/MS data to the X-ray structures of ClpP for *t* = 60 min, shown for single ClpP subunits (top row), and for complete tetradecamers (bottom row). Colors in (a) - (d) represent deuteration percentages, as defined in the legend. Gray elements in (a) - (d) were not covered by peptide mapping. In (c) selected elements are identified; note that only one of the two ADEP1 molecules that are in contact with the subunit is shown. Panels (e), (f): HDX difference map. Colored regions correspond to

|*average difference*| > 5% (eq. 4.2). Segments that exhibit elevated deuteration after ADEP1 binding are depicted in red. Segments with reduced deuteration are shown in blue. All other regions are depicted in gray.

This ligand-induced *de*stabilization is particularly pronounced for 17-23 (α_1) and 82-91 (β_3) which are part of the ADEP1 binding cleft (Figure 4-6c).[14-15] The N-terminal region (including β_{-1} and β_0, red in Figs. 6a-d) is almost completely deuterated after 60 min, regardless of ADEP1 binding.

An overview of the regions that undergo stabilization (blue) and destabilization (red) after addition of ADEP1 is provided in Figure 4-6e, f. This representation uses a 5% threshold, calculated as outlined in the Methods section. ADEP1-induced *de*stabilization is restricted to the head regions of the ClpP tetradecamer, whereas elements that are most strongly stabilized by ADEP1 are found in the equatorial (handle) region. The resulting red-blue-red pattern of Figure 4.6f bears a striking correlation with the ADEP1-induced domain movements that have been inferred from X-ray structural data (arrows in Figure 4-1d).[14, 15] Specifically, contraction of the equatorial belt is concomitant with enhanced HDX protection, i.e., a more stable H-bonding network in this region. Conversely, dilation of the apical barrel ends is accompanied by partial destabilization of the head domains.

4.3.3. Allosteric Nature of ADEP1 Binding

Ligand binding to a protein occurs spontaneously when the corresponding free energy change, $\Delta_{bind}G°$, is negative. This thermodynamic stabilization upon binding lowers the Boltzmann population of transiently populated excited conformers.[52-53] The resulting decrease in amide deuteration provides the basis of typical HDX ligand binding assays.[37,39,50-

[51] In some cases ligand-induced stabilization is most pronounced in the direct vicinity of the binding site.[37,54-57] Other systems show allosteric behavior, where the ligand affects regions that are remote from the site of interaction.[37,57-59]

Our HDX data reveal that the interaction of ADEP1 with ClpP causes both local changes and allosteric switching. Ligand binding in the apical region induces a major rigidification of the equatorial region. This long-distance effect requires the transduction of allosteric signals over ~30 Å, from the ADEP1 binding clefts to the handle elements α_5 and β_6'. What makes the ClpP behavior quite unusual is the fact that ADEP1 *destabilizes* some protein elements close to the binding site. At first sight, this effect seems to contradict the tenet that binding always results in a thermodynamic stabilization.[37,39,50-51] However, binding equilibria are not governed by local effects, but by the *overall* free energy change. $\Delta_{bind}G°$ is the sum of many individual contributions, each of which can be stabilizing (< 0) or destabilizing (> 0). Binding is a spontaneous process as long as the former outweigh the latter. Evidently, this is the case for the system considered here.

4.3.4. Implications for Product Release

The highly dynamic behavior of the free ClpP equatorial region seen in our HDX experiments (Figure 4-6a, b) is consistent with earlier NMR work.[25] Along with other observations,[10,26-27] those NMR data were interpreted in favor of a model where free ClpP as well as ClpP/AAA+ complexes release hydrolysis products via transiently formed equatorial openings. The results seen here point in a different direction. The pronounced structural stabilization in the handle regions (Figure 4-6c-f) makes it unlikely that ADEP1-bound ClpP

undergoes large opening/closing fluctuations that would be required for the formation of transient equatorial cavities. Instead, our HDX data are consistent with a scenario where product release occurs via the axial pores, as suggested previously.[13,23-24] In principle, the isotope exchange pattern of ADEP1-bound ClpP would also be compatible with the presence of *rigid* equatorial openings that could participate in

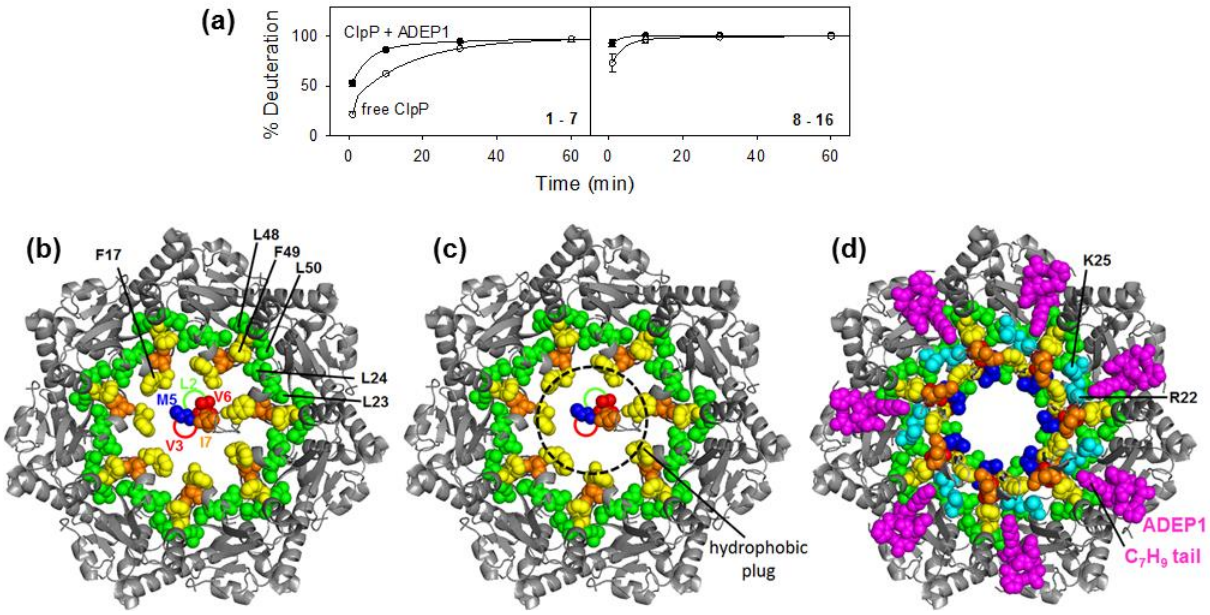

Figure 4-7: (a) Initial 60 min HDX period for peptides 1-7 and 8-16. (b) Top view of the axial pore region for free ClpP (1YG6).[9] Key nonpolar residues (I, L, V, F, M) are highlighted in color. The N-terminal region is shown only for the single subunit that adopts a "down" conformation in the pdb file.[9] Possible L2 and V3 positions (not resolved in the X-ray data) are indicated by circles. (c) Approximate location of the "hydrophobic plug" that will form by clustering of up to seven sets of L2/V3/M5/V6/I7 residues, when several N-termini adopt similar "down" conformations. (d) Top view of the ADEP1-bound open state (3MT6).[14] Highlighted residues correspond to those in (b), (c). In addition, R22 and K25 are shown in cyan (with δ-guanido and ε-amino groups omitted, as indicated in the text). Note how the outside of the hydrophobic ring is stabilized by interactions with the ADEP1 alkyl tails.

product release. Currently existing X-ray structures do not show any evidence of large equatorial openings.[14-15] Given the highly malleable nature of ClpP, however, it is possible that those crystal structures do not properly reflect all aspects of the handle domain behavior in solution.

4.3.5. N-Terminal Changes During ADEP1-Mediated Pore Opening

The key N-terminal segments that are involved in gating of the axial pore are 1-7 (ALVP tail and first three residues of β_{-1}) and 8-16 (β_{-1}, turn, β_0). The nearby region 24-31 (β_1) exhibits very low deuteration levels with and without ADEP1, suggesting that β_1 provides a rigid base for gating movements of the N-terminus. Segment 17-23 (α_1) serves as hinge between β_1 and the N-terminal region. Conformational switching of the latter may be facilitated by a "softening" of α_1, evident from its higher HDX levels after ADEP1 binding (red, Figure 4-6e).

Peptides 1-7 and 8-16 are among the most rapidly exchanging segments, both with and without ADEP1 (Figure 4-5, Figure 4-7a). This observation is consistent with earlier evidence of extensive N-terminal disorder.[9-10,12-13,15,21,26-27,35] Yet, it is surprising that the ADEP1-mediated pore opening transition is not accompanied by larger changes in the N-terminal HDX kinetics. Segment 8-16 shows almost no HDX protection, regardless of the presence of ADEP1. The crystal structure of ADEP1-bound ClpP shows H-bonding between β_{-1} and β_0.[14] However, our data imply that in solution these contacts are in rapid N-H···O=C $\leftrightarrow$ N-H O=C equilibrium, rendering the corresponding backbone hydrogens highly

susceptible to exchange. We attribute stabilization of the β_{-1}/β_0 open collar conformation to factors other than H-bonding (outlined below).

Compared to 8-16, peptide 1-7 shows more protection. Interestingly, HDX of 1-7 is faster after ADEP1 binding (Figure 4-7a, 4-6e). Because H-bonding in the β_{-1}/β_0 region is negligible (see previous paragraph), the alterations in the HDX behavior of 1-7 must be due to solvent accessibility differences.[45] In other words, segment 1-7 is less accessible in free ClpP than after ADEP1 binding. Hydrophobic clustering is the dominant contributor to solvent exclusion in proteins.[60-61] Strikingly, segment 1-7 mainly consists of nonpolar residues. These and other key nonpolar moieties have been highlighted in Figure 4-3 and Figure 4-7 to facilitate the following discussion.

As pointed out elsewhere,[7,15] a likely N-terminal structure for the closed-pore state of free ClpP in solution is the "down" conformation displayed by subunit C in pdb file 1YG6.[9] In this conformation M5, V6, and I7 are in the vicinity of the pore center. The first four residues are not resolved, but sequence dictates that L2 and V3 must be adjacent to M5, V6, and I7 (Figure 4-7b). All five of these amino acids are nonpolar.[62] Having multiple N-termini adopt similar "down" orientations will place up to $7 \times 5 = 35$ nonpolar residues in direct proximity to each other. We propose that clustering of these nonpolar moieties will result in a "hydrophobic plug" that is stabilized by the surrounding nonpolar head residues (F17, L23, L24, L48, F49, L50 from each subunit, Figure 4-7b). Figure 4-7c highlights the fact that such a hydrophobic network will block the axial pores of free ClpP. In support of this scenario, earlier studies already noted extensive hydrophobic contacts in the N-terminal region of free ClpP.[7,15] Also, mutations that lower the nonpolar character of the N-terminal region induce partial opening of the pore, [35,63] consistent with destabilization of the hydrophobic plug.

Why does ADEP1 binding open up the pore, and why does this transition increase the HDX levels of peptide 1-7? X-ray structure 3MT6[14] shows that the ADEP1-bound open collar state is devoid of an axial hydrophobic plug. Instead, the N-terminal residues L2, V3, M5, V6, I7 are in contact with a nonpolar interaction network comprising F17, L23, L24, L48, F49, L50 (Figure 4-7d). In the absence of firm H-bonds, we propose that this hydrophobic clustering is the key stabilizing factor of the β_{-1}/β_0 loops in the open collar state. Importantly, all seven ADEP1 molecules point their C_7H_9 alkyl tails towards the nonpolar moieties that are located around the rim of the pore. Clearly, the open state is stabilized by hydrophobic interactions between nonpolar residues and the ADEP1 alkyl tails (Figure 4-7d). Formation of these interactions after ADEP1 binding seems to be a major factor for triggering the transition to the open collar conformation. In addition, the opening event may be facilitated by the slight dilation of the head domains that occurs as the ADEP1 molecules wedge themselves into the binding clefts (arrows in Fig. 4-1e). We propose that the accelerated HDX kinetics of peptide 1-7 in the open state reflect the enhanced solvent accessibility of L2/V3/M5/V6/I7 after ADEP1-mediated disruption of the hydrophobic plug.

Interestingly, R22 and K25 participate in the closely packed nonpolar network of the open pore conformation (Figure 4-7d, cyan). It might seem surprising to see K and R participate in hydrophobic interactions, since both of these residues are charged. However, the charges are located at the end of nonpolar chains ($C_\alpha H$-CH_2-CH_2-CH_2-, and $C_\alpha H$-CH_2-CH_2-CH_2-, respectively), giving both K and R amphiphilic character. It is well known that this architecture allows K and R to participate in hydrophobic packing, while at the same time exposing their charged end groups to the solvent at the protein surface.[53,64] Such a scenario applies to the case of ADEP1-bound ClpP, as illustrated in Figure 4.7d (for clarity,

the solvent-exposed guanido and amino groups of R22 and K25 have been omitted in the Figure).

4.4. Conclusions

The interpretation of HDX measurements on protein-ligand systems is frequently guided by the expectation that structural stabilization effects will be most pronounced in the vicinity of the ligand, such that deuteration data can be used for binding site mapping.[65] Indeed, there are many proteins that behave according to this canonical scenario.[37,54-57] Unfortunately, such a simplistic "HDX footprinting" view is inadequate for systems that show allosteric behavior,[37,57] i.e., where the ligand affects structure and dynamics in regions that are remote from the binding site.[58-59] The ADEP1/ClpP system represents a case where a footprinting interpretation of HDX patterns is inadequate. A simplistic analysis of the measured HDX kinetics would erroneously suggest the equatorial region as ADEP1 binding site, because this is where deuteration changes are most pronounced.

The HDX/MS data of this study complement previous work on the interaction of ClpP with ADEP antibiotics. Our observations strongly suggest that the ADEP1-mediated opening of the ClpP axial pores involves switching between two different modes of hydrophobic packing. In free ClpP the clustering of nonpolar N-terminal residues yields a hydrophobic plug that is centered around the symmetry axis of the barrel, blocking access to the degradation chamber. ADEP binding dissolves this central plug by providing new hydrophobic anchor points (the seven alkyl tails on the *outside* of the pore) that nonpolar residues can bind to. By acting as hydrophobic nucleation sites, the ADEP1 molecules trigger switching to a conformation that has all seven N-terminal regions sequestered away from the

centerline of the barrel, thereby opening up the pore. Simply speaking, this gating mechanism relies on the "hydrophobic pull" exerted by ADEP1, causing a radial movement of nonpolar residues towards the outside.

Our view of the pore opening transition is consistent with X-ray structures of free[9,15] and ADEP1-bound ClpP[14] (Figure 4-7b-d). The scenario envisioned here helps resolve some of the differences[7] in the interpretation of earlier X-ray studies.[14-15] This reconciliation comprises (i) acknowledging the crucial role of hydrophobic clustering in the closed state as noted in ref.[15]; and (ii) accepting that ADEP1 binding triggers the formation of an N-terminal open collar as suggested in ref.[14] (Figure 4-1f, 4-7d). Our data imply that this collar is primarily stabilized by a network of hydrophobic moieties that comprises nonpolar side chains as well as the seven ADEP1 alkyl tails. Given the HDX evidence for the highly dynamic nature of the N-terminal regions, neither the hydrophobic plug in free ClpP, nor the collar formed after ADEP1 binding should be envisioned as static entities.

In future work, it will be interesting to conduct HDX measurements on ClpP in complex with AAA+ unfoldases. The C_7H_9 alkyl tail of ADEP1 mimics the first residue in the IGF/L loops of ClpA and ClpX [14-15,28-31] These IGF/L loops are essential for the association of AAA+ proteins with ClpP.[66] Therefore, the model proposed here for opening and stabilization of the ClpP axial pore by ADEP1 may be extendable to the ClpP interactions with AAA+ proteins. In the absence of high-resolution X-ray data for AAA+/ClpP complexes, HDX/MS might be able to prove or disprove such a proposal. Also, future investigations should explore whether the interaction of ClpP with ADEPs shows cooperative behavior, analogous to the T/R switching seen for hemoglobin and other proteins.[67-69]

4.5. References

1. Balch, W. E.; Morimoto, R. I.; Dillin, A.; Kelly, J. W., Adapting proteostasis for disease intervention. *Science* **2008,** *319* (5865), 916-919.

2. Gallastegui, N.; Groll, M., The 26S proteasome: assembly and function of a destructive machine. *Trends Biochem. Sci.* **2010,** *35* (11), 634-642.

3. Kress, W.; Maglica, Z.; Weber-Ban, E., Clp chaperone-proteases: structure and function. *Res. Microbiol.* **2009,** *160* (9), 618-628.

4. Corydon, T. J.; Bross, P.; Holst, H. U.; Neve, S.; Kristiansen, K.; Gregersen, N.; Bolund, L., A human homologue of Escherichia coli ClpP caseinolytic protease: recombinant expression, intracellular processing and subcellular localization. *Biochem. J.* **1998,** *331*, 309-316.

5. Katayama, Y.; Gottesman, S.; Pumphrey, J.; Rudikoff, S.; Clark, W. P.; Maurizi, M. R., The Two-component, ATP-dependent Clp Protease of *Escherichia coli*. *J. Biol. Chem.* **1988,** *263*, 15226-15236.

6. Baker, T. A.; Sauer, R. T., ClpXP, an ATP-powered unfolding and protein-degradation machine. *Biochim. Biophys. Acta* **2012,** *1823*, 15-28.

7. Alexopoulos, J. A.; Guarnéa, A.; Ortega, J., ClpP: A structurally dynamic protease regulated by AAA+ proteins. *J. Struct. Biol.* **2012,** *179*, 202-210.

8. Lupas, A.; Flanagan, J. M.; Tamura, T.; Baumeister, W., Self-compartmentalizing proteases. *Trends Biochem. Sci.* **1997,** *22*, 399-404.

9. Bewley, M. C.; Graziano, V.; Griffin, K.; Flanagan, J. M., The asymmetry in the mature amino-terminus of ClpP facilitates a local symmetry match in ClpAP and ClpXP complexes. *J. Struct. Biol.* **2006,** *153*, 113-128.

10. Gribun, A.; Kimber, M. S.; Ching, R.; Sprangers, R.; Fiebig, K. M.; Houry, W. A., The ClpP Double Ring Tetradecameric Protease Exhibits Plastic Ring-Ring Interactions, and the N Termini of Its Subunits Form Flexible Loops That Are Essential for ClpXP and ClpAP Complex Formation. *J. Bio. Chem.* **2005,** *280*, 16185-16196.

11. Hoffmann, R.; Reichert, I.; Wachs, W. O.; Zeppezauer, M.; Kalbitzer, H. R., H-1 AND P-31 NMR-SPECTROSCOPY OF PHOSPHORYLATED MODEL PEPTIDES. *Int. J. Pept. Protein Res.* **1994,** *44* (3), 193-198.

12. Szyk, A.; Maurizi, M. R., Crystal structure at 1.9Å of E. coli ClpP with a peptide covalently bound at the active site. *J. Struct. Biol.* **2006,** *156*, 165-174.

13. Wang, J.; Hartling, J. A.; Flanagan, J. M., The Structure of ClpP at 2.3 A° Resolution Suggests a Model for ATP-Dependent Proteolysis. *Cell* **1997,** *91*, 447-456.

14. Li, D. H. S.; Chung, Y. S.; Gloyd, M.; Joseph, E.; Ghirlando, R.; Wright, G. D.; Cheng, Y. Q.; Maurizi, M. R.; Guarne, A.; Ortega, J., Acyldepsipeptide Antibiotics Induce the Formation of a Structured Axial Channel in ClpP: A Model for the ClpX/ClpA-Bound State of ClpP. *Chem. Biol.* **2010,** *17* (9), 959-969.

15. Lee, B.-G.; Park, E. Y.; Lee, K.-E.; Jeon, H.; Sung, K. H.; Paulsen, H.; Rübsamen-Schaeff, H.; Brötz-Oesterhelt, H.; Song, H. K., Structures of ClpP in complex with acyldepsipeptide antibiotics reveal its activation mechanism. *Nat. Struct. Mol. Biol.* **2010,** *17*, 471-478.

16. Wang, J.; Hartling, J. A.; Flanagan, J. M., Crystal Structure Determination of Escherichia coli ClpP Starting from an EM-Derived Mask. *J. Struct. Biol.* **1998,** *124*, 151-163.

17. Thompson, M. W.; Singh, S. K.; Maurizi, M. R., Processive Degradation of Proteins by the ATP-dependent Clp Protease from Escherichia coli. *J. Biol. Chem.* **1994,** *269*, 18209-18215.

18. Jennings, L. D.; Lun, D. S.; Medard, M.; Licht, S., ClpP Hydrolyzes a Protein Substrate Processively in the Absence of the ClpA ATPase: Mechanistic Studies of ATP-Independent Proteolysis. *Biochemistry* **2008,** *47*, 11536-11546.

19. Choi, K.-H.; Licht, S., Control of Peptide Product Sizes by the Energy-Dependent Protease ClpAP. *Biochem.* **2005,** *44*, 13921-13931.

20. Kolygo, K.; Ranjan, N.; Kress, W.; Striebel, F.; Hollenstein, K.; Neelsen, K.; Steiner, M.; Summer, H.; Weber-Ban, E., Studying chaperone–proteases using a real-time approach based on FRET. *J. Struct. Biol.* **2009,** *168*, 267-277.

21. Kim, D. Y.; Kim, K. K., The Structural Basis for the Activation and Peptide Recognition of Bacterial ClpP. *J. Mol Biol.* **2008,** *379*, 760-771.

22. Effantin, G.; Ishikawa, T.; De Donatis, G. M.; Maurizi, M. R.; Steven, A. C., Local and Global Mobility in the ClpA AAA plus Chaperone Detected by Cryo-Electron Microscopy: Functional Connotations. *Structure* **2010,** *18* (5), 553-562.

23. Thompson, M. W.; Maurizi, M. R., Activity and Specificity of Escherichia coli ClpAP Protease in Cleaving Model Peptide Substrates. *J. Biol. Chem.* **1994,** *269*, 18201-18208.

24. Kim, Y.-I.; Burton, R. E.; Burton, B. M.; Sauer, R. T.; Baker, T. A., Dynamics of Substrate Denaturation and Translocation by the ClpXP Degradation Machine. *Mol. Cell* **2000,** *5*, 639-648.

25. Sprangers, R.; Gribun, A.; Hwang, P. M.; Houry, W. A.; Kay, L. E., Quantitative NMR spectroscopy of supramolecular complexes: Dynamic side pores in ClpP are important for product release. *Proct. Nat. Acad. Sci.* **2005,** *102*, 16678-16683.

26. Zhang, J.; Ye, F.; Lan, L.; Jiang, H.; Luo, C.; Yang, C.-G., Structural Switching of Staphylococcus aureus Clp Protease: A key to understanding protease dynamics. *J. Biol. Chem.* **2011,** *286*, 37590-37601.

27. Geiger, S. R.; Bottcher, T.; Sieber, S. A.; Cramer, P., A Conformational Switch Underlies ClpP Protease Function. *Angew. Chem. Int. Ed.* **2011,** *50*, 5749-5752.

28. Kirstein, J.; Hoffmann, A.; Lilie, H.; Schmidt, R.; Rubsamen-Waigmann, H.; Brotz-Oesterhelt, H.; Mogk, A.; Turgay, K., The antibiotic ADEP reprogrammes ClpP, switching it from a regulated to an uncontrolled protease. *EMBO Mol. Med.* **2009,** *1*, 37-49.

29. Sass, P.; Josten, M.; Famulla, K.; Schiffer, G.; Sahl, H.-G.; Hamoen, L.; Brötz-Oesterhelt, H., Antibiotic acyldepsipeptides activate ClpP peptidase to degrade the cell division protein FtsZ. *PNAS* **2011,** *108*, 17174-17479.

30. Schiefer, A.; Vollmer, J.; Lämmer, C.; Specht, S.; Lentz, C.; Ruebsamen-Schaeff, H.; Brötz-Oesterhelt, H.; Hoerauf, A.; Pfarr, K., The ClpP peptidase of Wolbachia endobacteria is a novel target for drug development against filarial infections. In *J. Antimicrob. Chemother.*, 2013; Vol. 68, pp 1790 –1800.

31. Brotz-Oesterhelt, H.; Beyer, D.; Kroll, H.-P.; Endermann, R.; Ladel, C.; Schroeder, W.; Hinzen, B.; Raddatz, S.; Paulsen, H.; Henninger, K.; Bandow, J. E.; Hans-Georg, S.;

Harald, L., Dysregulation of bacterial proteolytic machinery by a new class of antibiotics. *Nat. Med.* **2005,** *11*, 1082-1087.

32. Bewley, M. C.; Graziano, V.; Griffin, K.; Flanagan, J. M., Turned on for degradation: ATPase-independent degradation by ClpP. *J. Struct. Biol.* **2009,** *165* (2), 118-125.

33. Pan, Y.; Piyadasa, H.; O'Neil, J. D.; Konermann, L., Conformational Dynamics of a Membrane Transport Protein Probed by H/D Exchange and Covalent Labeling: The Glycerol Facilitator. *J. Mol. Biol.* **2012,** *416*, 400-413.

34. Milne, J. S.; Mayne, L.; Roder, H.; Wand, A. J.; Englander, S. W., Determinants of protein hydrogen exchange studied in equine cytochrome c. *Protein Sci.* **1998,** *7*, 739-745.

35. Religa, T. L.; Ruschak, A. M.; Rosenzweig, R.; Kay, L. E., Site-Directed Methyl Group Labeling as an NMR Probe of Structure and Dynamics in Supramolecular Protein Systems: Applications to the Proteasome and to the CIpP Protease. *J. Am. Chem. Soc.* **2011,** *133* (23), 9063-9068.

36. Iacob, R. E.; Engen, J. R., Hydrogen Exchange Mass Spectrometry: Are We Out of the Quicksand? *J. Am. Soc. Mass Spectrom.* **2012,** *23*, 1003-1010.

37. Percy, A. J.; Rey, M.; Burns, K. M.; Schriemer, D. C., Probing protein interactions with hydrogen/deuterium exchange and mass spectrometry-A review. *Anal. Chim. Acta* **2012,** *721*, 7-21.

38. Englander, S. W., Hydrogen Exchange and Mass Spectrometry: A Historical Perspective. *J. Am. Soc. Mass Spectrom.* **2006,** *17*, 1481-1489.

39. Konermann, L.; Pan, J.; Liu, Y., Hydrogen Exchange Mass Spectrometry for Studying Protein Structure and Dynamics. *Chem. Soc. Rev.* **2011,** *40*, 1224-1234.

40. Kaltashov, I. A.; Bobst, C. E.; Abzalimov, R. R.; Berkowitz, S. A.; Houde, D., Conformation and Dynamics of Biopharmaceuticals: Transition of Mass Spectrometry-Based Tools from Academe to Industry. *J. Am. Soc. Mass Spectrom.* **2010,** *21*, 323-337.

41. Liu, T.; Pantazatos, D.; Li, S.; Hamuro, Y.; Hilser, V. J.; Woods, V. L., Quantitative assessment of protein structural models by comparison of H/D exchange MS data with exchange behavior accurately predicted by DXCOREX. *J. Am. Soc. Mass Spectrom.* **2012,** *23*, 43-56.

42. Rey, M.; Forest, E.; Pelosi, L., Exploring the Conformational Dynamics of the Bovine ADP/ATP Carrier in Mitochondria. *Biochemistry* **2012,** *51* (48), 9727-9735.

43. Keppel, T. R.; Howard, B. A.; Weis, D. D., Mapping Unstructured Regions and Synergistic Folding in Intrinsically Disordered Proteins with Amide H/D Exchange Mass Spectrometry. *Biochemistry* **2011,** *50* (40), 8722-8732.

44. Trelle, M. B.; Hirschberg, D.; Jansson, A.; Ploug, M.; Roepstorff, P.; Andreasen, P. A.; Jørgensen, T. J. D., Hydrogen/Deuterium Exchange Mass Spectrometry Reveals Specific Changes in the Local Flexibility of Plasminogen Activator Inhibitor 1 upon Binding to the Somatomedin B Domain of Vitronectin. *Biochemistry* **2012,** *51* (41), 8256-8266.

45. Skinner, J. J.; Lim, W. K.; Bédard, S.; Black, B. E.; Englander, S. W., Protein dynamics viewed by hydrogen exchange. *Protein Sci.* **2012,** *21*, 996-1005.

46. Maurizi, M. R.; Thompson, M. W.; Singh, S. K.; Kim, S. H., Endopeptidase-CLP - ATP-Dependent Clp Protease from Escherichia coli. *Methods Enzymol.* **1994,** *244*, 314-331.

47. Leung, E.; Datti, A.; Cossette, M.; Goodreid, J.; McCaw, S. E.; Mah, M.; Nakhamchik, A.; Ogata, K.; Bakkouri, M. E.; Cheng, Y.-Q.; Wodak, S. J.; Eger, B. T.; Pai, E. F.; Liu, J.; Gray-Owen, S.; Batey, R. A.; Houry, W. A., Activators of Cylindrical

Proteases as Antimicrobials: Identification and Development of Small Molecule Activators of ClpP Protease. *Chem. Biol.* **2011,** *18*, 1167–1178.

48. Wales, T. E.; Fadgen, K. E.; Gerhardt, G. C.; Engen, J. R., High-Speed and High-Resolution UPLC Separation at Zero Degree Celsius. *Anal. Chem.* **2008,** *80*, 6815-6820.

49. Weis, D. D.; Engen, J. R.; Kass, I. J., Semi-Automated Data Processing of Hydrogen Exchange Mass Spectra Using HX-Express. *J. Am. Soc. Mass Spectrom.* **2006,** *17*, 1700-1703.

50. Zhu, M. M.; Rempel, D. L.; Du, Z.; Gross, M. L., Quantification of Protein-Ligand Interactions by Mass Spectrometry, Titration, and H/D Exchange: PLIMSTEX. *J. Am. Chem. Soc.* **2003,** *125*, 5252-5253.

51. Powell, K. D.; Ghaemmaghami, S.; Wang, M. Z.; Ma, L.; Oas, T. G.; Fitzgerald, M. C., A General Mass Spectrometry-Based Assay for the Quantitation of Protein-Ligand Binding Interactions in Solution. *J. Am. Chem. Soc.* **2002,** *124*, 10256-10257.

52. Bai, Y.; Sosnick, T. R.; Mayne, L.; Englander, S. W., Protein Folding Intermediates: Native State Hydrogen Exchange. *Science* **1995,** *269*, 192-197.

53. Creighton, T. E., *Proteins*. W. H. Freeman & Co: New York, **1993**.

54. Pan, J.; Han, J.; Borchers, C. H.; Konermann, L., Hydrogen/Deuterium Exchange Mass Spectrometry with Top-Down Electron Capture Dissociation for Characterizing Structural Transitions of a 17 kDa Protein. *J. Am. Chem. Soc.* **2009,** *131* (35), 12801–12808.

55. Sperry, J. B.; Smith, C. L.; Caparon, M. G.; Ellenberger, T.; Gross, M. L., Mapping the Protein–Protein Interface between a Toxin and Its Cognate Antitoxin from the Bacterial Pathogen Streptococcus pyogenes. *Biochemistry* **2011,** *50*, 4038–4045.

56. Bennett, M. J.; Barakat, K.; Huzil, J. T.; Tuszynski, J.; Schriemer, D. C., Discovery and characterization of the laulimalide-microtubule binding mode by mass shift perturbation mapping. *Chem. Biol.* **2010,** *17*, 725-734.

57. Chalmers, M. J.; Busby, S. A.; Pascal, B. D.; West, G. M.; Griffin, P. R., Differential hydrogen/deuterium exchange mass spectrometry analysis of protein-Ligand interactions. *Exp. Rev. Proteomics* **2011,** *8*, 43-59.

58. Kern, D.; Zuiderweg, E. R. P., The role of dynamics in allosteric regulation. *Curr. Op. Struct. Biol.* **2003,** *13*, 748-757.

59. Hilser, V. J.; Wrabl, J. O.; Motlagh, H. N., Structural and Energetic Basis of Allostery. In *Annu. Rev. Biophys.*, Rees, D. C., Ed. Annual Reviews: Palo Alto, **2012**; Vol. 41, pp 585-609.

60. Ball, P., More than a bystander. *Nature* **2011,** *478*, 467-468.

61. Uzawa, T.; Nishimura, C.; Akiyama, S.; Ishimori, K.; Takahashi, S.; Dyson, H. J.; Wright, P. E., Hierarchical folding mechanism of apomyoglobin revealed by ultra-fast H/D exchange coupled with 2D NMR. *Proc. Natl. Acad. Sci. U.S.A.* **2008,** *105*, 13859-13864.

62. Kyte, J.; Doolittle, R., A simple method for displaying the hydropathic character of a protein. *J. Mol. Biol.* **1982,** *157*, 105-132.

63. Lee, M. E.; Baker, T. A.; Sauer, R. T., Control of Substrate Gating and Translocation into ClpP by Channel Residues and ClpX Binding. *J. Mol. Biol.* **2010,** *399* (5), 707-718.

64. Das, U.; Hariprasad, G.; Ethayathulla, A. S.; Manral, P.; Das, T. K.; Pasha, S.; Mann, A.; Ganguli, M.; Verma, A. K.; Bhat, R.; Chandrayan, S. K.; Ahmed, S.; Sharma, S.; Kaur, P.; Singh, T. P.; Srinivasan, A., Inhibition of Protein Aggregation: Supramolecular Assemblies of Arginine Hold the Key. *Plos One* **2007,** *2* (11), e1176.

65. Lu, J.; Witcher, D. R.; White, M. A.; Wang, X.; Huang, L.; Rathnachalam, R.; Beals, J. M.; Kuhstoss, S., IL-1β Epitope Mapping Using Site-Directed Mutagenesis and Hydrogen-Deuterium Exchange Mass Spectrometry Analysis. *Biochemistry* **2005,** *44*, 11106-11114.

66. Martin, A.; Baker, T. A.; Sauer, R. T., Distinct static and dynamic interactions control ATPase-Peptidase communication in a AAA plus protease. *Mol. Cell* **2007,** *27* (1), 41-52.

67. Bellelli, A.; Brunori, M., Hemoglobin allostery: Variations on the theme. *Biochim. Biophys. Acta* **2011,** *1807* (10), 1262-1272.

68. Monod, J.; Wyman, J.; Changeux, J. P., On the Nature of Allosteric Transitions - A Plausible Model. *J. Mol. Biol.* **1965,** *12* (1), 88-&.

69. Dyachenko, A.; Gruber, R.; Shimon, L.; Horovitz, A.; Sharon, M., Allosteric mechanisms can be distinguished using structural mass spectrometry. *Proc. Natl. Acad. Sci. U. S. A.* **2013,** *110* (18), 7235-7239.

Chapter 5. Noncovalent Binding of a Cyclic Peptide Inhibitor to the Peptidyl-Prolyl Isomerase Pin1 Explored by Hydrogen Exchange Mass Spectrometry

5.1. Introduction

Proteins owe their specific biological functions to unique three-dimensional structures. The native fold of each protein is determined by numerous side chain interactions, as well as main chain contacts, i.e., hydrogen bonds that stabilize α-helices and β-sheets.[1] The partial double bond character of backbone C_α(CO)-(NH)C_α groups favors a coplanar arrangement of the six atoms adjacent to peptide linkages. Steric constraints dictate that the *trans* configuration is greatly preferred.[2] One exception to this rule are X-Pro bonds (where X can be any non-proline residue). The backbone-linked five-membered ring of Pro causes the *cis* and *trans* isomers of the corresponding peptide bond to be relatively close in free energy.[3-4] As a result, the occurrence of *cis* X-Pro bonds in native proteins is quite high, on the order of 7%.[5] The *cis-trans* isomerization of X-Pro bonds is nonetheless a slow process that is associated with an activation barrier on the order of 60 - 80 kJ mol^{-1}.[6-8]

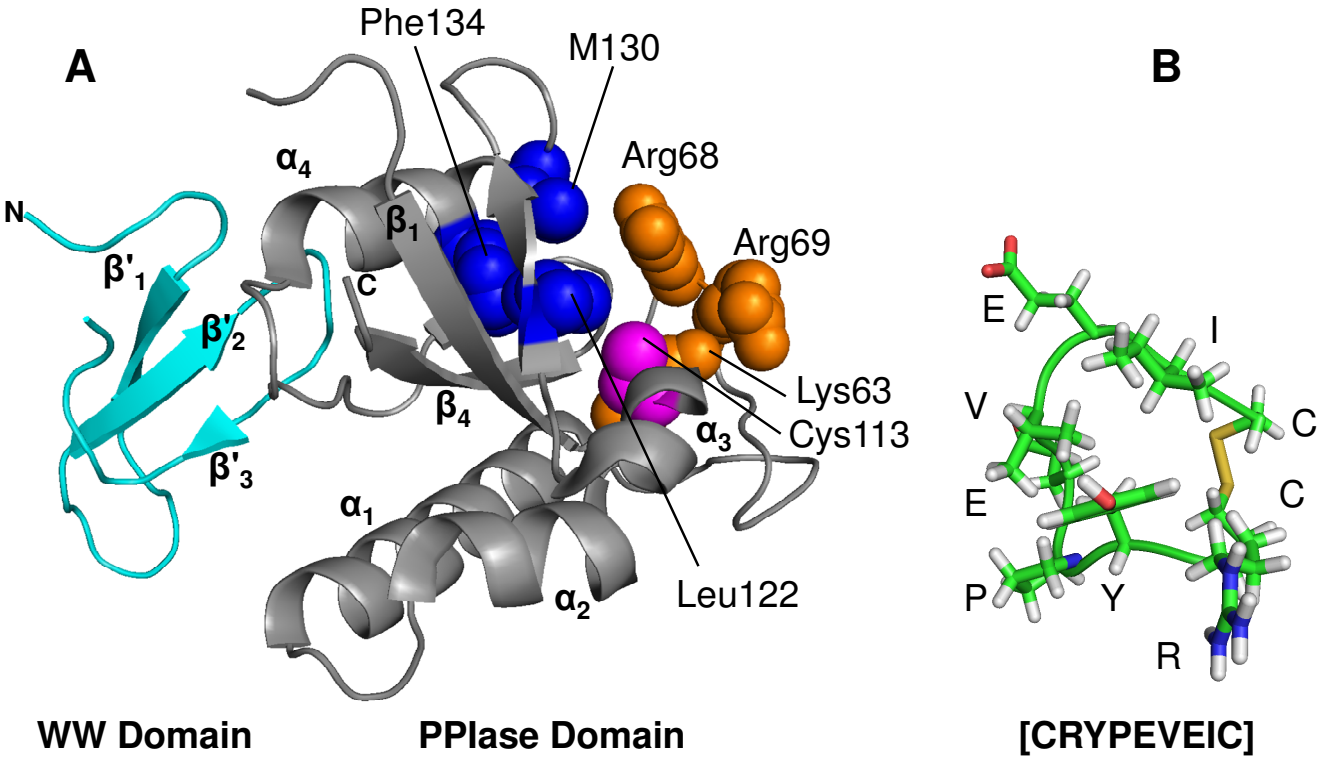

Figure 5-1: (A) Crystal structure of human Pin1 (PDB 3TCZ).[9] Selected active site residues and secondary structure elements are highlighted. Hydrophobic residues are shown in blue, cationic side chains are highlighted in orange, and the active site Cys113 is depicted in pink. The WW domain is colored cyan. Not all of the Pin1 residues were resolved in the X-ray data, causing the appearance of a discontinuous chain. (B) Representative NMR structure of the Pin1 inhibitor [CRYPEVEIC] in the free (unbound) state.[10] The square bracket notation is used to indicate the cyclic nature of the peptide.

Peptidyl-prolyl isomerases (PPIases) catalyze the *cis-trans* conversion of X-Pro bonds.[11] This group of enzymes comprises a number of well-known members such as cyclophilins and FK506-binding proteins.[3] Of particular interest for the current work, Pin1 is a PPIase that exhibits high specificity towards substrates where proline is preceded by phosphoserine or phosphothreonine (pSer-Pro or pThr-Pro).[3,12] Pin1 is involved in eukaryotic cell cycle regulation,[13] and as such it is a promising anticancer target.[14-17] The C-terminal domain of the largest subunit of RNA polymerase II is one of the primary Pin1 *in vivo* substrates,

highlighting the involvement of Pin1 in transcription regulation.[9,18] The phosphorylation-dependent substrate specificity of Pin1 is consistent with its central role in kinase/phosphatase mediated signaling pathways, many of which become deregulated in cancer.[19-20] In addition, Pin1 appears to be involved in disease states related to ageing, viral infections, asthma, and Alzheimer's disease.[21-25]

The 17.6 kDa amino acid sequence of Pin1 forms a N-terminal WW domain (residues 1-39) and a C-terminal PPIase domain (residues 45-163, Figure 5-1A).[9,12] The former consists of three antiparallel β strands (β1′ - β3′), whereas the latter has a mixed secondary structure comprising strands β1 - β4 and helices α1 - α4. The relatively close contacts seen between the two domains in X-ray structural data[9,12] may not adequately reflect the properties of Pin1 in solution where the WW and PPIase domains appear to be more independent of one another.[26] The reaction mechanism of Pin1 remains elusive, although Cys113 clearly represents one of the key active site residues.[27-28] Leu122, Met130, and Phe134 form a hydrophobic binding pocket that accommodates the substrate proline, whereas the cationic side chains of Lys63, Arg68, and Arg69 interact with the negatively charged phosphate.[12] While the catalytic function of Pin1 resides within the PPIase domain, the WW domain may represent the initial site of substrate recognition.[26,29]

The role of Pin1 as a potential drug target has sparked the development of custom-designed inhibitors that compete for binding with the natural pSer/pThr-Pro substrates.[9,30-37] Inhibitors carrying phosphate groups can act as substrate mimics; however, a problem with this approach is the limited membrane permeability of phosphorylated compounds which compromises their therapeutic potential.[35] Hence, the identification of non-phosphorylated Pin1 inhibitors remains an important goal. Peptide libraries are an interesting starting point for Pin1 inhibitor screening. Unfortunately, the loss of conformational entropy upon complex

formation tends to reduce the binding affinity of many peptides. A promising strategy to overcome this problem is the use of cyclic peptides that experience a lower entropic penalty upon noncovalent binding to the protein receptor.[38] Liu et al.[39] were the first to successfully employ such a strategy for the development of Pin1 inhibitors. Similarly, Duncan et al.[10] used phage display technology to identify the cyclic peptide [CRYPEVEIC] (square brackets are used to denote the cyclic structure) as a highly selective ligand for the Pin1 PPIase domain with a dissociation constant around 0.5 μM (Figure 5.1B). Cyclization of the peptide was achieved by disulfide formation of the two terminal -SH groups. NMR spectroscopy was successfully applied for elucidating the solution structure of free [CRYPEVEIC], but unfortunately conformational information obtained for the protein-ligand complex was extremely limited. Also, crystallization studies of the Pin1-[CRYPEVEIC] complex have been unsuccessful to date.[10]

Hydrogen/deuterium exchange (HDX) mass spectrometry (MS) is a widely used approach for examining protein structure, dynamics, and interactions.[40-51] Solvent-exposed N-H sites in unstructured regions undergo deuteration with rate constants on the order of 1 s^{-1}.[52] Exchange at backbone sites that are involved in hydrogen bonds (e.g., in α-helices or β-sheets) is much slower. HDX at these sites is mediated by structural fluctuations that lead to the transient disruption of hydrogen bonds, coupled with backbone N-H exposure to the solvent. Ligand binding usually stabilizes the protein, thereby reducing HDX rates. The largest changes tend to occur in the vicinity of the binding site, although allosteric effects can play a role as well.[50-51] It is also possible that some segments exhibit higher HDX rates after ligand binding, corresponding to local enhancements in protein dynamics.[48,53-55]

In the current work we use HDX/MS for exploring the response of Pin1 to [CRYPEVEIC] binding. Especially in cases where X-ray crystallographic data are not

available, HDX/MS can provide important insights into the nature of protein-ligand interactions.[50-51] Also, our aim was to identify highly mobile sequence regions in the Pin1-[CRYPEVEIC] complex. The presence of such dynamic elements often prevents proteins from crystallizing. It is likely that issues of this type were responsible for the lack of success in previous crystallization attempts.[10] It has been demonstrated for other proteins that HDX/MS can guide the design of truncated protein variants with enhanced crystallization propensity.[56] Our results demonstrate that [CRYPEVEIC] binding causes marked deuteration changes in the Pin1 PPIase domain. Many of these alterations reflect the occurrence of ligand-induced stabilization, but interestingly there is also a long sequence stretch that becomes more dynamic after [CRYPEVEIC] binding. These data yield novel information on the nature of Pin1-ligand interactions, and they provide the foundation for future crystallization trials on truncated protein constructs.

5.2. Experimental Section

5.2.1. Materials.

4-(2-Hydroxyethyl)-1-piperazineethanesulfonic acid (HEPES) was purchased from Sigma (St. Louis, MO, USA), and D_2O was from Cambridge Isotope Laboratories (Andover, MA). All chemicals were used as received. The Arg14Ala variant of human Pin1 was overexpressed in *E. coli* and isolated as described.[10,57] [CRYPEVEIC] was purchased from EZBiolab (Westfield, IN). The presence of the cyclic form was verified by ESI-MS, which resulted in a mass of 1109.5 Da, 2 Da less than expected for the linear amino acid sequence. This mass difference corresponds to the loss of two hydrogens as the terminal cysteine residues get linked via a -S-S- bond.

5.2.2. Backbone Amide Hydrogen/Deuterium Exchange Mass Spectrometry.

The experiments started with 100 μM Pin1 in 10 mM HEPES/100 mM NaCl (pH 7.7). [CRYPEVEIC]-bound samples were prepared by adding 2 μL of 25 mM [CRYPEVEIC] in water to 13 μL of Pin1 solution, resulting in a five-fold molar excess of ligand. These mixtures were pre-equilibrated for 24 h at 4 °C. Deuteration was conducted at room temperature. HDX was initiated by addition of 9 volumes of D_2O-based labeling buffer which had the same salt concentration as the stock solution, for a final measured pH of 7.7 and a protein concentration of 10 μM. For $K_d \approx 0.5$ μM[10] the fraction of bound protein under HDX conditions was estimated to be 99%. 30 μL aliquots were removed at various time points ranging from 1 to 360 min after initiating of labeling. These aliquots were quenched at pH 2.4 by addition of HCl on ice, followed by flash freezing in liquid nitrogen and storage at -80 °C. For spatially-resolved HDX/MS experiments, the aliquots were rapidly thawed to ~0 °C and manually injected into a nanoACQUITY UPLC with HDX technology (Waters, Milford, MA)[58] for desalting and peptide separation within 15 min on an equilibrated reversed phase column (BEH C18 1.7 μm, 1 mm × 100 mm) using a water/acetonitrile gradient in the presence of 0.1% formic acid at 35 μL min^{-1} . Online digestion was performed on a POROS pepsin column (2.1 mm × 30 mm) from Life Technologies/Applied Biosystems (Carlsbad, CA) at room temperature. The temperature for peptide trapping and reversed phase separation was set to 1 °C. Blank (water) injections in-between protein injections ensured the absence of sample carryover.

Mass analysis of peptides was performed on a Waters Synapt HDMS instrument with source and desolvation temperatures of 80 and 300 °C, respectively, a cone voltage of 30 V, and an electrospray voltage of 2.8 kV. The identity of each peptide was confirmed by tandem MS based on the known Pin1 sequence. Zero time point controls (m_0) for the correction of in-exchange were performed by exposing Pin 1 to quenching buffer, followed by D_2O exposure, resulting in the same final solution composition as for all other samples. Controls for fully exchanged Pin1 (m_{100}, for the correction of back exchange) were prepared by incubating 30 μM Pin 1 in labeling solution at pH 2.0 for 6 days. Biolynx 4.1 (Waters) and HX-Express[59] were employed to analyze the centroid mass of all peptides as a function of labeling time. Deuteration levels ($\%D$) were determined as

$$\% \ D = \frac{(m - m_0)}{(m_{100} - m_0)} \times 100\% \qquad (5.1)$$

Average deuteration differences for Figs. 5.6 were calculated as

$$average\ difference = \frac{1}{N} \sum \ (\%D_{[CRYPEVEIC\ ]} - \%D_{free}) \qquad (5.2)$$

The sum extends over the N = 6 time points that were measured for each peptide. All measurements were performed in triplicate. Error bars represent standard deviations. The Pin1 sequence numbering used here for reporting our data is consistent with that commonly used in the literature[9], where the active site cysteine corresponds to position 113. Hence, the

N-terminal residue is referred to as Lys6 (instead of Lys1). This implies that after the HDX analysis all residue numbers had to be increased by five.

5.3. Results and Discussion

Peptic digestion of Pin1 under HDX conditions resulted in 28 identifiable peptides, corresponding to a sequence coverage of 80 % (Figure 5-2). Even without any data processing, it is evident that the presence of [CRYPEVEIC] has noticeable effects on the structural dynamics of

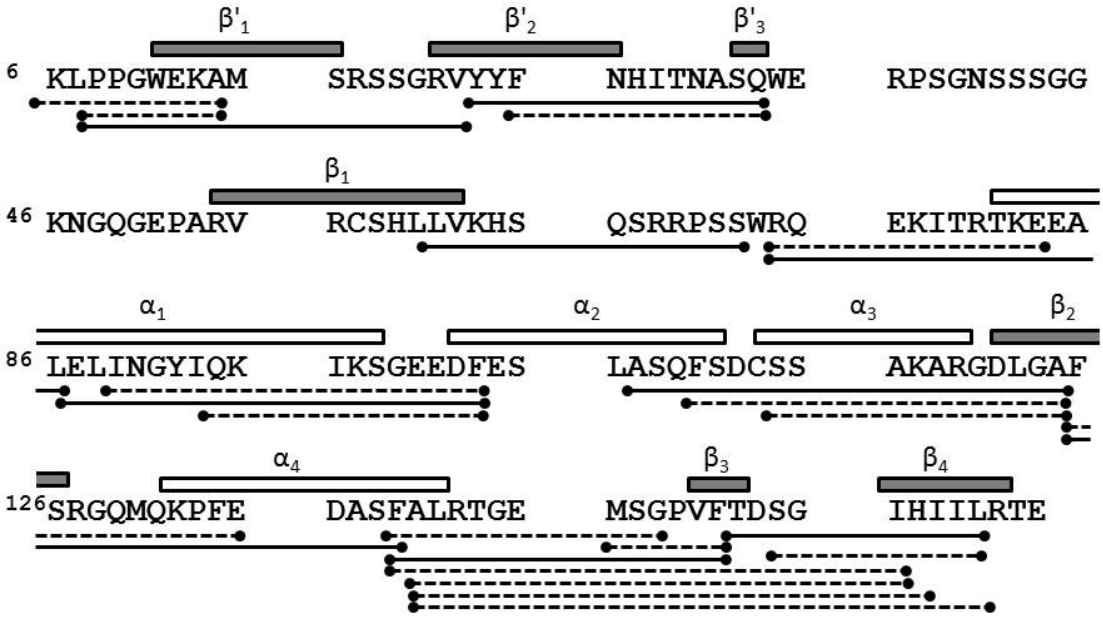

Figure 5-2: Sequence and secondary structure elements of Pin1, with the conventionally used residue numbering.[9] Solid lines represent peptides used for the graphic representation of deuteration levels in Figs. 5-5, 5-6. Dashed lines represent redundant peptides.

Pin1. The peptide behavior can be categorized into three groups as illustrated in Figure 5-3. Some peptides exhibited only very minor differences in their deuteration kinetics upon addition of the ligand (e.g., residues 140-160, Figure 5-3A). Others showed significantly reduced deuteration in the presence of [CRYPEVEIC], indicating the occurrence of ligand-induced rigidification (e.g., 139-151, Figure 5-3B). Interestingly, there were also some segments where deuteration was enhanced after [CRYPEVEIC] binding, such as 74-86 (Figure 5-3C).

A comprehensive overview of the spatially-resolved HDX kinetics is provided in Figure 5-4. These data illustrate that the deuteration behavior of the various Pin1 segments is highly dependent on the position within the sequence.

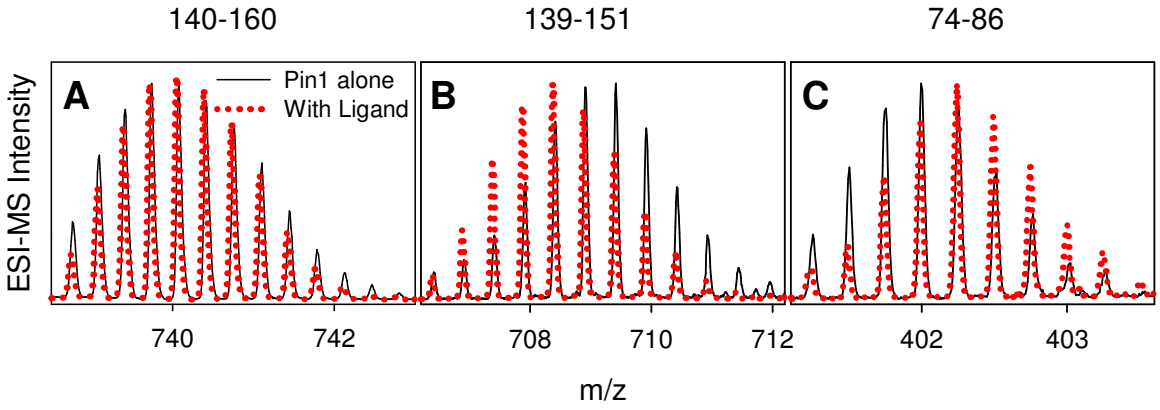

Figure 5-3: Unprocessed HDX/MS data for three Pin 1 peptic peptides recorded in the absence (black solid lines) and in the presence (red dotted lines) of [CRYPEVEIC] for a deuteration time of t = 360 min. The sequence range of the three peptides is indicated along the top.

Peptides towards the N-terminus display very rapid deuterium uptake, indicating that the corresponding protein regions are highly dynamic, with backbone N-H groups that are either unprotected or engaged in hydrogen bonds that are only marginally stable. In contrast, C-terminal segments exhibit a much higher protection against deuteration, reflecting the presence of stable secondary structure.

To facilitate a discussion of the Pin1 response to ligand binding, HDX data for a labeling time of 1 h were mapped to the X-ray structure of the protein (Figure 5-5). The N-terminal WW domain is displayed in red, signifying its near-complete deuteration both in the presence and in the absence of [CRYPEVEIC]. The extremely dynamic nature of this domain is somewhat unexpected, considering that isolated Pin1 WW constructs have served as model systems in folding experiments where they were treated as independently stable moieties.[60]

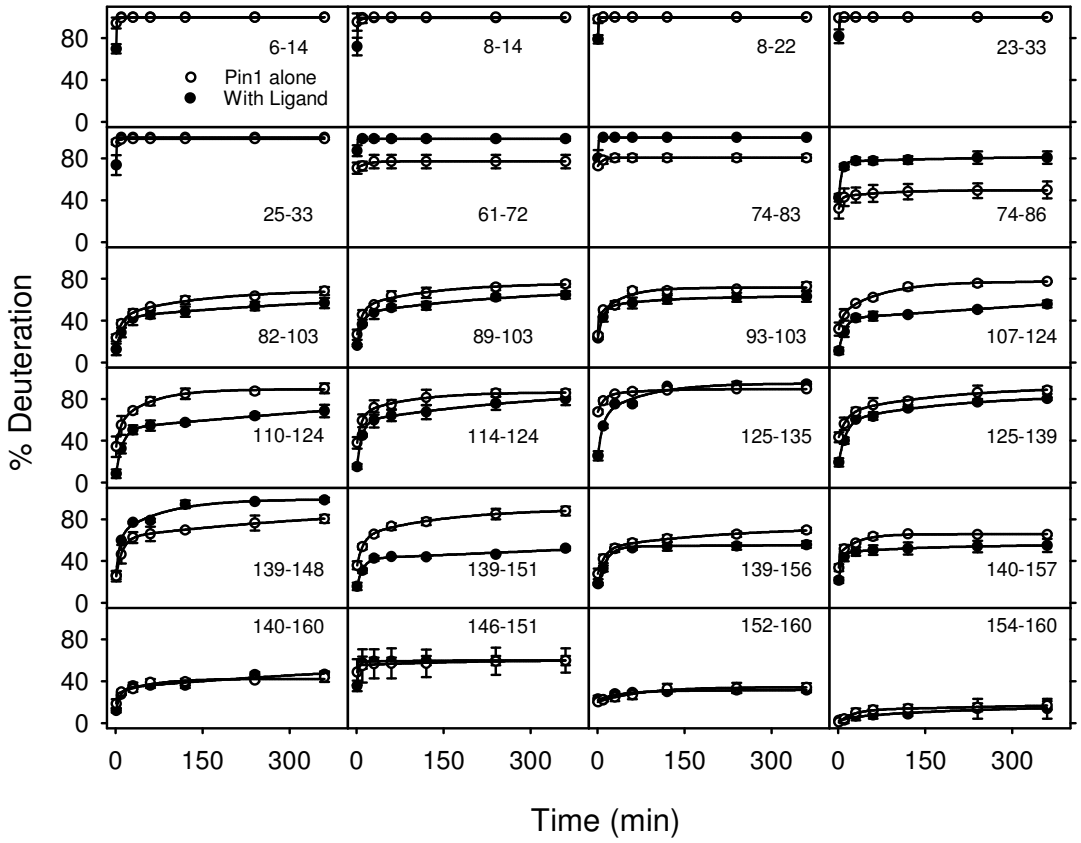

Figure 5-4: Normalized deuteration kinetics of Pin1 peptic peptides (%D, determined on the basis of eq. 5.1). Each panel shows data recorded in the absence of ligand (open circles) and in the presence of [CRYPEVEIC] (filled symbols). Lines are biexponential fits. Error bars represent standard deviations of triplicate measurements.

However, crystallization efforts of the isolated WW domain were unsuccessful for many years. Only very recently has it been possible to overcome this problem using a racemic mixture in the presence of small-molecule additives.[61] These crystallization difficulties have been attributed to the highly dynamic nature of the Pin1 WW domain.[61] Our HDX/MS data are in line with these findings, and they furthermore reveal that the WW domain remains highly dynamic even in the context of intact Pin1. The conformational flexibility of the WW domain is also consistent with the fact that all existing Pin1 X-rays structures have a number of unresolved residues in the N-

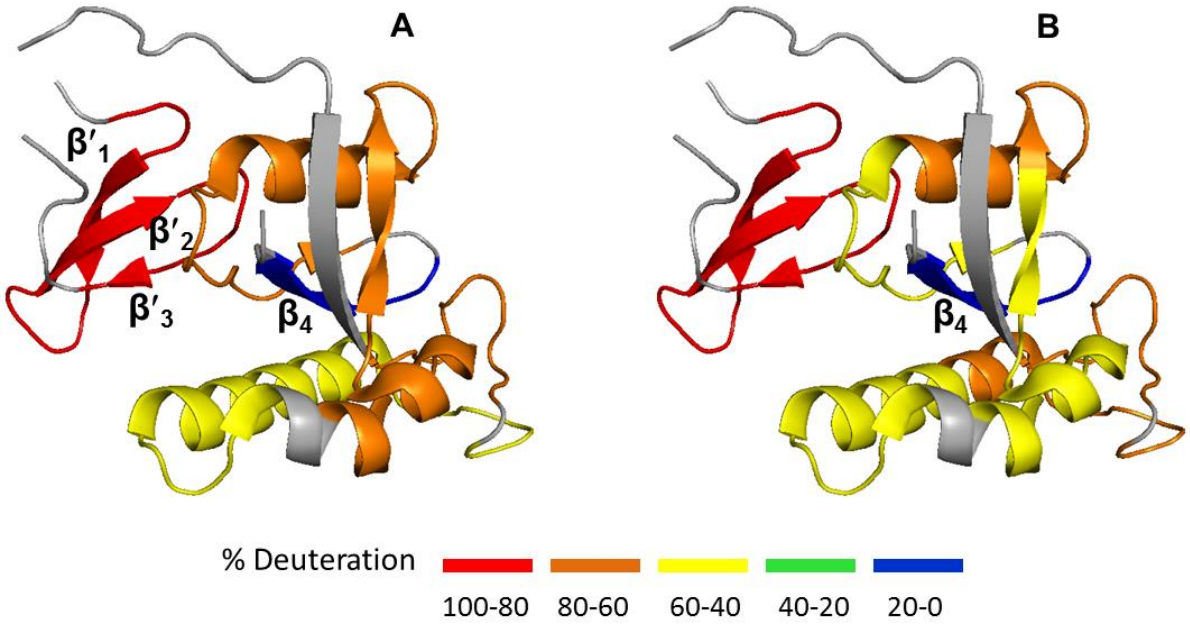

Figure 5-5: Mapping of the HDX data from Figure 5.4 to the crystal structure of Pin1 for a deuteration time of *t* = 60 min in the absence of ligand (A) and in the presence of [CRYPEVEIC]. Colors represent deuteration percentages as indicated in the legend. Gray color represents regions that were not covered during peptide mapping.

Terminal region.[9,12,62] In contrast to the WW domain, the PPIase domain of Pin1 showed deuteration kinetics that were much more distinct, consistent with the presence of well-developed secondary structure. Most of the PPIase domain elements displayed HDX levels ranging between 40 and 80% after one hour of deuteration (Figure 5-5, yellow and orange). The most protected element is β4 which is deeply buried (Figure 5-5, blue).

Changes in the deuteration pattern of Pin1 after [CRYPEVEIC] binding are displayed in Figure 5-6. Regions that underwent significant alterations upon addition of the ligand are highlighted in color, whereas all other segments are shown in gray. The color pattern of Figure 5-6 again highlights that ligand-induced changes are confined to the PPIase domain,

whereas the WW domain does not interact with [CRYPEVEIC]. This finding is consistent with recent chemical shift perturbation results.[10]

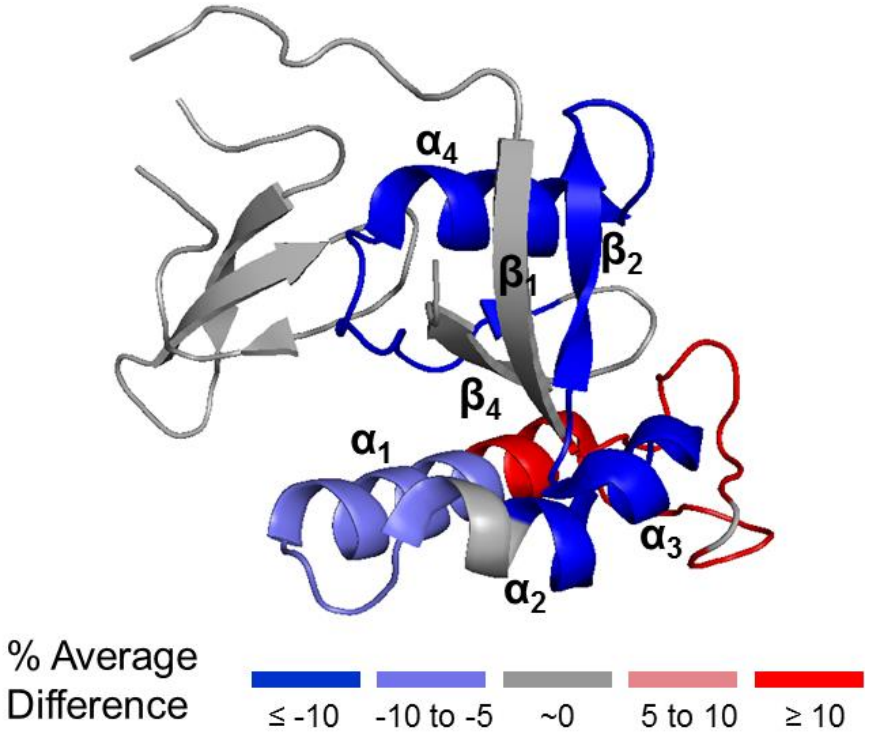

Figure 5-6: Deuteration difference map of Pin1 before and after [CRYPEVEIC] binding, calculated on the basis of eq. 5.2. Segments with reduced deuteration after ligand binding are represented in blue, while those with enhanced deuteration are shown in red, as indicated in the color legend.

Pronounced stabilization is seen for β2, α3, and α4 (Fig. 5-6, blue) which are known to be involved in substrate binding. β2 and α4 carry the residues that form the hydrophobic Pro binding pocket, whereas α3 comprises the active site Cys113 (cf. Figure 5-1A).[10,12]

Intriguingly, the sequence stretch covering residues 61 to 86 displayed elevated deuteration in the presence of [CRYPEVEIC], implying the occurrence of enhanced conformational dynamics after ligand binding (Figure 5-6, red). Most of these residues fold into a double-looped structure that connects β1 and α1. X-ray data[9] show that at least five N-H sites in this region form strong backbone hydrogen bonds. The destabilized region identified here

comprises the basic residues Lys63, Arg68, and Arg69 which bind the negatively charged phosphate of natural pSer-Pro or pThr-Pro substrates.[12] NMR shift perturbation data suggested that neither Lys63 nor Arg68 interact strongly with [CRYPEVEIC].[10] While the data of the current work cannot pinpoint individual residues, our HDX/MS results clearly demonstrate that residues in the 61-86 range do respond to the presence of the inhibitor. The observation of enhanced deuteration strongly suggests that these interactions are unfavorable. In other words, [CRYPEVEIC] binding to Pin1 distorts the 61-86 range in a way that weakens hydrogen bonding in this segment. Assuming that P4 of [CRYPEVEIC] occupies its canonical hydrophobic pocket (Figure 5-1A, blue)[12], it seems likely that steric clashes of Pin1 with either Y3 or E5 are responsible for destabilizing the 61-86 segment. One possibility is that the E5 carboxylate interacts with the positively charged side chains of Lys63, Arg68, or Arg69 by acting as a poor phosphate mimic. In any case, the enhanced deuterium uptake seen here for the "red" elements of Figure 5-6 originates from a partially distorted Pin1 structure that arises as the protein accommodates the inhibitor. The occurrence of ligand-induced destabilization in selected protein regions has been reported in a few previous studies on other systems.[48,53-55] In general, however, this phenomenon is uncommon because ligand binding is normally dominated by an overall protein stabilization that manifests itself as a reduction in deuteration levels.[46-47] Even for the Pin1-[CRYPEVEIC] interaction studied here such stabilizing effects are prevalent, seen from the many "blue" sequence regions in Figure 5-6.

5.4. Conclusions

The cyclic peptide [CRYPEVEIC] was recently identified as a potent Pin1 inhibitor, demonstrating that the presence of a phosphate group is not an absolute prerequisite for Pin1 binding.[10] In other words, the protein will also interact with compounds that do not possess the pSer-Pro or pThr-Pro motif found in natural substrates. [CRYPEVEIC] represents a promising lead compound for membrane-permeable anticancer agents. Efforts to refine the architecture of [CRYPEVEIC]-like compounds would greatly benefit from the availability of high resolution X-ray structures that reveal the exact mode of inhibitor binding to Pin1. The lack of success in generating suitable crystals of [CRYPEVEIC]-bound Pin1 thus represents a major impediment. One approach to deal with this type of problem is the use of "disorder-depleted" protein constructs that may be more amenable to crystallization. HDX/MS has previously been employed for identifying flexible regions that may interfere with crystal nucleation and growth.[56] The HDX/MS experiments of the current work identify the loop region of residues 61-86 as having an elevated degree of disorder after [CRYPEVEIC] binding. Protein constructs with truncations in this region may therefore be more amenable to the formation of high quality crystals than full-length Pin1. Crystallization trials on such constructs are currently underway, and the results of these efforts will be reported elsewhere.

From a more general perspective, [CRYPEVEIC] binding to Pin1 illustrates that ligand interactions can be associated with a complex pattern of stabilizing and destabilizing factors. In HDX/MS this leads to scenarios where some regions display lower deuteration whereas others are more deuterated in the presence of ligand (blue and red, respectively, in Fig. 5-6). There is a small but growing number of protein-ligand systems for which similar effects have been reported previously.[48,53-55] Recent work has demonstrated that it is even

feasible for ligand binding to accelerate HDX kinetics in a global fashion.[63] In any case, the observation of these and other phenomena illustrates the capability of HDX/MS to probe intricate details of biomolecular structure and interactions.

5.5. References

1. Anfinsen, C. B., Principles that Govern the Folding of Protein Chains. *Science* **1973,** *181*, 223-230.

2. Corey, R. B.; Pauling, L., Fundamental Dimensions of Polypeptide Chains. *Proc. R. Soc. London B* **1953,** *141* (902), 10-20.

3. Lu, P. K.; Finn, G.; Lee, H. T.; Nicholson, L. K., Prolyl cis-trans isomerization as a molecular timer. *Nat. Chem. Biol.* **2007,** *3*, 619-629.

4. Zimmerman, S. S.; Scheraga, H. A., Stability of cis, trans, and nonplanar peptide groups. *Macromolecules* **1976,** *9* (3), 408-416.

5. Stewart, D. E.; Sarkar, A.; Wampler, J. E., Occurence and Role of cis Peptide-Bonds in Protein Structures. *J. Mol. Biol.* **1990,** *214* (1), 253-260.

6. Grathwohl, C.; Wuthrich, K., NMR-Studies of the Rates of Proline Cis-Trans Isomerization in Oligopeptides. *Biopolymers* **1981,** *20* (12), 2623-2633.

7. Brandts, J. F.; Halvorson, H. R.; Brennan, M., Consideration of the Possibility That the Slow Step in Protein Denaturation Reactions Is Due to Cis-Trans Isomerism of Proline Residues. *Biochemistry* **1975,** *22*, 4953-4963.

8. Houry, W. A.; Scheraga, H. A., Nature of the Unfolded State of Ribonuclease A: Effect of Cis-Trans X-Pro Peptide Bond Isomerisation. *Biochemistry* **1996,** *35*, 11719-11733.

9. Zhang, M. M.; Wang, X. J.; Chen, X.; Bowman, M. E.; Luo, Y. H.; Noel, J. P.; Ellington, A. D.; Etzkorn, F. A.; Zhang, Y., Structural and Kinetic Analysis of Prolyl-isomerization/Phosphorylation Cross-Talk in the CTD Code. *ACS Chem. Biol.* **2012,** *7* (8), 1462-1470.

10. Duncan, K. E.; Dempsey, B. R.; Killip, L. E.; Adams, J.; Bailey, M. L.; Lajoie, G. A.; Litchfield, D. W.; Brandl, C. J.; Shaw, G. S.; Shilton, B. H., Discovery and Characterization of a Nonphosphorylated Cyclic Peptide Inhibitor of the Peptidylprolyl Isomerase, Pin1. *J. Med. Chem.* **2011,** *54* (11), 3854-3865.

11. Schiene-Fischer, C.; Aumuller, T.; Fisher, G., Peptide Bond cis/trans Isomerases: A Biocatalysis Perspective of Conformational Dynamics in Proteins. In *Molecular Chaperones*, Jackson, S., Ed. Springer-Verlag Berlin: Berlin, **2013**; Vol. 328, pp 35-67.

12. Ranganathan, R.; Lu, K. P.; Hunter, T.; Noel, J. P., Structural and functional analysis of the mitotic rotamase Pin1 suggests substrate recognition is phosphorylation dependent. *Cell* **1997,** *89* (6), 875-886.

13. Lu, K. P.; Hanes, S. D.; Hunter, T., A human peptidyl-prolyl isomerase essential for regulation of mitosis. *Nature* **1996,** *380*, 544-547.

14. Uchida, T.; Takamiya, M.; Takahashi, M.; Miyashita, H.; Ikeda, H.; Terada, T.; Matsuo, Y.; Shirouzu, M.; Yokoyama, S.; Fujimori, F.; Hunter, T., Pin1 and Par14 Peptidyl Prolyl Isomerase Inhibitors Block Cell Proliferation. *Chem. Biol.* **2003,** *10*, 15-24.

15. Rustighi, A.; Zannini, A.; Tiberi, L.; Sommaggio, R.; Piazza, S.; Sorrentino, G.; Nuzzo, S.; Tuscano, A.; Eterno, V.; Benvenuti, F.; Santarpia, L.; Aifantis, I.; Rosato, A.; Bicciato, S.; Zambelli, A.; Sal, G. D., Prolyl-isomerase Pin1 controls normal and cancer stem cells of the breast. *EMBO J.* **2014,** *6*, 99-119.

16. Lu, K. P., Prolyl isomerase Pin1 as a molecular target for cancer diagnostics and therapeutics. *Cancer Cell* **2003,** *4* (3), 175-180.

17. Wang, X. D. J.; Etzkorn, F. A., Peptidyl-prolyl isomerase inhibitors. *Biopolymers* **2006,** *84* (2), 125-146.

18. Xu, Y. X.; Hirose, Y.; Zhou, X. Z.; Lu, K. P.; Manley, J. L., Pin1 modulates the structure and function of human RNA polymerase II. *Genes Dev.* **2003,** *17* (22), 2765-2776.

19. Blume-Jensen, P.; Hunter, T., Oncogenic kinase signalling. *Nature* **2001,** *411*, 355-365.

20. St-Denis, N. A.; Litchfield, D. W., From birth to death: The role of protein kinase CK2 in the regulation of cell proliferation and survival. *Cell. Mol. Life Sci.* **2009,** *66* (11-12), 1817-1829.

21. Lee, T.-H.; Pastorino, L.; Lu, K. P., Peptidyl-prolyl cis–trans isomerase Pin1 in ageing, cancer and Alzheimer disease. *Expert Rev. Mol. Med.* **2011,** *13*, 1-26.

22. Guito, J.; Gavina, A.; Palmeri, D.; Lukac, D. M., The Cellular Peptidyl-Prolyl cis/trans Isomerase Pin1 Regulates Reactivation of Kaposi's Sarcoma-Associated Herpesvirus from Latency. *J. Virol.* **2014,** *88*, 647.

23. Lonati, E.; Brambilla, A.; Milani, C.; Masserini, M.; Palestini, P.; BulbarellI, A., Pin1, a new player in the fate of HIF-1α degradation: an hypothetical mechanism inside vascular damage as Alzheimer's disease risk factor. *Front. Cell. Neurosci.* **2014,** *8*, 1-11.

24. Wang, J.-Z.; Zhu, W.-D.; Xu, Z.-X.; Du, W.-T.; Zhang, H.-Y.; Sun, X.-W.; Wang, X.-H., Pin1, endothelial nitric oxide synthase, and amyloid-b form a feedback signaling loop involved in the pathogenesis of Alzheimer's disease, hypertension, and cerebral amyloid angiopathy. *J. Med. Hypotheses* **2014,** *82*, 145-150.

25. Inoue, K. I.; Takano, H.; Kumagai, Y., Pin 1 blockade in asthma by naphthoquinone? *J. Allergy Clin. Immunol.* **2008,** *121* (4), 1064-1064.

26. Jacobs, D. M.; Saxena, K.; Vogtherr, M.; Bernado, P.; Pons, M.; Fiebig, K. M., Peptide binding induces large scale changes in inter-domain mobility in human Pin1. *J. Biol. Chem.* **2003,** *278* (28), 26174-26182.

27. Bailey, M. L.; Shilton, B.; Brandl, C. J.; Litchfield, D. W., The Dual Histidine Motif in the Active Site of Pin1 Has a Structural Rather than Catalytic Role. *Biochem* **2008,** *47*, 11481-11489.

28. Behrsin, C. D.; Bailey, M. L.; Bateman, K. S.; Hamilton, K. S.; Wahl, L. M.; Brandl, C. J.; Shilton, B. H.; Litchfield, D. W., Functionally important residues in the peptidyl-prolyl isomerase Pin1 revealed by unigenic evolution. *J. Mol. Biol.* **2007,** *365* (4), 1143-1162.

29. Lu, P. J.; Zhou, X. Z.; Shen, M.; Lu, K. P., Function of WW Domains as Phosphoserine- or Phosphothreonine-Binding Modules. *Science* **1999,** *283*, 1325-1328.

30. Bayer, E.; Thutewohl, M.; Christner, C.; Tradler, T.; Osterkamp, F.; Waldmann, H.; Bayer, P., Identification of hPin1 inhibitors that induce apoptosis in a mammalian Ras transformed cell line. *Chem. Commun.* **2005**, 516-518.

31. Daum, S.; Erdmann, F.; Fischer, G.; Feaux de Lacroix, B.; Hessamian-Alinejad, A.; Houben, S.; Frank, W.; Braun, M., Aryl Indanyl Ketones: Efficient Inhibitors of the Human Peptidyl Prolyl cis/trans Isomerase Pin1 *Angew. Chem.* **2006,** *45*, 7454-7458.

32. Braun, M.; Hessamian-Alinejad, A.; Féaux de Lacroix, B.; Alvarez, B. H.; Fischer, G., Novel Spiroannulated 3-Benzofuranones. Synthesis and Inhibition of the Human Peptidyl Prolyl cis/trans Isomerase Pin1. *Molecules* **2008,** *13*, 995-1003.

33. Guo, C.; Hou, X.; Dong, L.; Dagostino, E.; Greasley, S.; Ferre, R.; Marakovits, J.; Johnson, M. C.; Matthews, D.; Mroczkowski, B.; Parge, H.; VanArsdale, T.; Popoff, I.; Piraino, J.; Margosiak, S.; Thomson, J.; Los, G.; Murray, B. W., Structure-based design of novel human Pin1 inhibitors (I). *Bioorg. Med. Chem.* **2009,** *19*, 5613-5616.

34. Tatara, Y.; Lin, Y.-C.; Bamba, Y.; Mori, T.; Uchida, T., Dipentamethylene thiuram monosulfide is a novel inhibitor of Pin1. *biochem. Biophys. Res. Comm.* **2009,** *384*, 394-398.

35. Dong, L.; Marakovits, J.; Hou, X.; Guo, C.; Greasley, S.; Dagostino, E.; Ferre, R.; Johnson, M. C.; Kraynov, E.; Thomson, J.; Pathak, V.; Murray, B. W., Structure-based design of novel human Pin1 inhibitors (II). *Bioorg. Med. Chem.* **2010,** *20*, 2210-2214.

36. Potter, A.; Oldfield, V.; Nunns, C.; Fromont, C.; Ray, S.; Northfield, C. J.; Bryant, C. J.; Scrace, S. F.; Robinson, D.; Matossova, N.; Baker, L.; Dokurno, P.; Surgenor, A. E.; Davis, B.; Richardson, C. M.; Murray, J. B.; Moore, J. D., Discovery of cell-active phenyl-imidazole Pin1 inhibitors by structure-guided fragment evolution. *Bioorg. Med. Chem.* **2010,** *20*, 6483-9488.

37. Aluise, C. D.; Rose, K.; Boiani, M.; Reyzer, M. L.; Manna, J. D.; Tallman, K.; Porter, N. A.; Marnett, L. J., Peptidyl-prolyl cis/trans-Isomerase A1 (Pin1) Is a Target for Modification by Lipid Electrophiles. *Chem. Res. Toxicol.* **2013,** *26* (2), 270-279.

38. Katz, B. A.; Johnson, C.; Cass, R. T., Structure-based design of high affinity streptavidin binding cyclic peptide ligands containing thioether crosslinks. *J. Am. Chem. Soc.* **1995,** *117* (33), 8541-8547.

39. Liu, T.; Liu, Y.; Kao, H.-Y.; Pei, D., Membrane Permeable Cyclic Peptidyl Inhibitors against Human Peptidylprolyl Isomerase Pin1. *J. Med. Chem.* **2010,** *53*, 2494-2501.

40. Konermann, L.; Pan, J.; Liu, Y., Hydrogen Exchange Mass Spectrometry for Studying Protein Structure and Dynamics. *Chem. Soc. Rev.* **2011,** *40*, 1224-1234.

41. Kaltashov, I. A.; Bobst, C. E.; Abzalimov, R. R., Mass spectrometry-based methods to study protein architecture and dynamics. *Protein Sci.* **2013,** *22* (5), 530-544.

42. Iacob, R. E.; Engen, J. R., Hydrogen Exchange Mass Spectrometry: Are We Out of the Quicksand? *J. Am. Soc. Mass Spectrom.* **2012,** *23*, 1003-1010.

43. Englander, S. W., Hydrogen exchange and mass spectrometry: A historical perspective. *J. Am. Soc. Mass Spectrom.* **2006,** *17* (11), 1481-1489.

44. Rob, T.; Liuni, P.; Gill, P. K.; Zhu, S. L.; Balachandran, N.; Berti, P. J.; Wilson, D. J., Measuring Dynamics in Weakly Structured Regions of Proteins Using Microfluidics-Enabled Subsecond H/D Exchange Mass Spectrometry. *Anal. Chem.* **2012,** *84*, 3771-3779.

45. Johnson, R. S.; Walsh, K. A., Mass spectrometric measurement of protein amide hydrogen exchange rates of apo- and holo-myoglobin. *Protein Sci.* **1994,** *3*, 2411-2418.

46. Powell, K. D.; Ghaemmaghami, S.; Wang, M. Z.; Ma, L.; Oas, T. G.; Fitzgerald, M. C., A General Mass Spectrometry-Based Assay for the Quantitation of Protein-Ligand Binding Interactions in Solution. *J. Am. Chem. Soc.* **2002,** *124*, 10256-10257.

47. Zhu, M. M.; Rempel, D. L.; Du, Z. H.; Gross, M. L., Quantification of protein-ligand interactions by mass spectrometry, titration, and H/D exchange: PLIMSTEX. *J. Am. Chem. Soc.* **2003,** *125* (18), 5252-5253.

48. Asuru, A. P.; An, M.; Busenlehner, L. S., Dissection of Porphyrin-Induced Conformational Dynamics in the Heme Biosynthesis Enzyme Ferrochelatase. *Biochemistry* **2012,** *51* (36), 7116-7127.

49. Keppel, T. R.; Howard, B. A.; Weis, D. D., Mapping Unstructured Regions and Synergistic Folding in Intrinsically Disordered Proteins with Amide H/D Exchange Mass Spectrometry. *Biochemistry* **2011,** *50* (40), 8722-8732.

50. Percy, A. J.; Rey, M.; Burns, K. M.; Schriemer, D. C., Probing protein interactions with hydrogen/deuterium exchange and mass spectrometry-A review. *Anal. Chim. Acta* **2012,** *721*, 7-21.

51. Chalmers, M. J.; Busby, S. A.; Pascal, B. D.; West, G. M.; Griffin, P. R., Differential hydrogen/deuterium exchange mass spectrometry analysis of protein-Ligand interactions. *Exp. Rev. Proteomics* **2011,** *8*, 43-59.

52. Bai, Y.; Milne, J. S.; Mayne, L.; Englander, S. W., Primary Structure Effects on Peptide Group Hydrogen Exchange. *Proteins: Struct., Funct., Genet.* **1993,** *17*, 75-86.

53. Sowole, M. A.; Alexopoulos, J. A.; Cheng, Y.-Q.; Ortega, J.; Konermann, L., Activation of ClpP Protease by ADEP Antibiotics: Insights from Hydrogen Exchange Mass Spectrometry. *J. Mol. Biol.* **2013,** *425* (22), 4508-4519.

54. Burke, J. E.; Babakhani, A.; Gorfe, A. A.; Kokotos, G.; Li, S.; Woods, V. L.; McCammon, J. A.; Dennis, E. A., Location of Inhibitors Bound to Group IVA Phospholipase A(2) Determined by Molecular Dynamics and Deuterium Exchange Mass Spectrometry. *J. Am. Chem. Soc.* **2009,** *131* (23), 8083-8091.

55. Bobst, C. E.; Zhang, M.; Kaltashov, I. A., Existence of a Noncanonical State of Iron-Bound Transferrin at Endosomal pH Revealed by Hydrogen Exchange and Mass Spectrometry. *J. Mol. Biol.* **2009,** *388* (5), 954-967.

56. Pantazatos, D.; Kim, J. S.; Klock, H. E.; Stevens, R. C.; Wilson, I. A.; Lesley, S. A.; Woods, V. L., Rapid refinement of crystallographic protein construct definition employing enhanced hydrogen/deuterium exchange MS. *Proc. Natl. Acad. Sci. U. S. A.* **2004,** *101* (3), 751-756.

57. Innes, B.; Bailey, M.; Brandl, C. J.; Shilton, B.; Litchfield, D. W., Non-catalytic participation of the Pin 1 peptidyl-prolyl isomerase domain in target binding. *Front. Physiol.* **2013,** *4*, 1-10.

58. Wales, T. E.; Fadgen, K. E.; Gerhardt, G. C.; Engen, J. R., High-Speed and High-Resolution UPLC Separation at Zero Degree Celsius. *Anal. Chem.* **2008,** *80*, 6815-6820.

59. Weis, D. D.; Engen, J. R.; Kass, I. J., Semi-automated data processing of hydrogen exchange mass spectra using HX-Express. *J. Am. Soc. Mass Spectrom.* **2006,** *17* (12), 1700-1703.

60. Jager, M.; Dendle, M.; Kelly, J. W., Sequence determinants of thermodynamic stability in a WW domain-An all-beta-sheet protein. *Protein Sci.* **2009,** *18* (8), 1806-1813.

61. Mortenson, D. E.; Kreitler, D. F.; Yun, H. G.; Gellman, S. H.; Forest, K. T., Evidence for small-molecule-mediated loop stabilization in the structure of the isolated Pin1 WW domain. *Acta Crystallogr. Sect. D-Biol. Crystallogr.* **2013,** *69*, 2506-2512.

62. Zhang, Y.; Daum, S.; Wildemann, D.; Zhou, X. Z.; Verdecia, M. A.; Bowman, M. E.; C., L.; Hunter, T.; Lu, K. P.; Fischer, G.; Noel, J. P., Structural Basis for High-Affinity Peptide Inhibition of Human Pin1. *ACS Chem. Biol.* **2007,** *2*, 320-328.

Chapter 6. Summary and Future Work

6.1. Summary

The work described in this thesis showed how both global and local HDX-MS analysis can be used for the study of protein structure. Spatially resolved HDX information gives useful information about the regions of the protein undergoing conformational changes however, global probing is always a useful first experiment. Global probing is usually fast and it cuts down on unnecessary experiments. Also, the experimental conditions can be fine-tuned prior to enzymatic digests. The ultimate goal in this work was to improve the understanding of protein-ligand binding interactions as it pertains to HDX-MS.

In Chapter 2, native oxy-Hb and aquomet-Hb were exposed to deuterium. It was found that deuteration pattern in these two proteins were quite different with aquomet-Hb having a higher deuterium uptake after 6 hours. HDX analysis at the peptide level indicates that crystallized Hb does not represent the solution-phase structure adequately. Oxy-Hb also showed an increase in the deuterium uptake near the heme binding site.

In subsequent studies (Chapter 3), the structural dynamics in hemoglobin and myoglobin were studied. Heme binding to apo-Mb resulted in a decrease in deuterium incorporated into the backbone of the protein. This result is in agreement with other HDX binding studies. Binding of oxygen to hemoglobin or myoglobin, however, resulted in an increase in the uptake of deuterium with hemoglobin exhibiting the larger increase of the two proteins. It appears that the increase in measured HDX kinetics was not limited to multimeric proteins like hemoglobin. A thermodynamic model for the different scenarios encountered in HDX measurements is thus provided in this chapter.

Having established that protein-ligand interactions can lead to both stabilization or destabilization of the protein receptor, Chapter 3 explored the interaction between an antibacterial drug target ClpP and ADEP (an antibiotic compound). Binding cause noticeable changes at the binding site, but allosteric interactions can be triggered as well. This is particularly important for protein-ligand studies that seek to map the binding site of a drug to its target. The results also suggest that ligand binding to ClpP induces an opening of the axial pore as demonstrated in the increased HDX kinetics in this region.

Chapter 5 focused on the structural changes in Pin 1 a peptidyl prolyl isomerase. CREPEVEIC, a cyclic peptide, is a known inhibitor of Pin 1 however efforts to crystallize Pin1-CRYPEVEIC complex have proved unsuccessful. The HDX kinetics of Pin 1 in the WW domain remains unchanged in the presence of ligand. The PPIase domain, however, shows a dramatic difference before and after ligand binding. Of particular interest is a group of residues in the loop region known to interact with the phosphate groups of the ligand. This loop became destabilized after ligand binding due to steric effect.

6.2. Future Work

6.2.1. Application of HDX to Other Proteins

HDX is a powerful tool for probing the structural dynamics of proteins, but this technique works best only for soluble proteins. The size and type of systems that can be studied using HDX-MS are endless. The goal is to study larger and more complex systems. The work in Chapter 4 looks at ClpP with a small binding partner. It will be interesting to investigate ClpP interaction with AAA+ proteins such as ClpX or ClpA. [1-3] Global and peptide analysis will help understand how ClpP functions with its natural binding partner. The experiment can

also be tuned to look at the structural changes in ClpA (ClpX) as a function of binding to ClpP. Another interesting class of protein to study is integral membrane proteins.

Integral membrane proteins represent a large proportion of the current drug targets which indicates their role in cellular processes. Membrane proteins are water insoluble and prone to aggregation. They represent the most difficult proteins to study by HDX-MS. Previous MS structural studies have utilized detergents as solubilizing agents which allows the acquisition of global HDX information. [4-5] It will be interesting to explore the development of improved HDX-MS protocols for membrane proteins

6.2.2. Application of HDX to Intrinsically Disordered Proteins (IDPs)

IDPs represent a special family of proteins lacking a unique tertiary structure at physiological pH. IDPs are predicted to perform various function and they have been shown to be associated with human diseases like cancer and neurodegenerative diseases.[6] HDX is routinely used to detect disordered regions in a protein. The ability of HDX to report on the structure of the polypeptide chain gives it an advantage over other optical methods that rely of select chromophores. HDX has been successfully applied in the study of the interaction between ACTR (activator of thyroid and retinoid receptors) and CBP (binding domain of the CREB binding protein).[7] Extending this technique to other IDPs would be very informative.

6.3. References

1. Kress, W.; Maglica, Z.; Weber-Ban, E., Clp chaperone-proteases: structure and function. *Res. Microbiol.* **2009,** *160* (9), 618-628.

2. Baker, T. A.; Sauer, R. T., ClpXP, an ATP-powered unfolding and protein-degradation machine. *Biochim. Biophys. Acta* **2012,** *1823*, 15-28.

3. Choi, K.-H.; Licht, S., Control of Peptide Product Sizes by the Energy-Dependent Protease ClpAP. *Biochem.* **2005,** *44*, 13921-13931.

4. Pan, Y.; Stocks, B. B.; Brown, L.; Konermann, L., Structural Characterization of an Integral Membrane Protein in its Natural Lipid Environment by Oxidative Methionine Labeling and Mass Spectrometry. *Anal. Chem.* **2009,** *81*, 28-35.

5. Pan, Y.; Ruan, X.; Valvano, M. A.; Konermann, L., Validation of Membrane Protein Topology Models by Oxidative Labeling and Mass Spectrometry. *J. Am. Soc. Mass Spectrom.* **2012,** *23*, 889-898.

6. Forman-Kay, J. D.; Mittag, T., From Sequence and Forces to Structure, Function, and Evolution of Intrinsically Disordered Proteins. *Structure* **2013,** *21* (9), 1492-1499.

7. Keppel, T. R.; Howard, B. A.; Weis, D. D., Mapping Unstructured Regions and Synergistic Folding in Intrinsically Disordered Proteins with Amide H/D Exchange Mass Spectrometry. *Biochemistry* **2011,** *50* (40), 8722-8732.

Appendix **I-P**ermissions

SPRINGER LICENSE
TERMS AND CONDITIONS

May 27, 2015

This is a License Agreement between Modupeola A Sowole ("You") and Springer ("Springer") provided by Copyright Clearance Center ("CCC"). The license consists of your order details, the terms and conditions provided by Springer, and the payment terms and conditions.

All payments must be made in full to CCC. For payment instructions, please see information listed at the bottom of this form.

License Number	3636001051751
License date	May 25, 2015
Order Content Publisher	Springer
Order Content Publication	Journal of The American Society for Mass Spectrometry
Order Content Title	Comparative Analysis of Oxy-Hemoglobin and Aquomet-Hemoglobin by Hydrogen/Deuterium Exchange Mass Spectrometry
Order Content Author	Modupeola A. Sowole
Order Content Date	Jan 1, 2013
Volume number	24
Issue number	7
Type of Use	Thesis/Dissertation
Portion	Full text
Number of copies	10000
Author of this Springer article	Yes and you are a contributor of the new work
Order reference number	None
Title of your thesis / dissertation	Hydrogen Exchange Mass Spectrometry for Studying Protein-Ligand Interactions
Expected completion date	Aug 2015

Estimated size(pages)	200
Total	**0.00 USD**

Terms and Conditions

Introduction

The publisher for this copyrighted material is Springer Science + Business Media. By clicking "accept" in connection with completing this licensing transaction, you agree that the following terms and conditions apply to this transaction (along with the Billing and Payment terms and conditions established by Copyright Clearance Center, Inc. ("CCC"), at the time that you opened your Rightslink account and that are available at any time at http://myaccount.copyright.com).

Limited License

With reference to your request to reprint in your thesis material on which Springer Science and Business Media control the copyright, permission is granted, free of charge, for the use indicated in your enquiry.

Licenses are for one-time use only with a maximum distribution equal to the number that you identified in the licensing process.

This License includes use in an electronic form, provided its password protected or on the university's intranet or repository, including UMI (according to the definition at the Sherpa website: http://www.sherpa.ac.uk/romeo/). For any other electronic use, please contact Springer at (permissions.dordrecht@springer.com or permissions.heidelberg@springer.com).

The material can only be used for the purpose of defending your thesis limited to university-use only. If the thesis is going to be published, permission needs to be re-obtained (selecting "book/textbook" as the type of use).

Although Springer holds copyright to the material and is entitled to negotiate on rights, this license is only valid, subject to a courtesy information to the author (address is given with the article/chapter) and provided it concerns original material which does not carry references to other sources (if material in question appears with credit to another source, authorization from that source is required as well).

Permission free of charge on this occasion does not prejudice any rights we might have to charge for reproduction of our copyrighted material in the future.

Altering/Modifying Material: Not Permitted

You may not alter or modify the material in any manner. Abbreviations, additions, deletions and/or any other alterations shall be made only with prior written authorization of the author(s) and/or Springer Science + Business Media. (Please contact Springer at (permissions.dordrecht@springer.com or permissions.heidelberg@springer.com)

Reservation of Rights

Springer Science + Business Media reserves all rights not specifically granted in the combination of (i) the license details provided by you and accepted in the course of this licensing transaction, (ii) these terms and conditions and (iii) CCC's Billing and Payment terms and conditions.

Copyright Notice:Disclaimer

You must include the following copyright and permission notice in connection with any reproduction of the licensed material: "Springer and the original publisher /journal title, volume, year of publication, page, chapter/article title, name(s) of author(s), figure number(s), original copyright notice) is given to the publication in which the material was originally published, by adding; with kind permission from Springer Science and Business Media"

Warranties: None

Example 1: Springer Science + Business Media makes no representations or warranties with respect to the licensed material.

Example 2: Springer Science + Business Media makes no representations or warranties with respect to the licensed material and adopts on its own behalf the limitations and disclaimers established by CCC on its behalf in its Billing and Payment terms and conditions for this licensing transaction.

Indemnity

You hereby indemnify and agree to hold harmless Springer Science + Business Media and CCC, and their respective officers, directors, employees and agents, from and against any and all claims arising out of your use of the licensed material other than as specifically authorized pursuant to this license.

No Transfer of License

This license is personal to you and may not be sublicensed, assigned, or transferred by you to any other person without Springer Science + Business Media's written permission. No

Amendment Except in Writing

This license may not be amended except in a writing signed by both parties (or, in the case of Springer Science + Business Media, by CCC on Springer Science + Business Media's behalf).

Objection to Contrary Terms
Springer Science + Business Media hereby objects to any terms contained in any purchase order, acknowledgment, check endorsement or other writing prepared by you, which terms are inconsistent with these terms and conditions or CCC's Billing and Payment terms and conditions. These terms and conditions, together with CCC's Billing and Payment terms and conditions (which are incorporated herein), comprise the entire agreement between you and Springer Science
+ Business Media (and CCC) concerning this licensing transaction. In the event of any conflict between your obligations established by these terms and conditions and those established by CCC's Billing and Payment terms and conditions, these terms and conditions shall control.
Jurisdiction
All disputes that may arise in connection with this present License, or the breach thereof, shall be settled exclusively by arbitration, to be held in The Netherlands, in accordance with Dutch law, and to be conducted under the Rules of the 'Netherlands Arbitrage Instituut' (Netherlands Institute of Arbitration).***OR:***
All disputes that may arise in connection with this present License, or the breach thereof, shall be settled exclusively by arbitration, to be held in the Federal Republic of Germany, in accordance with German law. Other terms and conditions:
v1.3

Questions? customercare@copyright.com or +1-855-239-3415 (toll free in the US) or +1-978-646-2777.

Gratis licenses (referencing $0 in the Total field) are free. Please retain this printable license for your reference. No payment is required.

ELSEVIER LICENSE
TERMS AND CONDITIONS

May 27, 2015

This is a License Agreement between Modupeola A Sowole ("You") and Elsevier ("Elsevier") provided by Copyright Clearance Center ("CCC"). The license consists of your order details, the terms and conditions provided by Elsevier, and the payment terms and conditions.

All payments must be made in full to CCC. For payment instructions, please see information listed at the bottom of this form.

Supplier	Elsevier Limited The Boulevard,Langford Lane Kidlington,Oxford,OX5 1GB,UK
Registered Company Number	1982084
Customer name	Modupeola A Sowole
Customer address	Department of Chemistry London, ON N6G 5B7
License number	3636000406054
License date	May 25, 2015
Licensed content publisher	Elsevier
Licensed content publication	Journal of Molecular Biology
Licensed content title	Activation of ClpP Protease by ADEP Antibiotics: Insights from Hydrogen Exchange Mass Spectrometry
Licensed content author	Modupeola A. Sowole,John A. Alexopoulos,Yi-Qiang Cheng,Joaquin Ortega,Lars Konermann
Licensed content date	15 November 2013
Licensed content volume number	425
Licensed content issue number	22
Number of pages	12
Start Page	4508
End Page	4519
Type of Use	reuse in a thesis/dissertation
Portion	full article
Format	both print and electronic
Are you the author of this Elsevier article?	Yes
Will you be translating?	No
Title of your thesis/dissertation	Hydrogen Exchange Mass Spectrometry for Studying Protein-Ligand Interactions
Expected completion date	Aug 2015
Estimated size (number	200

of pages)	
Elsevier VAT number	GB 494 6272 12
Price	0.00 USD
VAT/Local Sales Tax	0.00 USD / 0.00 GBP
Total	**0.00 USD**

Terms and Conditions

INTRODUCTION

1. The publisher for this copyrighted material is Elsevier. By clicking "accept" in connection with completing this licensing transaction, you agree that the following terms and conditions apply to this transaction (along with the Billing and Payment terms and conditions established by Copyright Clearance Center, Inc. ("CCC"), at the time that you opened your Rightslink account and that are available at any time at http://myaccount.copyright.com).

GENERAL TERMS

2. Elsevier hereby grants you permission to reproduce the aforementioned material subject to the terms and conditions indicated.
3. Acknowledgement: If any part of the material to be used (for example, figures) has appeared in our publication with credit or acknowledgement to another source, permission must also be sought from that source. If such permission is not obtained then that material may not be included in your publication/copies. Suitable acknowledgement to the source must be made, either as a footnote or in a reference list at the end of your publication, as follows:
"Reprinted from Publication title, Vol /edition number, Author(s), Title of article / title of chapter, Pages No., Copyright (Year), with permission from Elsevier [OR APPLICABLE SOCIETY COPYRIGHT OWNER]." Also Lancet special credit - "Reprinted from The Lancet, Vol. number, Author(s), Title of article, Pages No., Copyright (Year), with permission from Elsevier."
4. Reproduction of this material is confined to the purpose and/or media for which permission is hereby given.
5. Altering/Modifying Material: Not Permitted. However figures and illustrations may be altered/adapted minimally to serve your work. Any other abbreviations, additions, deletions and/or any other alterations shall be made only with prior written authorization of Elsevier Ltd. (Please contact Elsevier at permissions@elsevier.com)
6. If the permission fee for the requested use of our material is waived in this instance, please be advised that your future requests for Elsevier materials may attract a fee.
7. Reservation of Rights: Publisher reserves all rights not specifically granted in the combination of (i) the license details provided by you and accepted in the course of this licensing transaction, (ii) these terms and conditions and (iii) CCC's Billing and Payment terms and conditions.
8. License Contingent Upon Payment: While you may exercise the rights licensed immediately upon issuance of the license at the end of the licensing process for the transaction, provided that you have disclosed complete and accurate details of your proposed use, no license is finally effective unless and until full payment is received from you (either by publisher or by CCC) as provided in CCC's Billing and Payment terms and conditions. If full payment is not received on a timely basis, then any license preliminarily granted shall be deemed automatically revoked and shall be void as if never granted. Further, in the event that you breach any of these terms and conditions or any of CCC's Billing and Payment terms and conditions, the license is automatically revoked and shall be void as if never granted. Use of materials as described in a revoked license, as well as any use of the materials beyond the scope of an unrevoked license, may constitute copyright infringement and publisher reserves the right to take any and all action to protect its copyright in the materials.
9. Warranties: Publisher makes no representations or warranties with respect to the licensed material.
10. Indemnity: You hereby indemnify and agree to hold harmless publisher and CCC, and their respective officers, directors, employees and agents, from and against any and all claims arising out of your use of the licensed material other than as specifically authorized pursuant to this license.
11. No Transfer of License: This license is personal to you and may not be sublicensed, assigned, or transferred by you to any other person without publisher's written permission.
12. No Amendment Except in Writing: This license may not be amended except in a writing signed by both parties (or, in the case of publisher, by CCC on publisher's behalf).
13. Objection to Contrary Terms: Publisher hereby objects to any terms contained in any purchase order, acknowledgment, check endorsement or other writing prepared by you, which terms are inconsistent with these terms and conditions or CCC's Billing and Payment terms and conditions. These terms and conditions, together with CCC's Billing and Payment terms and conditions (which are incorporated herein), comprise the entire agreement between you and publisher (and CCC) concerning this licensing transaction. In the event of any conflict between your obligations established by these terms and conditions and those established by CCC's Billing and Payment terms and conditions,

these terms and conditions shall control.
14. Revocation: Elsevier or Copyright Clearance Center may deny the permissions described in this License at their sole discretion, for any reason or no reason, with a full refund payable to you. Notice of such denial will be made using the contact information provided by you. Failure to receive such notice will not alter or invalidate the denial. In no event will Elsevier or Copyright Clearance Center be responsible or liable for any costs, expenses or damage incurred by you as a result of a denial of your permission request, other than a refund of the amount(s) paid by you to Elsevier and/or Copyright Clearance Center for denied permissions.

LIMITED LICENSE

The following terms and conditions apply only to specific license types:
15. **Translation**: This permission is granted for non-exclusive world **English** rights only unless your license was granted for translation rights. If you licensed translation rights you may only translate this content into the languages you requested. A professional translator must perform all translations and reproduce the content word for word preserving the integrity of the article. If this license is to re-use 1 or 2 figures then permission is granted for non-exclusive world rights in all languages.
16. **Posting licensed content on any Website**: The following terms and conditions apply as follows: Licensing material from an Elsevier journal: All content posted to the web site must maintain the copyright information line on the bottom of each image; A hyper-text must be included to the Homepage of the journal from which you are licensing at http://www.sciencedirect.com/science/journal/xxxxx or the Elsevier homepage for books at http://www.elsevier.com; Central Storage: This license does not include permission for a scanned version of the material to be stored in a central repository such as that provided by Heron/XanEdu.
Licensing material from an Elsevier book: A hyper-text link must be included to the Elsevier homepage at http://www.elsevier.com . All content posted to the web site must maintain the copyright information line on the bottom of each image.

Posting licensed content on Electronic reserve: In addition to the above the following clauses are applicable: The web site must be password-protected and made available only to bona fide students registered on a relevant course. This permission is granted for 1 year only. You may obtain a new license for future website posting.
17. **For journal authors:** the following clauses are applicable in addition to the above:
Preprints:
A preprint is an author's own write-up of research results and analysis, it has not been peer-reviewed, nor has it had any other value added to it by a publisher (such as formatting, copyright, technical enhancement etc.).
Authors can share their preprints anywhere at any time. Preprints should not be added to or enhanced in any way in order to appear more like, or to substitute for, the final versions of articles however authors can update their preprints on arXiv or RePEc with their Accepted Author Manuscript (see below).
If accepted for publication, we encourage authors to link from the preprint to their formal publication via its DOI. Millions of researchers have access to the formal publications on ScienceDirect, and so links will help users to find, access, cite and use the best available version. Please note that Cell Press, The Lancet and some society-owned have different preprint policies. Information on these policies is available on the journal homepage.
Accepted Author Manuscripts: An accepted author manuscript is the manuscript of an article that has been accepted for publication and which typically includes author-incorporated changes suggested during submission, peer review and editor-author communications.
Authors can share their accepted author manuscript:

- immediately
  - via their non-commercial person homepage or blog
  - by updating a preprint in arXiv or RePEc with the accepted manuscript
  - via their research institute or institutional repository for internal institutional uses or as part of an invitation-only research collaboration work-group
  - directly by providing copies to their students or to research collaborators for their personal use
  - for private scholarly sharing as part of an invitation-only work group on commercial sites with which Elsevier has an agreement
- after the embargo period
  - via non-commercial hosting platforms such as their institutional repository via
  - commercial sites with which Elsevier has an agreement

In all cases accepted manuscripts should:

- link to the formal publication via its DOI

- bear a CC-BY-NC-ND license - this is easy to do
- if aggregated with other manuscripts, for example in a repository or other site, be shared in alignment with our hosting policy not be added to or enhanced in any way to appear more like, or to substitute for, the published journal article.

Published journal article (JPA): A published journal article (PJA) is the definitive final record of published research that appears or will appear in the journal and embodies all value-adding publishing activities including peer review co- ordination, copy-editing, formatting, (if relevant) pagination and online enrichment.
Policies for sharing publishing journal articles differ for subscription and gold open access articles:
Subscription Articles: If you are an author, please share a link to your article rather than the full-text. Millions of researchers have access to the formal publications on ScienceDirect, and so links will help your users to find, access, cite, and use the best available version.
Theses and dissertations which contain embedded PJAs as part of the formal submission can be posted publicly by the awarding institution with DOI links back to the formal publications on ScienceDirect.
If you are affiliated with a library that subscribes to ScienceDirect you have additional private sharing rights for others' research accessed under that agreement. This includes use for classroom teaching and internal training at the institution (including use in course packs and courseware programs), and inclusion of the article for grant funding purposes.
Gold Open Access Articles: May be shared according to the author-selected end-user license and should contain a CrossMarklogo, the end user license, and a DOI link to the formal publication on ScienceDirect. Please refer to Elsevier's postingpolicy for further information.
18. **For book authors** the following clauses are applicable in addition to the above: Authors are permitted to place a brief summary of their work online only. You are not allowed to download and post the published electronic version of your chapter, nor may you scan the printed edition to create an electronic version. **Posting to a repository:** Authors are permitted to post a summary of their chapter only in their institution's repository.
19. **Thesis/Dissertation**: If your license is for use in a thesis/dissertation your thesis may be submitted to your institution in either print or electronic form. Should your thesis be published commercially, please reapply for permission. These requirements include permission for the Library and Archives of Canada to supply single copies, on demand, of the complete thesis and include permission for Proquest/UMI to supply single copies, on demand, of the complete thesis. Should your thesis be published commercially, please reapply for permission. Theses and dissertations which contain embedded PJAs as part of the formal submission can be posted publicly by the awarding institution with DOI links back to the formal publications on ScienceDirect.

Elsevier Open Access Terms and Conditions
You can publish open access with Elsevier in hundreds of open access journals or in nearly 2000 established subscription journals that support open access publishing. Permitted third party re-use of these open access articles is defined by the author's choice of Creative Commons user license. See our openaccesslicensepolicy for more information.
Terms & Conditions applicable to all Open Access articles published with Elsevier:
Any reuse of the article must not represent the author as endorsing the adaptation of the article nor should the article be modified in such a way as to damage the author's honour or reputation. If any changes have been made, such changes must be clearly indicated.
The author(s) must be appropriately credited and we ask that you include the end user license and a DOI link to the formal publication on ScienceDirect.
If any part of the material to be used (for example, figures) has appeared in our publication with credit or acknowledgement to another source it is the responsibility of the user to ensure their reuse complies with the terms and conditions determined by the rights holder.
Additional Terms & Conditions applicable to each Creative Commons user license:
CC BY: The CC-BY license allows users to copy, to create extracts, abstracts and new works from the Article, to alter and revise the Article and to make commercial use of the Article (including reuse and/or resale of the Article by commercial entities), provided the user gives appropriate credit (with a link to the formal publication through the relevant DOI), provides a link to the license, indicates if changes were made and the licensor is not represented as endorsing the use made of the work. The full details of the license are available at http://creativecommons.org/licenses/by/4.0.
CC BY NC SA: The CC BY-NC-SA license allows users to copy, to create extracts, abstracts and new works from the Article, to alter and revise the Article, provided this is not done for commercial purposes, and that the user gives appropriate credit (with a link to the formal publication through the relevant DOI), provides a link to the license, indicates if changes were made and the licensor is not represented as endorsing the use made of the work. Further, any new works must be made available on the same conditions. The full details of the license are available at

NRC RESEARCH PRESS LICENSE TERMS AND CONDITIONS

May 27, 2015

This is a License Agreement between Modupeola A Sowole ("You") and NRC Research Press ("NRC Research Press") provided by Copyright Clearance Center ("CCC"). The license consists of your order details, the terms and conditions provided by NRC Research Press, and the payment terms and conditions.

All payments must be made in full to CCC. For payment instructions, please see information listed at the bottom of this form.

License Number	3636001111552
License date	May 25, 2015
Order Content Publisher	NRC Research Press
Order Content Publication	Canadian Journal of Chemistry
Order Content Title	Noncovalent binding of a cyclic peptide inhibitor to the peptidyl-prolyl isomerase Pin1, explored by hydrogen exchange mass spectrometry
Order Content Author	Modupeola A. Sowole, Brendan T. Innes, Mahasilu Amunugama, et al
Order Content Date	Jan 1, 2015
Volume number	93
Issue number	1
Type of Use	Thesis/Dissertation
Requestor type	Author (original work)
Format	Print and electronic
Portion	Full article
Order reference number	None
Title of your thesis / dissertation	Hydrogen Exchange Mass Spectrometry for Studying Protein-Ligand Interactions
Expected completion date	Aug 2015
Estimated size(pages)	200
Total	**0.00 USD**
Terms and Conditions	

General Terms & Conditions

Permission is granted upon the requester's compliance with the following terms and conditions:

1. A credit line will be prominently placed in your product(s) and include: for books the author, book title, editor, copyright holder, year of publication; for journals the author, title of article, title of journal, volume number, issue number, and the inclusive pages. The credit line must include the following wording: "© 2008 Canadian Science Publishing or its licensors. Reproduced with permission," except when an author of an original article published in 2009 or later is reproducing his/her own work.

2. The requester warrants that the material shall not be used in any manner that may be derogatory to the title, content, or authors of the material or to Canadian Science Publishing, including but not limited to an association with conduct that is fraudulent or otherwise illegal.

3. Permission is granted for the term (for Books/CDs-Shelf Life; for Internet/Intranet-In perpetuity; for all other forms of print-the life of the title) and purpose specified in your request. Once term has expired, permission to renew must be made in writing.

4. Permission granted is nonexclusive, and is valid throughout the world in English and the languages specified in your original request. A new permission must be requested for revisions of the publication under current consideration.

5. Canadian Science Publishing cannot supply the requester with the original artwork or a "clean copy."

6. If the Canadian Science Publishing material is to be translated, the following lines must be included: The authors, editors, and Canadian Science Publishing are not responsible for errors or omissions in translations.

v1.4

A**ppendix** II-C**urriculum** V**itae**

Name: MODUPEOLA SOWOLE

Education

Ph.D. 2011-2015	The University of Western Ontario, Canada.
M.Sc. 2009-2011	The University of Western Ontario, Canada.
M.Sc. 2005-2006	The University of Lagos, Nigeria.
B.Sc. 1998-2002	The University of Lagos, Nigeria.

Selected Scholarships and Awards

Canadian Society of Mass Spectrometry Travel Award	2014
Graduate Thesis Research Award	2013
Canadian Society for Chemistry Award	2013

Research/Work Experience

Research / Teaching Assistant	University of Western Ontario	2009-2015
Graduate Fellow	University of Lagos	2008-2009
Graduate/Teaching Assistant	University of Lagos	2005-2006

Publications

1. B. T. Innes, M. A Sowole, L. Gyenis, M. Dubinsky, L. Konermann, D. W. Litchfield, C. J. Brandl, and B. H. Shilton (**2015**) "Peroxide-Mediated Oxidation and Inhibition of the Peptidyl-Prolyl Isomerase Pin1" *Biochim. Biophys. Acta*, *1852,* 905-912

2. M. A. Sowole, B. T. Innes, M. Amunugama, D. W. Litchfield, C. J. Brandl, B. H. Shilton, and L. Konermann (**2015**) "Noncovalent Binding of a Cyclic Peptide Inhibitor to the Peptidyl-Prolyl Isomerase Pin1 Explored by Hydrogen Exchange Mass Spectrometry" *Can. J. Chem., 93,* 44-50

3. L. Konermann, A. D. Rodriguez, M. A. Sowole, (**2014**) "Type 1 and Type 2 Scenarios in Hydrogen Exchange Mass Spectrometry Studies on Protein-Ligand Complexes" *Analyst,* 139, 6078-6087

4. M. A. Sowole and L. Konermann, (**2014**) "Effects of Protein-Ligand Interactions on Hydrogen/ Deuterium Exchange Kinetics: Canonical and Non-Canonical Scenarios" *Anal. Chem*., 86*,* 6715-6722

5. L. Konermann, S. Vahidi , and M. A. Sowole, (**2014**) "Mass Spectrometry Methods for Studying Structure and Dynamics of Biological Macromolecules" *Anal. Chem.*, 86, 213-232

6. M. A. Sowole, J. A. Alexopoulos, Y.-Q. Cheng, J. Ortega and L. Konermann, (**2013**) "Activation of ClpP Protease by ADEP Antibiotics: Insights from Hydrogen Exchange Mass Spectrometry" *J. Mol. Biol.,* 425, 4508–4519

7. M. A. Sowole and L. Konermann, (**2013**) "Comparative Analysis of Oxy- Hemoglobin and Aquomet-Hemoglobin by Hydrogen/Deuterium Exchange Mass Spectrometry" *J. Am. Soc. Mass Spectrom.* 24, 997-1005

8. M. A. Sowole and H.-B. Kraatz, (**2012**) "Electrochemical detection of hepatitis C viral NS3-4A protease." *Analyst.,* 137, 1120-1124

Selected Poster and Oral presentations

1. **2014:** M. A. Sowole; Protein-Ligand Interactions Studied by Hydrogen Exchange Mass Spectrometry, 27th annual Tandem Mass Spectrometry Workshop Dec 3-6, Lake Louise Alberta Canada. **Oral Presentation**

2. **2014:** M. A. Sowole and L. Konermann; Does Protein-Ligand Binding Generally Induce Reduced Deuteration Rates? Globin Oxygenation Studies Provide Insights Into HDX Fundamentals. 62nd ASMS Conference on Mass Spectrometry and Allied Topics. Jun., 15-19, Baltimore MD, United States. **Poster Presentation**

3. **2014:** M. A. Sowole and L. Konermann; Thermodynamic Aspects of Protein-Ligand Interactions Probed by Hydrogen Exchange Mass Spectrometry. 97th Canadian Chemistry Conference and Exhibition. Jun., 1-5, Vancouver, B.C, Canada. **Oral Presentation**

4. **2013:** M. A. Sowole and L. Konermann; Effector Binding Causes Major Changes in the Structure and Dynamics of the ClpP Protease Complex: A HDX/MS Investigation. 61th ASMS Conference on Mass Spectrometry and Allied Topics, June 8-14, Minneapolis, United State. **Oral Presentation**

5. **2012:** M. Sowole and L. Konermann; Conformational Dynamics of Hemoglobin in Different Ligation states studied by HDX mass spectrometry. 60th ASMS Conference on

Mass Spectrometry and Allied Topics, May 20-24, Vancouver, Canada. **Poster Presentation**